BOKU UNIVERSITY

Master Thesis

Phenotyping of European soybean varieties with different time to maturity for drought tolerance

Submitted by

Benedikt Johannes PILLER, B.Sc.

In the framework of the Master programme

Nutzpflanzenwissenschaften

In partial fulfilment of the requirements for the academic degree

Diplom-Ingenieur

Vienna, April 2025

Supervisor

Ao. Univ. Prof. Dr. Johann Vollmann
Institut für Pflanzenzüchtung
Department für Agrarwissenschaften
Universität für Bodenkultur Wien

Affidavit

I hereby declare that I have authored this master thesis independently, and that I have not used any assistance other than that which is permitted. The work contained herein is my own except where explicitly stated otherwise. All ideas taken in wording or in basic content from unpublished sources or from published literature, as well as those which were generated using artificial intelligence tools, are duly identified and cited, and the precise references included.
I further declare that this master thesis has not been submitted, in whole or in part, in the same or a similar form, to any other educational institution as part of the requirements for an academic degree.
I hereby confirm that I am familiar with the standards of Scientific Integrity and with the guidelines of Good Scientific Practice, and that this work fully complies with these standards and guidelines.

Vienna, April 10, 2025

_____

Benedikt PILLER (*manu propria)*

What we observe is not nature itself, but nature exposed to our method of questioning.

- Werner Heisenberg

For Megi

Acknowledgements

Ao. Prof. Johann Vollmann for his sunny and soft-spoken manner to guide me through the experiments for my master thesis. He showed me how scientific work routine is applied to practical field experiments. A great thank you for all constructive suggestions during the process of the present work.
Charlotte Nothelfer for her great perseverance in field sampling and data collection. Her willingness to work for this project is invaluable and enabled the success of this master thesis.
My parents for their belief to my master studies and to give me the possibility to use a thermal infrared camera for the purpose of plant phenotyping.
A special thank goes to my girlfriend Megi for her mental support and her inestimably huge 'Hilfsbereitschaft' during the whole period of my master studies.

Preface

The research work reported here was partly supported by the European Union through the Legume Generation project (Boosting innovation in breeding for the next generation of legume crops for Europe) under Horizon Europe grant number 101081329.

Abstract

Soybean is the major crop for high-protein feed and food in Europe, however domestic production is low due to non-adapted varieties for drought events and time to maturity. Especially, drought stress during growing season can cause severe yield loss in soybean. The present work focused on phenotyping of European soybean varieties of maturity groups (MG) 000 – I, grown in Tulln (Austria) under rainfed conditions. Phenotyping traits were visually scored and screened by hyperspectral and thermal imaging (TIR) techniques. Varietal differences in time to flowering, time to maturity (ttm), plant height, stomatal density, yield, 16 hyperspectral reflectance indices and canopy temperature were examined. Furthermore, TIR method was evaluated for two daytimes (12:00h, 15:00h) and applied for simplified Crop Water Stress Index (siCWSI). Results showed significant differences in ttm between MG. Plant height showed a positive relationship with ttm, while yield reached an optimum at MG 00. Stomatal density of European soybean varieties was published first time: stomatal density was significantly different and ranges between 203.4 and 322.2 stomata/mm². Soybean of MG 000 showed significant correlation between yield and chlorophyll index, red edge inflection point, water indices WI-1, NWI-2 and NWI-4. Later maturing soybean sets had less relationship between indices and yield. Correlation between siCWSI and morphological traits were higher at 15:00h than at 12:00h. Plant phenotyping is a crucial process to improve genetic material due to drought tolerance and ttm and predicting yield. These findings will contribute to a better understanding of varietal differences in European soybean varieties.

Kurzfassung

Die Sojabohne ist die wichtigste Proteinpflanze für Nahrungs- und Futtermittel in Europa, aber die heimische Produktion ist wegen nicht angepasster Sorten niedrig. Besonders Trockenstress während der Vegetationszeit kann zu hohem Ertragsausfall führen. Diese Masterarbeit beschäftigt sich mit der Phänotypisierung von europäischen Sojabohnen-Sorten der Reifegruppen (RG) 000 – I, die im Feldversuch in Tulln (Österreich) angebaut wurden. Phänotypische Merkmale wurden visuell ermittelt und mithilfe von Hyperspektroskopie und Thermographie untersucht. Sortenunterschiede wurden unter anderem in den Merkmalen Blütezeit, Reifezeit, Stomatadichte, Ertrag, 16 Hyperspektral-Indizes und Blatt-Temperatur überprüft. Darüber hinaus wurde die Thermographie-Methode an zwei Tageszeiten (12 und 15 Uhr) untersucht und der simplified Crop Water Stress Index (siCWSI) angewendet. Die Ergebnisse zeigten signifikante Unterschiede zwischen den RG für die Reifezeit. Während Wuchshöhe positiv mit Reifezeit korrelierte, gab es beim Ertrag ein Optimum bei RG 00. Die Stomatadichte von europäischen Sojabohnensorten (RG 00) wurde erstmals publiziert, welche signifikante Unterschiede im Bereich von 203.4 bis 322.2 Stomata/mm² zeigte. Sojabohnen der RG 000 korrelierten signifikant zwischen Ertrag und Chlorophyll Index, Red Edge Inflection Point, Wasserstress-Indizes WI-1, NWI-2 und NWI-4. Spät reifende Sojabohnen zeigten weniger Zusammenhang zwischen Hyperspektral-Indizes und Ertrag. Sojabohnensorten zeigten signifikant unterschiedliche Blatt-Temperatur um 15 Uhr an allen Tagen. Die Korrelation zwischen siCWSI und morphologischen Merkmalen war höher um 15 Uhr als um 12 Uhr. Phänotypisierung ist für die Pflanzenzüchtung eine sehr wichtige Aufgabe, um genetisches Material bezogen auf Trockentoleranz und Reifezeit verbessern zu können und den möglichen Ertrag vorherzusagen. Diese Erkenntnisse sollen für ein besseres Verständnis über Sorten-Unterschiede in europäischen Sojabohnensorten beitragen.

Table of contents

List of Figures

List of Tables

List of abbreviations

Abbreviation	Description
ABA	Abscisic acid
CEST	Central Europe Summer Time
CWSI	Crop water stress index
das	Day after sowing
CT	Canopy temperature
doy	Day of the year
IR	Infrared radiation
LSD5	Least significant difference at p-value of 5%
MG	Maturity group
NIR	Near infrared reflectance
r	Coefficient of correlation
RE	Red edge
SD	Stomatal density
siCWSI	Simplified crop water stress index
TIR	Thermal infrared imaging
T-reprod	reproductive time
ttf	Time to flowering
ttm	Time to maturity
UAV	Unmanned aerial vehicles

Parameter	Variable	Unit
dT_c	Air canopy temperature differential	℃
R	Precipitation sum	mm
rad_g	Global Radiation	W/m²
rH	Relative humidity	%
T_{wet}	Canopy temperature at fully transpiring leaves	℃
T_{dry}	Canopy temperature at non-transpiring leaves	℃
T_{max}	Maximum canopy temperature	℃
T_{min}	Minimum canopy temperature	℃
T_a	Air temperature	℃
T_c	Canopy temperature	℃
T_s	Soil temperature	℃
VPD	Vapor pressure deficit	kPa

1 Introduction

Soybean (*Glycine max* [L.] MERR.) belongs to the legume family and is able to live in symbiosis with nitrogen-fixing bacteria. Plant available nitrogen is used for plant development and production of protein-rich seeds. In comparison to other legume crops, soybean seeds have very high crude protein content about 40% and, additionally, high oil contents about 20% (Mannan et al., 2022).

These qualitative properties have made soybean the major protein and oil crop in the world, which provides a huge supply in global protein food and feed. According to FAOSTAT (2024), globally harvested area of soybean has reached about 137 million hectars with a seed production over 371 million tonnes in the year 2023. In sharp contrast, European Union (EU) soybean production 2023 was about 2.86 million tonnes in a harvested area of 0.985 million ha that results in less than 1% of global soybean seed (FAOSTAT, 2024).

Only EU imports of both soybeans (15 million tonnes) and soybean meal (21 million tonnes) in year 2023 maintain high demand for plant-based protein which is mainly used as feed source in livestock production (FAOSTAT, 2024). This large 'protein gap' in EU has led to strong dependency on soybean trade from Brazil, Argentinia and United States in the last decades (Boerema et al., 2016). The balance sheet for EU feed protein (Commission, 2024) displays that soybean meal determines about 17% of total feed protein use, but only 4% of soybean meal is from EU origin. European Union's 'farm to fork' strategy 2020 initiated governmental efforts boosting domestic production of soybean and other legumes in Europe (Commision, 2020).

However, in northern Europe soybean production is limited to both temperature and light requirements during summer season, while in southern part of Europe dry climate conditions restrict soybean yields due to water shortage (Rotundo et al., 2024). Basically, these climatic challenges are faced in breeding programs achieving high environmental tolerance and adaptations to abiotic stress factors.

1.1 Soybean maturity groups

Soybean is a short-day crop with relatively high temperature requirements, which is difficult to obtain satisfactory yield in temperate climate regions, especially in the northern part of European continent. Soybean is sensitive to photoperiod and temperature, that means flowering stage is induced by daylength. Therefore, soybean cultivation is limited to northern latitudes of Europe because of too long days in summer season (Staniak et al., 2023). Genetic variation in photoperiodic sensitivity affects flowering time associated with maturity date (Kumudini, 2010). Needs for better declaration of soybean growing regions, resulted in a classification system with uniform maturity groups (MGs), mainly based on latitudes (Miladinović and Djordjević, 2011).

Figure 1 displays five zones of soybean MGs in Europe: varieties in MG I are basic varieties with a vegetation period of 120 to 135 days, while varieties in MG II are relatively late (135-145 days). Earlier soybean varieties belong to MG 0 (110-120 days, early), MG 00 (mid-early) or MG 000 (very early). In

case of climatic stress conditions and interactions between variety and environment, soybean vegetation period can be changed (Miladinović and Djordjević, 2011).

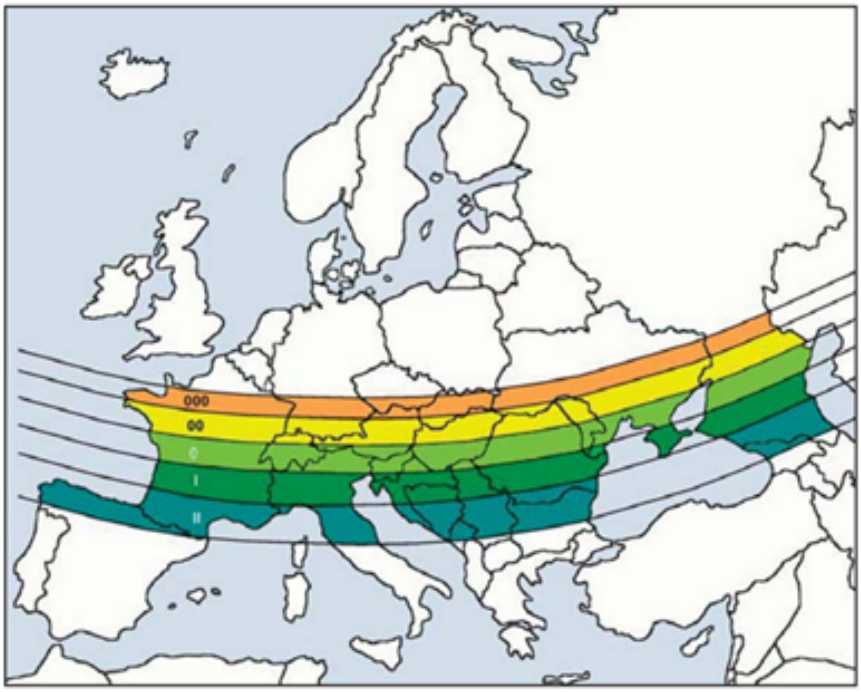

Figure 1: Soybean maturity groups in Europe range from very early (MG 000) to late (MG II) varieties; published by (Miladinović and Djordjević, 2011).

1.2 Abiotic stress in soybean

Soybean is characterized as a more stress tolerant species than other legume crops, nevertheless, different abiotic stresses will damage soybean's development and grain yield (Mannan et al., 2022). Main environmental stress factors during soybean's life-cycle are light requirements due to daylength, high and low temperatures, and both water shortage and water excess as well.

Adverse weather conditions strongly modify light, temperature and water on a high amplitude which result in reduced yield by approximately 30% compared to optimum (Staniak et al., 2023). Soybean has its optimal growing temperature (T_{opt}) at a level of 30 °C (Hesketh et al., 1973) in vegetative phase and 23-26 °C in reproductive phase (Hatfield et al., 2011), while T_{opt} decreases from anthesis (26 °C) to post-anthesis period (23 °C) (Luo, 2011).

Low temperatures induce **cold stress** to plants and have the highest negative effects to soybean growth and yield during germination stage and flowering stage, respectively. Chilling temperatures of 12/6 °C (day/night) after sowing will prolong germination and will delay emergence (Staniak et al., 2021b); additional high soil moisture can cause seed rotting which results in inhomogeneous field emergence and low plant density (Yamaguchi et al., 2014).

At flowering stage, chilling conditions at a temperature level of 17/13 °C (day/night) adversely affect plant height, number of nodes, stem dry mass, number and weight of pods, number and weight of seeds,

and consequently, seed yield (Staniak et al., 2021a). Cold stress to soybean primarily occurs in regions of high latitudes (e.g. Poland, Canada and Japan) and also in higher altitudes at low-mountain range, for example in parts of Switzerland.

On the other side of temperature range are hot weather conditions which induce **heat stress** to soybean. Both high air temperatures and solar radiation can cause heat stress in plants which is associated to drought stress. It's difficult to distinguish the effects of heat stress from drought stress in soybean. Both stresses usually occur together and multiply the effects to soybean (Poudel et al., 2024; Ergo et al., 2018). Air temperatures above 35℃ will evaporate the same amount of water that soybean plants allow to transport from roots to leaves in their vessels. In this case, heat leads to very similar water-deficit stress compared to drought (Ye et al., 2018).

As long as there is a sufficient level of moisture available in soil, temperatures above 32℃ in reproductive phase (Poudel et al., 2023a) are determined as heat stress conditions for soybean cultivars. Each degree above optimal growing temperature will reduce seed weight by approximately 7% combined with drought conditions (Poudel et al., 2024).

Drought stress appears in plants, when evaporative requirements can not be fulfilled or are restricted to a non-sufficient level. The evaportative demand of soybean varies over the period of soybean development and is mainly determined by climate region. Soybean genotypes, that are growing in temperate regions, use about 450–700 mm of water during the growing season, if day temperatures will reach around 30℃ (Dogan et al., 2007). In cooler climatic regions (e.g. Poland), soybean's potential evaporative demand is determined to 350-400 mm within life-cycle (Rolbiecki et al., 2023).

The effects of drought stress to plants, drought resistance mechanisms in soybeans and its consequences to plant breeding for more drought-tolerant varieties are described in the following sections.

1.3 Climate change and drought stress

The continuous increase of carbon dioxide (CO_2) concentration in the atmosphere from 317 ppm in year 1960 to more than 425 ppm in year 2024 (www.gml.noaa.gov, seen: 30.01.2025) will highly influence climatic conditions and, in consequence, stimulate global warming. Higher temperatures and climatic fluctuations lead to extreme weather conditions like heat and drought events or other abiotic factors, which strongly affect to plants.

Especially drought stress, defined as lack of moisture, is considered as the most severe abiotic stress to plants. The severity of drought depends on many variables such as occurence and distribution of precipitation, amount of evaporation and water storing capability in soils (Farooq et al., 2009).

In a situation of drought stress, soybean and, in general, all plant species are influenced in traits based on morphological, physiological and molecular level and, consequently, their mutual implications.

1.3.1 Morphological changes under drought stress

Crop growth

Growth is based on mitosis which consists of cell division, cell enlargement and differentiation with their

complex interactions. Low water availability causes a decrease of turgor pressure in plant cells. Low cell turgor disrupts mitosis and reduces following physiological processes for plant growth. Therefore, cell development is estimated as one of the most drought-sensitive traits (Taiz et al., 2010). The occurrence of drought is accompanied by water shortage and affects the quantitative and qualitative plant growth, and finally, yield of harvested biomass (Khatun et al., 2021). In general, plant growth decreases under drought stress, while root to shoot ratio increases. This means, roots are promoted to grow deeper and more extensive in soil layers with still enough moisture content (Farooq et al., 2009).

Drought-induced crop growth in the vegetative phase is exposed to several morphological traits: decreased internode length, number of nodes, plant height, height of first pod set and smaller leaves as well. Internodes that started to grow under stress conditions were shorter resulting in lower plants (Staniak et al., 2023).

Yield

Plant development and yield reduction is mainly dependent on the phenological stage, when drought stress is occurred. Following abbreviations of development stages in soybean were classified according to Fehr et al. (1971). Early phases of water deficit during germination and emergence (VE) stage can lower germination potential Helms et al. (1997). Although, water stress within vegetative phase (V3 and later vegetative stages) shows no negative effect to grain yield. In contrast, most drought-vulnerable development phase is the period of flowering and the following reproductive stages, which have greatest water requirements in soybean's life-cycle (Khatun et al., 2021).

If drought is occurring during bloom in soybean (R2), flowers wilt and are aborted. The flowering period itself is shortened and flowers are not well developed due to dry conditions. On the other hand, flowering time of 3-4 weeks can compensate yield loss for short-term drought events. Water deficit at pod setting (R3) and seed-filling (R5) stages is highly sensitive for plant reproduction, because during this period number of seeds per pod and the seed weight is determined (Staniak et al., 2023). In soybean, drought events during the reproductive stage causes yield reduction of 40% or even more (Samarah et al., 2006).

In figure 2, the effect of drought stress on grain yield in rice is displayed which was applied at different growth stages. The highest yield loss is observed, when drought was induced at flowering stage. Smaller drought effects to yield were observable either at vegetative growth stage and in late grain filling phase. For soybean, yield loss caused by drought stress events might show a similar pattern than in rice.

1.3.2 Physiological changes under drought stress

Water relation traits

Relative water content, leaf water potential, stomatal conductance, rate of transpiration, leaf and canopy temperature are important properties which define plant's water status. Low humidity and high temperatures are mainly prevalent in arid and semi-arid environments and cause an increase of transpiration

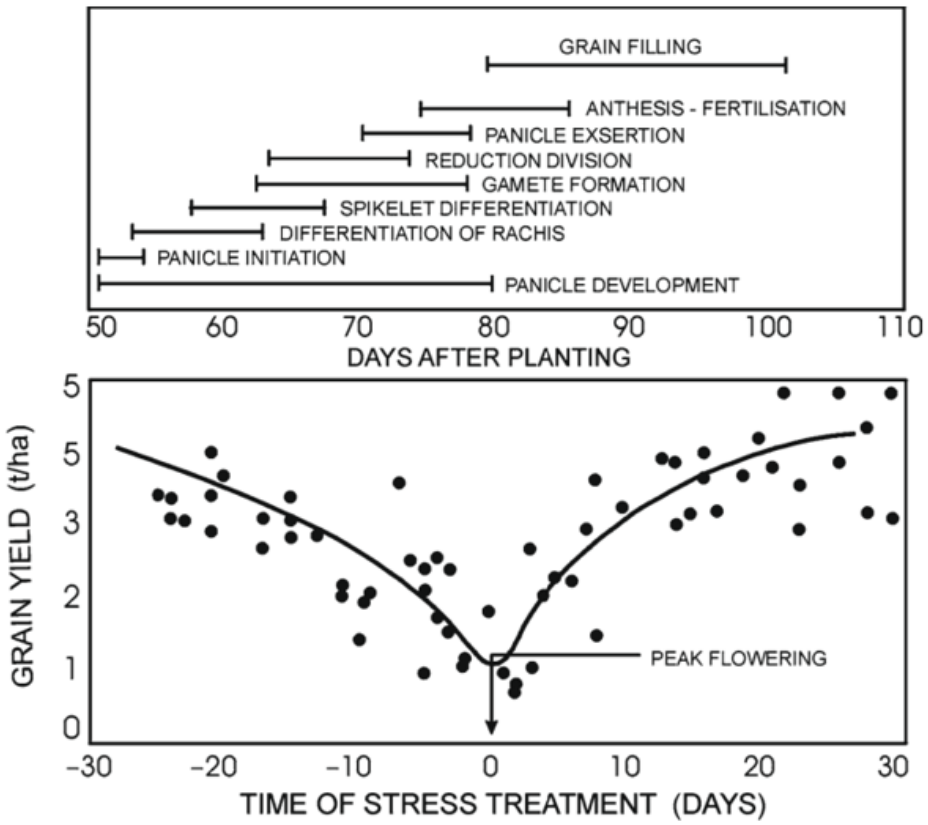

Figure 2: The effect of drought stress on grain yield at different growth stages in rice; upper panel shows several phases of development, lower panel shows the grain yield according to the time of stress treatment; published by Blum (2011).

rate in plants and a raised evaporative demand in the atmosphere. High transpiration rate enables cooler microclimate surrounding leaves and, in larger scale, surrounding plant canopy.

Transpiration and evaporative demand are mainly driven by vapor pressure deficit (VPD) (Grossiord et al., 2020), a meteorological parameter based on air temperature and relative air humidity. In common, high VPD results in high transpiration rate, but in case of simultaneously high soil water content, plants are not or slightly drought-stressed.

If plants are drought-stressed due to high VPD and low amount of plant-available water in soil, leaf water potential decreases and also relative water content is reduced in leaves compared to well-watered group (Hossain et al., 2014).

Breaking down to cell level, low RWC means low osmotic potential and following turgor loss. Accumulation of osmotic active molecules in the liquid phase will prevent overhasty cell death. Phenotyping for low water potential is often expressed in transient canopy wilting on water-stressed days (Ye et al., 2018). Another phenomenon related to drought stress is leaf senescence, which mainly occurs during reproductive stages (Brevedan and Egli, 2003). A contrary mechanism under drought stress is called 'stay green', which is mainly a non-functional behaviour in plants caused by transient drought stress

during flowering stage. Stay green is maintenance of chlorophyll in leaves as a compensation from degraded reproductive organs (Farooq et al., 2017).

Infinite water loss is prevented by closure of stomata. In dry environments where VPD is greater than 2.0 kPa, transpiration is limited by stomatal closure in photosynthetic active tissues, especially in leaves (Fletcher et al., 2007). High stomatal resistance reduces the cooling effect of transpiration, in the following canopy and leaf temperature increases. Canopy temperature and stomatal conductance were negatively correlated (Gates, 1968).

In drought trial with soybean, stomatal conductance was reduced by 95% under drought, while canopy temperature was measured by +2℃ above control (Poudel et al., 2023b). In contrast, combination of drought and heat stress show reduced stomatal conductance (93%) and increased canopy temperature of +8℃ compared to a reference with ideal growing conditions (Poudel et al., 2024).

Nutrient relations and nitrogen fixation

Low moisture in soil affects plants negatively in their acquisition of nutrients by roots. Nutrient transport from roots to shoots is dependent on transpiration flow. Drought stress will decline transpiration rate due to stomatal closure, and lead to impaired nutrient uptake, transport and unloading mechanisms (Fahad et al., 2017). Less concentration levels of nitrogen and phosphorous in plant biomass are linked to decreased concentration or activity of nutrient-uptake proteins for nitrogen and phosphorus after induced drought event (Bista et al., 2018).

In legume family, nitrogen fixation with symbiotic soil-living bacteria (e.g. *Rhizobia* spp.) is impaired in water-deficit environments. In consequence, dry phases during plant growth results in decreased infection and nodulation of roots, lower nodule size and a loss of lenticels in soybean nodules (Farooq et al., 2017). Contrary results was shown by another study, that measured a higher nodule size for moderate drought stress at vegetative stages (Lumactud et al., 2023).

The ability of symbiotic N_2 fixation in nodules is dependent on nitrogenase activity, which is regulated by oxygen level and, indirectly, by carbohydrate supply. Water shortage in nodules causes both reduced supply of carbohydrates and O_2 limitation in infected cells, followed by a decrease of nitrogenase activity. Furthermore, less nitrogen is available for protein biosynthesis, which is crucial for legumes, leading to reduction in grain yield (Serraj et al., 1999; Staniak et al., 2023).

Photosynthesis, respiration and oxidative damage

Major effect of drought is the reduction in photosynthesis and following decline of carbohydrate fixation. Photosynthetic activity is affected by either stomatal or non-stomatal limitations. In dry environments, stomatal closure prevents water loss and, simultaneously, restricts CO_2 availability for carboxylation in Calvin cycle in chloroplasts. Non-stomatal effects to photosynthesis are changes in photosynthetic pigments and components, which mitigate the damaged photosynthetic apparatus and diminished activities of Calvin cycle enzymes (Farooq et al., 2009).

Respiration is a metabolic process which uses photosynthetic fixed carbohydrates for growth and maintenance of plant tissues. In soybean, the fraction of daily accumulated photosynthates which were

allocated to roots was about 38%. Furthermore, about 40% of this fraction is used for root respiration including symbiotic *Rhizobium* (Harris et al., 1985). Water-deficit in soil leads to both higher respiration rates in roots and reduced photosynthetic capacity in green plant parts, which may result in a negative carbon balance.

Another physiological phenomenon in stressed plants is an increased generation of reactive oxygen species (ROS), mainly produced in chloroplasts, mitochondria and peroxisoms (Apel and Hirt, 2004). ROS are oxygen radicals which react with proteins, lipids and even with deoxyribonucleic acid (DNA), and cause oxidative damage in plant cells. Production of ROS is linear with severity of drought stress, which results in increased peroxidation of membrane lipids and degradation of nucleic acids, and higher damage of structural and functional proteins (Farooq et al., 2009).

In summary, water shortage induces drought stress and has several effects to plant's physiology and growth. Nevertheless, a wide range of adaptations has evolved in plant species to withstand drought events.

1.4 Drought resistance mechanisms in plants

Plants response to drought stress with several adaptations in morphology, physiology and biochemistry against dehydration and water deficit. The level of dehydration depends on stress intensity and duration as well as on adaptive traits to prevent water loss in plants. The term 'drought resistance' is defined as the ability to survive under drought stress due to defense responses in plants (Bandurska, 2022).

Plants use various drought resistance mechanisms which can be classified into three groups: drought escape, dehydration avoidance and dehydration tolerance. Figure 3 shows an overview of traits related to drought resistance in soybean.

Drought escape

One component of drought resistance is drought escape, where plants will complete their life cycle before dry periods may occur. Annual crops have commonly shortened their vegetative and reproductive phase instead of complete failure in arid and semi-arid regions (Bandurska, 2022). In soybean, early maturing cultivars have an advantage to match plant development with periods of sufficient soil moisture level compared to genotypes with later maturity time (Manavalan et al., 2009).

From an agronomic perspective, drought escape is an important resistance mechanism for plant users, such as farmers and plant breeders, in limited water environments (Blum, 2011). In these areas, grain production may be rather possible with early maturing cultivars, however, yield is linked to the length of crop duration under suitable weather conditions. This means for drought escape, any decrease of plant's lifetime will limit crop yield (Turner et al., 2001).

Dehydration avoidance

Dehydration avoidance combines strategies which aim to maintain high water status in plants and post-

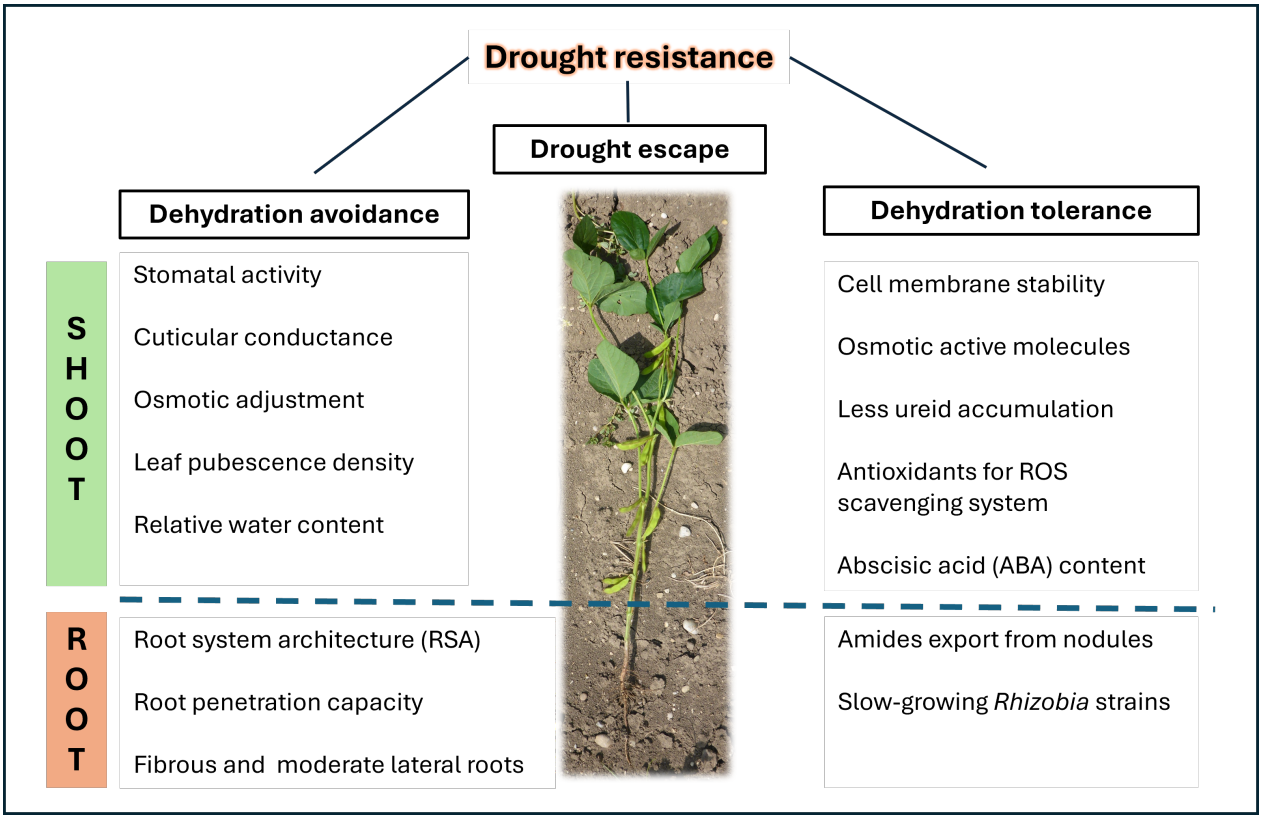

Figure 3: Traits for drought resistance in soybean, grouped for dehydration avoidance, drought escape and dehydration tolerance; adapted from Manavalan et al. (2009).

pone dehydration as long as possible under conditions of soil or atmospheric water stress (Blum, 2011). In general, dehydration avoidance can be split into root-related and shoot-related traits in soybean.

Roots are the key plant organ for adaptation to drought. **Root-related traits** focus on enhanced water uptake capacity even in drought-prone environments and are summarized in the term root system architecture. Root architectural traits consist of root surface area, length, and lateral root number, as well as depth penetration capacity and fibrous lateral roots (Joshi et al., 2022). In soybean, one of the major factors for rooting depth is taproot elongation rate in vegetative phase. Induced water stress during early reproductive growth stages (R1-R2) affects large increase in root growth, while drought stress at R4 stage show less additional root growth (Manavalan et al., 2009).

Shoot-related traits belong to all plant responses in green tissue and especially in leaves. These traits are responsible to store water, maintain leaf water potential under drought stress, prevent high water loss and, therefore, improve water use efficiency in plant. One initial response due to adverse environmental conditions is active closure of stomata, which occurs even at low stress level. Stomatal closure, induced by turgor loss in guard cells, regulates transpiration rate due to high water potential in leaves. Morpho-physiological adjustments in stomata and leaves can contribute to a water-saving strategy: mild water stress resulted in higher stomatal density, especially on abaxial leaf surface (Toum et al., 2022). Sinclair et al. (2010) showed in a study that water conservation strategies lead to higher grain yields in soybean, mainly caused by early decrease in stomatal conductance according to soil

drying and by limiting the maximum transpiration rate. Furthermore, there is a non-stomatal transpiration pathway, which might be recognized: cuticular conductance describes the permeability of water vapor through outer leaf layer, when stomata are tightly closed. In comparison to stomata, cuticular conductance is non-variable in a short timescale. If cuticle is conductive, effective transpiration control through stomata is limited. Low cuticular conductance was found for plants which produce a wax layer on cuticle. (Blum, 2011).

Another morphological adaptations to stress, including drought, can be distinguished at leaf level in soybean. Commonly, leaf pubescence is existant in xerophytic plants, but also in crop plants like soybean. Leaf hairs will increase albedo value of plant canopy. Leaves with high pubescence density allow a higher reflectance and less transmittance of incident radiation than glabrous leaves (Blum, 2011). Furthermore, effects of pubescence color and orientation on spectral reflectance. Tawny pubescence reflected more light in near-infrared spectrum than grey colored trichomes. Leaves with curly trichomes reflected more radation than leaves with erected or appressed leaf hairs (Doughty et al., 2011). In literature, pubescence density is highlighted as a crucial adaptive trait in soybean for drought-stressed environments. More dense hairy leaves positively influence vegetative vigor, root density and extension, while leaf temperature is cooler and photosynthesis is enhanced (Manavalan et al., 2009).

Summarizing, high plant water status in dry environments is caused by several mechanisms like stomatal closure and osmotic adjustment. These drought-related responses avoid fast dehydration in soybean leaves and is expressed in the phenomenon of canopy wilting. Drought-adapted genotypes show slow or delayed canopy wilting during daytime (Ye et al., 2018; Fletcher et al., 2007).

Dehydration tolerance

For severe and long-term drought periods, plants cannot avoid dehydration any longer by mechanisms mentioned above. In this case, plants use another component of drought resistance: dehydration tolerance. Dehydration tolerance describes the ability to survive and continue metabolism even at low water status in plant cells. Some relevant traits in dehydration tolerance are cell membrane stability, biosynthesis of antioxidants for ROS scavenging and osmoprotectants for osmotic adjustment in cells.

Drought-tolerant soybeans maintain higher proline and other osmotica as well as higher chlorophyll content and water status in their leaves. Cell membrane stability and lethal water or osmotic potential will be physiological factors for dehydration tolerance in theory. However, both concepts can not be applied in breeding programs to determine genotypes with improved drought resistance (Turner et al., 2001).

Prevalence of osmotic active molecules (or osmoprotectants) in cells with low water potential keep the functions of cellular processes because of their ability of osmotic adjustment. Osmoprotectants are low-molecular-weight molecules, such as proline, glycinebetaine and γ-aminobutyric acid, that are usually non toxic even at high cytosolic concentrations. For severely dry conditions, accumulation and additional biosynthesis of osmoprotectants leads to cell survival, although leaf water potential is low (Turner et al., 2001). Drought tolerance and reproductive success of a plant is also associated with the ability to store reserves in vegetative organs, especially in leaves and stem for later remobilization for

grain development. The potential for storing reserves depends on leaf size and stem length, respectively (Farooq et al., 2017).

Increased oxidative damage under stress conditions is restricted by enhanced activity of antioxidants, including enzymes such as peroxide dismutase and peroxidase, and non-enzymatic metabolites like β-carotenes and ascorbic acid. Antioxidants protect chloroplast's damage against reactive oxidative species and maintain photosynthetic activity under stress factors (Farooq et al., 2009).

Symbiotic nitrogen fixation is another root-related trait negatively affected by drought stress. In comparison to host plants, symbiotic bacteria are quite resistant to low soil moisture (Serraj et al., 1999). Another research showed that more drought-tolerant legume species mainly export amides (principally glutamin and asparagine, such as in chickpea, faba bean and alfalfa) in the nodule xylem, while more drought sensitive species export big amounts of ureides (allantoin and allantoic acid, e.g. soybean and cowpea) to xylem (Sinclair and Serraj, 1995). Therefore, low ureide concentration in plant tissues will indicate drought tolerance in N_2 fixation, also found within soybean varieties (Blum, 2011).

Stomatal closure in pro-longed stress periods is fixed by abscisic acid (ABA), a growth inhibitor, which is called as a stress hormone. ABA is mainly produced under stress in roots and is transported to leaves via xylem. In leaf cells, ABA is responsible to inhibit stomatal aperture by lowering pH in guard cells followed by turgor loss (Khatun et al., 2021).

In summary, the wide range of morphological, physiological and biochemical traits can be used to improve yield and yield stability of crops in drought-prone environments which is a contribution to drought resistance (Turner et al., 2001). According to Blum (2011), following potential drought resistance mechanisms are listed regarding to the reproductive process and yield:

1. Drought escape is a mechanism with agronomic relevance to circumvent drought-prone phases.
2. Plant dehydration avoidance to conserve reproductive organ water status. This mechanism has most effectiveness to prevent failure of the reproductive process in plants.
3. Dehydration tolerance keeps the carbohydrate status of the plant on a sufficient level.
4. Low status of abscisic acid (ABA) or low sensitivity for ABA in plant.

1.5 Managing drought stress

1.5.1 Farming adaptations

Drought resistance can be induced by agronomic features in agriculture. A practical solution of drought escape is to use early planting time. Furthermore, farmer's choice for soybean cultivars of earlier maturity groups will shift the drought-sensitive flowering and pod filling stages into early summer months with low risk for drought stress (Ye et al., 2018). High plant density and low row spacing will affect water use efficiency negatively for soybean, that's why lower plant densities on field improve soybean's growth and yield components in dry environments (Nadeem et al., 2019).

Drought stress can be alleviated for plants with amendments of plant growth regulators. Foliar application of hormones improve drought stress, such as gibberrelic acid brassinolide and ABA.The exogenous use of osmoprotectants e.g. proline and glycinebetaine, will support drought tolerance in plants and maintenance of leaf water status (Farooq et al., 2009). Application of plant growth promoting rhizobacteria enhances growth of plants under stress producing growth regulators and improving water and nutrient uptake in plants (Ullah and Farooq, 2022).

1.5.2 Physiological breeding for drought resistance

Plants under drought stress show another behaviour than in well watered conditions. Some characteristics have evolved as useful in breeding programs due to the ability to easy and fast screening during crop development. Soybean germplasms with lower canopy temperature, higher chlorophyll content and higher specific leaf weight show high stress tolerance to water deficit (Jumrani and Bhatia, 2019). The phenomenon of slow-wilting genotypes is also linked to better dehydration avoidance than fast-wilting soybean lines (Sinclair et al., 2010).

Plant breeding for drought resistance is a highly relevant, but complex undertaking and has only success, if some issues are recognized. In field trials, drought stress is not imposed equally from year to year. Drought events differ in duration, intensity and occurrence according to growth stage from one growing season to another.

Avoiding these weather uncertainties, Blum (2011) suggested to establish a managed stress environment due to site homogeneity, controlled water regime as pot experiments in greenhouses or field trials under rainout shelters. Additionally, a reference trial under well-watered conditions allows to determine drought tolerant genotypes according to yield or other quantitative traits.

However, in plant breeding programs thousands of breeding lines are grown on field and may be evaluated to traits which are related to drought resistance. Managed stress environments in such an extent are not applicable in many breeding programs and companies for mass selection to drought resistant cultivars (Reynolds, 2012).

Focusing on field trials under rain-fed conditions, these experiments are exposed to variable and unpredictable drought events, nevertheless, relative drought stress can be observed between genotypes. Evaluating relative drought stress means to look for phenotypic differences between genotypes for a certain timepoint or date. These phenotypic differences in one selection trait may change in a changed environment from one timepoint to another. This implicates that several breeding traits for drought resistance depend on plant physiology and, in consequence, on plant's response to environmental framework at a certain observation moment.

Therefore, physiology plays a crucial role in breeding programs focused on plant's behaviour to environmental stress. New research insights in plant physiology can be applied in plant breeding for early generation selection using high-throughput screening techniques (Reynolds, 2012).

Jackson et al. (1996) summarized three aspects how physiologists can support the breeder:

(i) identification of suitable environments in which to conduct selection trials,

(ii) identification of selection criteria for focused introgression programs and

(iii) identification of traits as indirect selection criteria in core breeding programs.

Physiological breeding aims to improve use-efficiency of essential resources like irradiance, water and nutrients. Regarding to drought adaptation, water use efficiency (WUE) is one important factor determining grain yield and biomass. However, WUE is too abstract for practical use and can only indirectly be measured by other traits, which can be observed in the field during drought stress. Furthermore, Nadeem et al. (2019) stated, that various other physiological traits have been used to screen for DS tolerance, including smaller leaf area, leaf area maintenance, root and shoot biomass, osmotic adjustment, pod number per plant, and 100-grain weight.

From beginnings to present, plant selection and breeding strategies were and are based on phenotyping in the field. Development of new technical screening devices has enlarged the possibilities measuring physiological traits. Among of them, two selection criteria for stress evaluation are canopy temperature and spectral reflectance. The technical approaches for these traits are thermal infrared cameras and hyperspectral cameras which extends the range of breeders vision into infrared range of electromagnetic spectrum.

Nevertheless, accumulated knowledge about drought-resistance is quite limited so far because the genetic background is often poorly understood. There's a need to reveal the genetic bases of any drought-associated trait (Nadeem et al., 2019). In the last decades, the emergence of molecular screening methods and computational capacity has enabled to assess the genotypic value of plants. Genotyping methods, e.g. quantitative trait locus (QTL) mapping and genome wide association study (GWAS), are responsible for increased progress in plant breeding programmes. Genotyping is a fast and currently cost-effective technique to achieve the breeding aim and improve genetic material in crop plants (Abou-Elwafa and Shehzad, 2021; Matei et al., 2018).

However, crop breeding for enhanced stress tolerance in plants is quite more complex. Beside plant genotype, plant performance under drought stress is dependent on environmental factors, severity and duration of drought and also physiological processes. The complexity of drought stress to plant's life cycle in performance and reproductivity is shown in its inheritance pattern, high genotype-environment interactions and low-heritability (Abou-Elwafa and Shehzad, 2021). Therefore, phenotyping methods are still more important in plant breeding for stress tolerance.

1.6 Phenotyping methods

In plant breeding, phenotyping is a traditional approach to select individual plants due to their more favorable characteristics in a certain trait. Plant's phenotype is the optical detectable appearance of a species, which is clearly affected by genetic variation within a population. Additionally, environmental factors have strong influence to the phenotype. In general, phenotype (P) is the combination of geno-

type (G) and environment (E) and genotype-environment (GxE) interaction (see equation 1). The term 'environment' is used for both spatial and temporal difference between two observations to the same genotype (Becker, 2011).

$$P = G + E + GxE \tag{1}$$

The choice of a phenotyping method is accounted to its practical application in the field and its potential meaningfulness in data evaluation. Phenotyping has the claim to observe a certain trait with an appropriate method which is (i) simple to use, (ii) relatively fast, (iii) precise, (iv) low-cost and (iv) objective (Blum, 2011; Abebe et al., 2023). In reality, all methods will be limited to at least one of these properties. The combination of several methods can alleviate the weakness of some phenotyping approaches.

Approaches in phenotyping can be grouped in classical and image-based methods. Classical methods include visual scoring, direct measurements and destructive harvest and are limited to the visible light spectrum. Image-based phenotyping methods use non-destructive technologies to study plant traits in a certain bandwidth of the electromagnetic spectrum (Al-Tamimi et al., 2022). In the following sections some phenotyping methods described with their advantages and problems.

1.6.1 Classical phenotyping

Classical field phenotyping is the traditional approach to determine plant traits and select according to these findings. This approach combines primarily low-input methods and observe eye-visual plant characteristics.

Visual scoring

Visual scoring is a direct and non-destructive process to differentiate and rank plants only on visible signs. The observed trait is graded on a scale according to its markedness. Commonly, a numbered scale from 1 to 9 is applied, where as 1 is determined for a low, 9 for a high performance in one trait. For some traits, alternative scoring scales, e.g. numbers from 1 to 5, can be appropriate. Scoring is widely applied to morphological, phenological and agronomic plant characteristics.

Scored morphological traits are often strongly associated with genotype such as flower colour, pubescence colour, pubescence density or leaf shape. These traits are usually scored once during the vegetation period.

Phenological plant characteristics can be observed to a certain timepoint or a short period of plant's life cycle and can be expressed as emerging status or development score during vegetative stages. In contrast to other scoring traits, phenological stages, like flowering time (ttf) and time to mature (ttm), are often determined to the day of the year (doy) or day after sowing (das) for a better temporal classification.

Agronomic traits were also visually estimated on a scale, including characteristics such as lodging, pod shattering and pod set. Moreover, occurrence and degree of severity of diseases and pests to plant trials can be scored to determine tolerant germplasms on the field.

Visual scoring in the field is a simple approach and points to a low-costing method without additional devices, but tends to be subjective. Personal bias can be reduced by manuals with clearly defined signs and shared scoring assessments in the field.

Non-destructive measurements

For more objective phenotyping, plant traits can be measured directly with simple and mobile devices. Non-destructive measurements can be done by measuring stick to determine plant height, for instance. Another measurement device is SPAD meter to determine relative chlorophyll content as a dimensionless SPAD value (Uddling et al., 2007).

Destructive measurements

Some phenotyping methods are destructive because plant organs or the whole plant are removed from the field. Common choice for destructive measurements are leaf samples because these plant parts can easily be modified and measured to certain traits, unless the whole plant is alive. A destructive leaf trait, which is related to drought stress, is leaf water content, for instance. Harvested grain yield or biomass are other destructive harvest traits.

Phenotyping of harvested plant material is independent to environmental conditions. Some traits need specialized and non-mobile measurement devices for evaluation, that makes sampling necessary. Destructively measured traits generate results which are more likely precise than scored traits. Although, the destructive harvest approach is time-consuming and labour-intensive (Al-Tamimi et al., 2022).

1.6.2 Image-based phenotyping

High-throughput phenotyping

In contrast to high-throughput genotyping, phenotyping was mainly based on classical methods which were labor-intensive, time-consuming, and partly with low accuracy due to individual bias issues, for instance different experience levels or shortage of time. In recent two decades, image-based techniques were introduced to plant breeding and have obtained an important position as non-destructive and objective phenotyping tools. These technologies enlarge the screening possibilities to the complete spectral range of electromagnetic wavelength. With image-based phenotyping either morphological and physiological traits can be observed. Moreover, imaging techniques enable to detect biochemical content and composition of molecular ingredients in plants, and also abiotic and biotic plant stress (Abebe et al., 2023).

The data of imaging-based techniques are used to detect indirect traits which have a high correlation to another trait of interest. In case of field phenotyping, image-based results are strongly influenced by the environmental conditions. Standardizing the data leads to the calculation of indices. This is an appropriate way to find patterns or similarities within spatially and temporally different measurements. Image-based sensors include a number of techniques across the electromagnetic spectrum: magnetic resonance imaging (MRI), thermal infrared imaging (TIR) light detection and ranging (LiDAR), visible

imaging (VIS), hyperspectral imaging, fluorescence imaging (FLU), X-ray computed tomography (CT) and positron emission tomography (PET) are used for different purposes (Al-Tamimi et al., 2022). Spectra of imaging sensors, which are widely used for high-throughput phenotyping, are shown in figure 4.

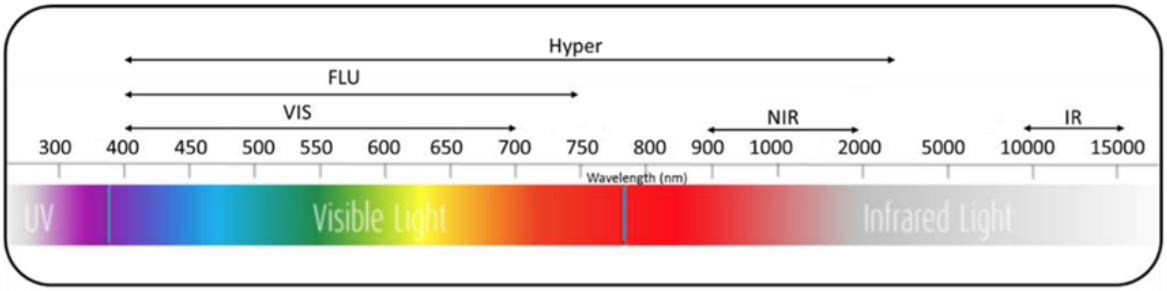

Figure 4: Electromagnetic spectrum and applied spectral phenotyping techniques in different ranges of wavebands; published by Biswas et al. (2020).

Image-based phenotyping of plants under drought stress was applied for a range of sensor techniques: RGB sensors in visible range (400-700 nm); NIR sensors in near-infrared spectrum (700-1440 nm); infrared thermal sensors (7-15 µm); hyperspectral sensors combining a spectrum in visible, NIR and short-wave infrared (SWIR) bandwidth (400-2500 nm); fluorescence sensors in detection of blue, green, red and NIR wavelengths (Kim et al., 2021).

All these sensor types are able to operate on several measurement platforms. Handheld solutions are compact and light-weight and enable the operator to be flexible in the field. There is a good spatial resolution, but it takes time to measure all plots on the field. Therefore, handheld measurements are likely to be exposed to changing environmental conditions. Additionally, manual use can bring problems to objectivity by individual bias.

Another sensor platform is also ground-based, but mounted on vehicles. These vehicles can move over the field and screen plots separately in a consistant manner. This platform leads to more objective results than hand-held devices, but has the same disadvantage with temporal changes in the environment.

In contrast to before mentioned platforms, remote phenotyping techniques are on a high-throughput level of data collection. Airborne phenotyping platforms can screen large areas in a short period of time and includes techniques such as unmanned aerial vehicles (UAV) (Bian et al., 2019), helicopters (Deery et al., 2016) and spider cams (Bai et al., 2019).

Plant phenotyping with UAV increases the phenotypic scale and the temporal frequencies of observations. Remote sensing with UAV is a low-cost variant compared to helicopters and spider cams. Although, remote sensing has variance in the spatial resolution which alters on altitude and speed of the airborne system (Kim et al., 2021).

In this work, only handheld solutions were used for imaged-based phenotyping. Focusing on two sensor techniques which are widely used for evaluating drought stress: thermal imaging and hyperspectral reflectance will be described closer in the following sections.

1.6.3 Thermal imaging

Thermal imaging (TIR, also known as 'infrared thermography') is an integrative phenotyping method to evaluate leaf temperature on plants. In a larger scale, whole plots are observed to get information about the canopy temperature (CT). Thermal imaging methods are used either as hand-held devices and as airborne thermal imaging platforms for direct and easy measurements without interfering with the crop (Pask, 2012).

The thermal sensor transform infrared radiation in the range of 3-5 µm or 7-14 µm emitted from the observed object into visible images. Thermal cameras allow to visualize plant temperature in black and white or colored graphics where each pixel is a temperature value of the target area, e.g. a field plot (Abebe et al., 2023).

Focusing on the technical issues, the reliability of CT measurements is dependent on the resolution and sensitivity of the sensor. There are two types of devices: cryogenic and non-cryogenic instruments. Cryogenic instruments are able to cool the sensor and improve image resolution during data collection in the field. However, this type of instrument is more expensive. Cheaper solutions are non-cryogenic devices, which produce images of lower quality (Blum, 2011).

In the beginning of thermal sensing, plant breeders used simple infrared thermometers which allow to do point-measurements in plots. These low-cost and light-weight instruments were widely used as hand-held devices to get insights how plant temperature can be applied in plant breeding programs for stress tolerance (Blum et al., 1982). In the last two decades, plant breeders mainly use the emerged thermal imaging technique to apply for high-throughput phenotyping. TIR enhances data availability for canopy temperature and can be scaled to multi-plot measurements in large-scale breeding designs to save time and labour. (Deery et al., 2016).

TIR is able to detect differences in CT caused by changes in plant's water flow due to stomatal closure. Canopy temperature is related to physiological traits like transpiration rate, stomatal conductance and leaf water content (Leinonen and Jones, 2004). In comparison to these physiological traits mentioned above, CT measurement is a quick method to evaluate thermal differences between genotypes.

Beside the advantages, there are some challenges for the use of TIR in field experiments. Infrared thermography is highly influenced by environmental factors. Therefore, some limitations have to be considered. Reliable measurement conditions for TIR are provided on days with clear sky and little or no wind. Further, the plant surfaces has to be dry and not wet from dew or rain. Days with low relative humidity (rH <60%) and warm air temperature (T_a > 15 ℃) are suggested for CT measurements (Pask, 2012). Furthermore, the time of the day is relevant to get comparable measurement data. For low water stress treatments take measurements from 11:00h to 14:00h, when the plant is most water stressed. For severe stress treatments take measurements in the late morning, from two hours before solar noon to solar noon to detect drought adapted genotypes (under water scarcity, drought adapted genotypes have the ability to recover plant water status during night allowing higher level of transpiration and photosynthetic activity during the morning than non-adapted genotypes)(). Another important issue for thermal plant phenotyping is the developmental stage. The begin of CT measurements is possible, when

the canopy sufficiently covers the ground to avoid sensing temperature of soil. Soil is commonly much warmer than the surrounding plants. The best time to examine canopy temperature is the reproductive stages after anthesis (V3-V5 in soybean). The measurements have to be stopped in the advent of senescence, when first yellowing leaves occur (Pask, 2012).

After raw data collection, canopy temperature is linked to ambient weather conditions during the the measurement period. The biggest effect to CT is the ambient air temperature (T_a). For a better understanding of plant's temperature response to environment, some thermal-based indices were established including reference measurements and meteorological data, respectively. Selection of thermal-based indices were described in chapter 1.7.1.

1.6.4 Hyperspectral imaging and reflectance

Hyperspectral imaging (HSI) observes the reflectance of electromagnetic wavebands between a range of 250-2500 nm, containing UV, VIS, NIR and SWIR. Each pixel of a hyperspectral image contains a spatial and a spectral information. If the focus lays on spectroscopy, the sequence of several hundreds of wavebands is combined to a hyperspectral matrix, so-called reflectance curve. Reflectance curve represents the spectral range of all observed wavebands on the x-axis and displays the degree of reflectance according to each waveband on the y-axis (Abebe et al., 2023).

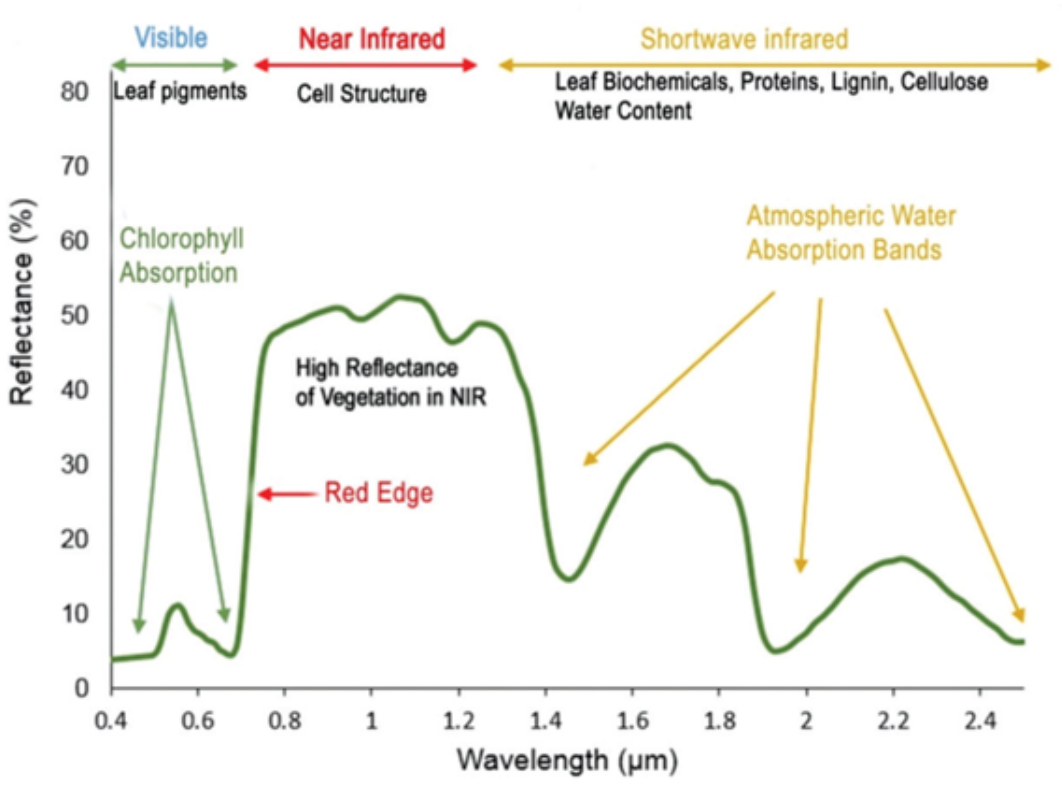

Figure 5: Spectral reflectance curve of vegetation. Major absorption regions and reflectance features are indicated; published by (Roman and Ursu, 2016).

Figure 5 illustrates a reflectance curve calculated by hyperspectral measurement data. In VIS range refelectance is minimum due to chlorophyll absorption. The transition from low reflected VIS to high reflectance NIR range is called the Red Edge (RE). The slope of RE can be used to determine water stress. Spectral reflectance is clearly decreasing above a wavelength level of 1400 nm, where SWIR range begins. Three local reflectance minima are shown across SWIR range caused by high absorption bands of atmospheric water (Roman and Ursu, 2016)

The hyperspectral imaging camera has four different scanning types: (1) point scanning, (2) line scanning, (3) area scanning and (4) single shot scanning. The most common type is a line scanning camera, which captures hyperspectral images when it moves from one side to another, e.g. in a field plot (Xie and Yang, 2020).

The HSI method is a rapid, non-destructive and automated phenotyping technique which enables the indirect evaluation of several physiological and morphological traits in plants. Applied to plant breeding, biochemical properties like pigment, water and nutritional content can be classified with spectral reflectance on known wavelengths. Changes in hyperspectral reflectance between two observations are used to examine plant's physiology, e.g. nutritional status, development stage and responses to the environment. HSI is an uprising and powerful tool for early detection of symptoms affected by abiotic and biotic stresses in plants (Mishra et al., 2017).

Plants under high-stress conditions show a changed spectral reflectance beyond the visible range which indicates their adaptation to the environment. In general, stressed plants have a lower reflectance curve than non-stressed plants, shown in figure 6. Thus, variety differences with HSI can be determined for the same ambient conditions at one observation timepoint.

In a situation of drought stress, certain NIR-SWIR spectral bands were found to reflect water (Reynolds, 2012). These insights have been widely accepted. In the following, a big range of indices were developed to assess plant water status (see chapter below) (Braga et al., 2021).

Furthermore, HSI data is used to predict quantitative traits, such as yield, biomass and height under stress conditions, e.g. transitional water deficit.

Devices for HSI are still expensive and their application is only affordable in large breeding programs and in state-owned institutions. Another challenge researchers faced, is HSI data evaluation. Hyperspectral imaging is a phenotyping method which creates huge amounts of data. Analyzing hyperspectral data requires capacities in data mining and machine learning. This challenge is well-known and there is motivation to cope this problem for high-throughput pathways in phenotyping (Römer et al., 2012).

1.7 Plant phenotyping indices

Plant phenotyping indices are dimensionless values to describe plants for a specific trait or behavior under certain stress conditions. In case of drought stress, specialized indices for waterlimited environments were proposed.

Drought indices characterize drought levels in quantitative measures by using one or several variables, also called indicators. These indicators are either meteorological-based, e.g. air temperature,

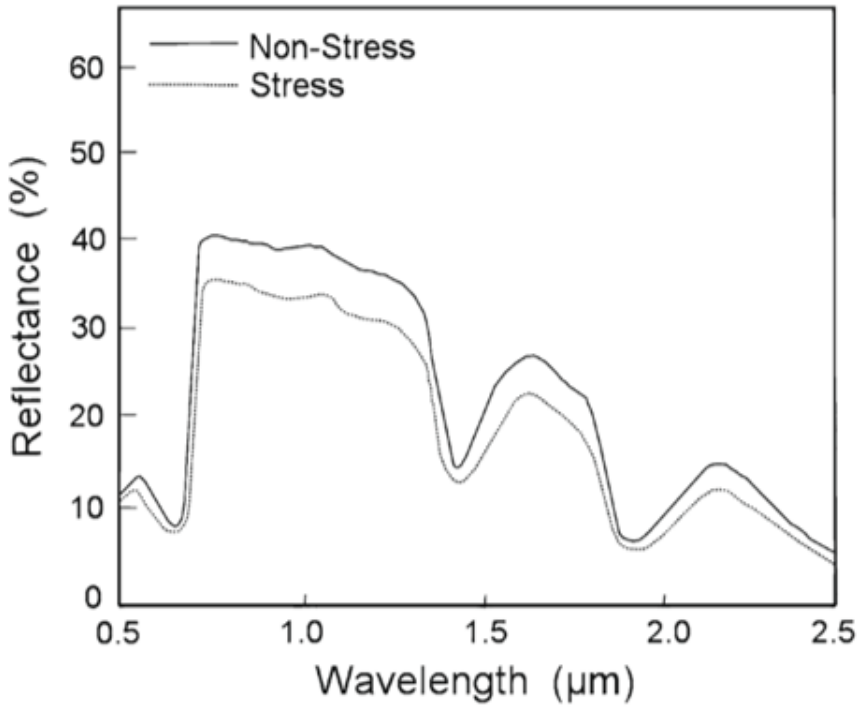

Figure 6: Typical reflectance curve for a stressed and non-stressed leaf ranging from VIS to SWIR; published by Blum (2011).

relative air humidity or solar radiation, or hydrological-based, like precipitation and groundwater level, or plant-based as soil moisture and leaf water content of crop plants (Zargar et al., 2011).

Some drought indices are used to determine short-term abnormal dryness (Crop Moisture Index, CMI), other indices determine long-term drought more effectively (e.g. Palmer Drought Index, PDI) (Blum, 2011).

Plant breeding for drought adaptation needs indices which allow to account water status in plants as a numeric value. A range of indices and parameters, which evaluate water stress, are based on temperature measurements at plant organs which are related to transient drought stress in plants. Some parameters need only meteorological values and still other indices use spectral reflectance of wavelengths to determine drought stress in plants.

Vapor Pressure Deficit (VPD)

The vapor pressure deficit (VPD) was used to define objective conditions based on water relations and evaporative demand in the environment. Findings of Anderson (1936) show that VPD is more sensitive to indicate water vapour condition than relative humidity (rH) allows to do. Therefore, VPD describes the interaction of plants with the ambient atmosphere more precisely. The equation for calculating VPD (in kPa) needs only weather parameter rH in % and air temperature (T_a) in ℃ (Struthers et al., 2015). Formula 2 contains saturation vapor pressure, e_s in millibars (mb), which is calculated with equation 3.

Unit conversion from mb to kPa is done with factor 0.1, shown in following equation:

$$VPD = (e_s * 0.1) * \frac{100 - R_h}{100} \quad \text{[kPa]}, \tag{2}$$

$$e_s = 6.11 * \exp\left[\frac{L}{R_v} * \left(\frac{1}{273} - \frac{1}{273 + T_a}\right)\right] \quad \text{[mb]} \tag{3}$$

where L is the latent heat of vaporization with $2.5{*}10^6$ $\frac{\text{J}}{\text{kg}}$, R_v is gas constant for water vapor with 461 $\frac{\text{J}}{\text{kg}*\text{K}}$ and T_a is measured air temperature in Kelvin (T_a (°C) + 273.15). In soybean, VPD values above a threshold of 1.5-2.0 kPa indicate plant's response to beginning water stress, which is resulted in reduced transpiration. This threshold is mainly reached around midday, while 'slow-wilting' genotypes will limit the transpiration rate and keep this level in rising VPD on afternoon, while non-adapted cultivars even increase in their transpiration rate (Fletcher et al., 2007). Applied to this phenotypic variation in soybean cultivars, QTL mapping is used to identify the genetic basis of canopy water use to rising VPD (Monnens et al., 2024).

1.7.1 Thermal-based indices

Canopy air temperature differential (dT_c)

The canopy air temperature differential (dT_c) is a simple normalization of measured canopy temperature substracted by the ambient air temperature, see equation 4. Well-watered plants show dT_c values both negative and around 0 K. Water stressed plants will show reduced transpiration rate by closing stomata, which is associated with a lower cooling capacity. In consequence, leaf and canopy temperature increase relatively to air temperature. In some studies, a threshold of dT_c above +2 K will indicate water stress in plants.

$$\delta T = T_c - T_a \tag{4}$$

Crop water stress index (CWSI)

The crop water stress index (CWSI) was developed to indicate drought stress in plants (Idso et al., 1981). The idea of this index was to set the actual evaporation in relation to potential evaporation in a non-stressed environment. CWSI is widely used for abiotic and biotic stress detections and for irrigation timing, even if Maes and Steppe (2012) call for attention to 'stable' weather conditions during thermal canopy measurements in humid and temperate climate regions.

The values for CWSI ranges from 0 to 1, where 0 describes a situation of fully water-saturated crop plants (no water stress) and 1 is the value for completely non-transpiring plants (high water stress). Applied to cultivars screening, (Ucak and Arslan, 2023) suggested for chickpea, that CWSI values up to 0.28 are considered for resistant genotypes, the CWSI values between 0.29 and 0.37 show moderately resistant genotypes. Furthermore, cultivars with CWSI values 0.38 and 0.49 are moderately sensitive, and CWSI values over 0.50 describe sensitive genotypes.

Three approaches were used to determine CWSI: an analytical, an empirical and a direct approach. The analytical and empirical approaches have hampered for a practical application due to large input requirements (Maes and Steppe, 2012).

In contrast, the direct approach uses only directly measured canopy temperatures (Jones, 1999). Following input parameters were measured: the actual canopy temperature (T_c) of crop leaves, the potential canopy temperature of fully transpiring or wet leaves (T_{wet}), as a lower baseline, and the temperature of non-transpiring or dry leaves (T_{dry}), as an upper baseline. CWSI is calculated in following equation:

$$CWSI = \frac{T_c - T_{wet}}{T_{dry} - T_{wet}} \tag{5}$$

In a low scale of samples, the reference measurement of T_{wet} was done at fully water sprayed leaves, while T_{dry} was determined on leaves covered with petroleum jelly. The generation of artificial surface references is labor-intensive and dedicated to errors (Maes and Steppe, 2012).

The emergence of thermal imaging enabled to measure temperatures with spatial differences. In the following, a simplified CWSI (siCWSI) was introduced, which determines the lower and upper baseline as the average of the lowest 0.5% and highest 0.5% of values in the canopy temperature histogram (Bian et al., 2019).

1.7.2 Spectral reflectance indices

Spectral reflectance indices (SRI) are numerical markers that use either wavelengths or wavebands of the electromagnetic sprectrum. SRI have the aim to create quantitative relationship of changes in electromagnetic spectra with changes in physiological variables on plant canopy surface. One big advantage of SRI is the ability to summarize a large amount of data into a few numerical values (Reynolds, 2012).

Vegetation indices

Vegetation indices estimates photosynthetic size of a canopy. Commonly, healthy canopy vegetation absorbs most light in VIS region and reflects most light in NIR region. In contrast, sparse developed or unhealthy canopy vegetation show low absorption level in visible and higher absorption content in NIR spectrum range. This effect is mainly caused by decreased chlorophyll content in stressed vegetation (Araus et al., 2001).

A widely-known vegetation index is the normalized difference vegetation index (NDVI), which compare a red wavelength in the visible spectrum with a wavelength in the NIR range (Rouse et al., 1973). NDVI was successfully used to predict yields in corn and also for soybean. High accuracy for yield prediction is shown at seed-filling stages (R5-R6) because of senescing vegetation (Christenson et al., 2016). Furthermore, a range of simple ratio vegetation indices (SRVI) were developed for predicting yield in soybean based on canopy spectral reflectance on 454-950 nm bands (Zhang et al., 2019).

Chlorophyll and other indices

Another group of SRI are specialized indices for evaluation of chlorophyll and other pigment concentrations. For a change in chlorophyll a and b content, chlorophyll indices, such as PSSRa and PSSRb, were very sensitive at a reflectance wavelength at 675 nm and lower at 550 nm. Red edge (RE) indices also estimate with canopy chlorophyll content focused on the red edge, a spectral region within 680-780 nm. Some nitrogen indices allow to detect the status of nitrogen in plants (Reynolds, 2012).

Water indices

Plant leaves may be composed about 40-80% water by weight. Water indices were developed to indicate canopy water status, including parameters such as stomatal conductance, leaf water potential, relative water content and canopy temperature. Water indices are based on reflectance of specific wavebands in NIR and SWIR region, which were detected for high water absorption (see figure 5). Some well-known (liquid) water absorption bands are approximately at 760 nm, 970 nm, 1190 nm, 1450 nm and 1950 nm (Reynolds, 2012). The reflectance in these regions is masked by water content, and can be used to generate indices for further relationship.

In detail, highest absorption rates of radiation were found in the 1300-1500 nm region of the spectrum. However, the reflectance is saturated for low water contents. That's why this SWIR range has low application for detection of water status, especially under drought conditions (Reynolds, 2012).

Early water index development was done due to remote sensing of vegetation. Normalized Difference Water Index (NDWI) uses the spectral reflectance of 860 nm and 1240 nm and is sensitive to changes in water content in vegetation canopies (Gao, 1996).

For ground-based spectroscopy devices several indices were established in the NIR region for wavelengths 850, 880, 900, 920, 930 and 970 nm (see table 4). Peñuelas et al. (1993) developed Water Index (WI) based on the simple ratio of 900 nm and 970 nm reflectance. Furthermore, three water indices (WI-1, WI-2, WI-3) were focused on wavelengths 915, 940 and 990 nm, which allow to predict seed yield and maturity in soybean during reproductive phase, after a drought event has occurred (Christenson et al., 2016). Another water indices are Normalized Difference water indices (NWI) based on wavelengths above.

1.8 Scientific questions

The aim of this work was to compare European soybean genotypes from maturity group (MG) 000, MG 00 and MG 0/I for their adaptations to drought stress and to find significant differences in physiological and agronomic characteristics. Another objective was the attempt to evaluate the methodology of hyperspectral and thermal imaging technique for physiological plant breeding.
Scientific questions of this work are:

1. Are there significant differences between genotypes for grain yield in MG 000, MG 00 and MG 0/I?
2. What is the influence of time to maturity to yield?
3. Are there significant differences in reproductive period between maturity groups?
4. Are there significant differences between genotypes of MG 00 for stomatal density?
5. Which of 16 hyperspectral reflectance indices can show highest correlation with grain yield in soybean MG 000, MG 00 and MG 0/I?
6. How strong is the correlation between grain yield and siCWSI in soybean varieties?
7. Is siCWSI a useful parameter to determine water stress in soybean?

2 Material and Methods

2.1 Location and site

Variety field experiments with soybean were grown under rainfed conditions in Tulln in Lower Austria, 25 km northwest of Vienna (GPS: 48°19'3" N, 16°04'7" E; elevation: 178 m above sea level). Tulln is located at the transition of the oceanic and the contintental climate zone. The location has a general humid climate (period 1995-2024) with annual mean temperature of 11.1 °C and summarized precipitation of 674 mm/year (figure 7, data: GeoSphere Austria (2024)). The local climate is strongly shaped by Danube river. The area of research fields is former alluvial land.

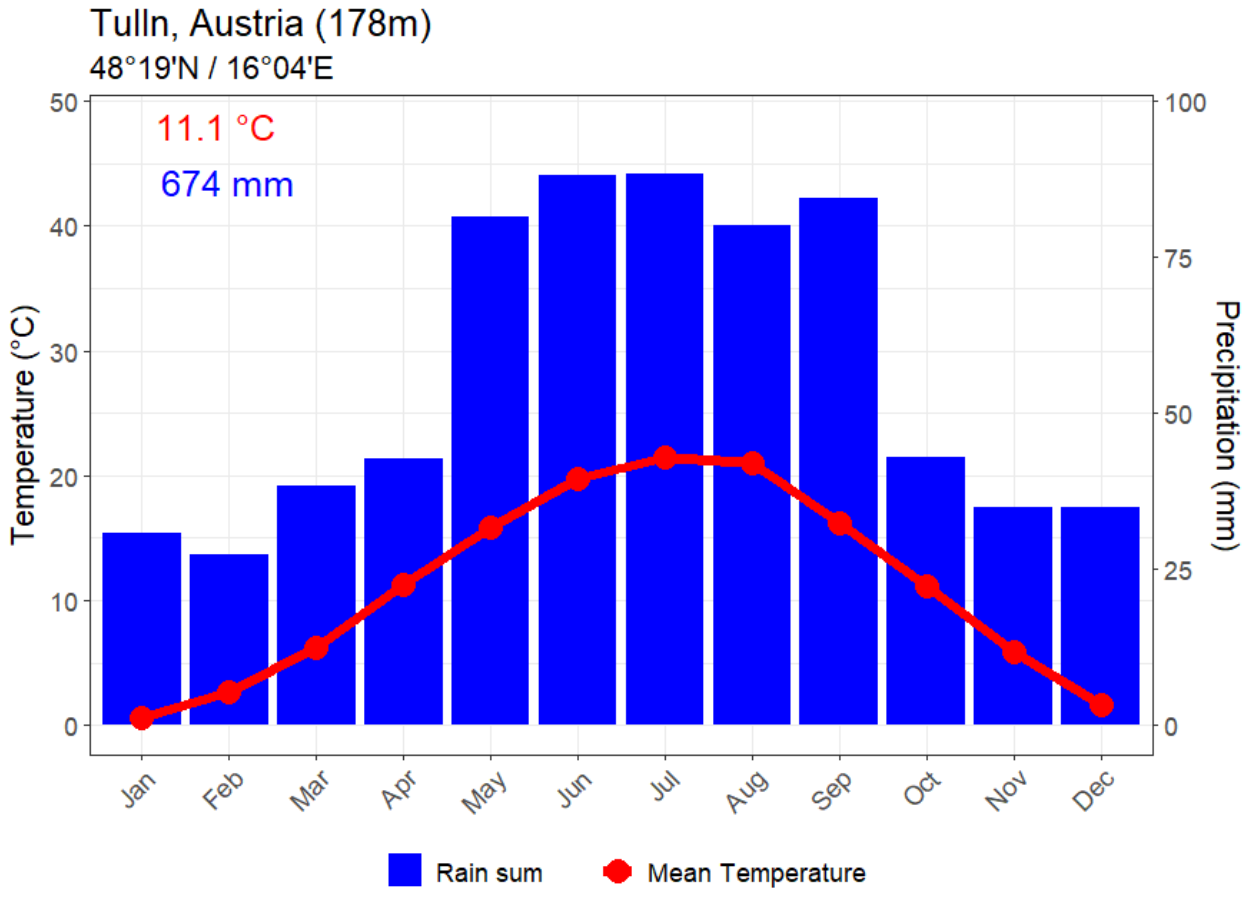

Figure 7: Climate diagram from Tulln, Lower Austria with monthly mean temperatures and monthly summarized precipitation in the period 1995-2024.

Soil type is primarily calciferous Tschernosem with neutral soil reaction (pH = 6.9), good water storage capacity and low water porosity. In a descending order of soil depth, horizontal layers consist of silty-loam (0-70 cm), loamy sand with high content of gravel and rock (70-80 cm), and a bedrock with slight gleyification (90-120 cm). Soil conditions across the experimental design are homogeneous and the area is counted as high quality farmland (www.bodenkarte.at, accessed: 26.08.2024).

2.1.1 Weather data collection

Information about weather parameter for the experimental site is collected by an installed BOKU-own weather station (type: Adcon A733), which records weather variables in intervals of 15 minutes. The logged weather data is online available at https://dnw-web.boku.ac.at/dnw/wetter_form_uft.php. Following weather parameters were selected:

- air temperature (T_a) in ℃
- global radiation (rad_g) in W/m²
- relative humidity (rH) in %

Weather data was used to display environmental conditions for each timepoint, when measurements for thermal or hyperspectral imaging were conducted.

For calculation of climate data focused on Tulln, meteorological parameters (T_a, rH and precipitation sums R in mm) were requested on online services of GeoSphere Austria (2024). The obtained data was collected by meteorological weather station Langenlebarn located about 6 km away from Tulln.

2.1.2 Weather of growing season 2024

The 1995-2024 climate normal for Tulln computed a mean seasonal T_a of 17.6℃ and a summarized total R of 465.1 mm for Tulln between May and October (Table 1). The soybean season lasted from mid of May to mid of October. The growing season 2024 was extraordinarily warm, on average 2.0℃ over the climate norm. In all months in the season 2024, T_a was minimum 1.4℃ (April) and maximum 3.6℃ (August) warmer compared to climate norm.

Table 1: Meteorological variables, monthly mean air temperatures (T_a) and rainfall sums (R) during the 2024 growing season. The climate norms represent the time period between 1995 and 2024.

Month	May	Jun	Jul	Aug	Sep	Oct	**Total**
Mean air temperatures, T_a (℃)							*Mean*
Climate norm	15.8	19.8	21.4	21.0	16.2	11.1	**17.6**
2024	17.2	21.1	24.0	24.6	17.8	12.7	**19.6**
Precipitation sums, R (mm)							*Sum*
Climate norm	81.4	88.0	88.3	80.0	84.3	43.1	**465.1**
2024	60.9	116.2	47.3	35.9	447.2	56.6	**764.1**
Relative humidity, rH (%)							*Mean*
Climate norm	65.0	64.3	63.7	66.5	73.0	78.9	**68.6**
2024	65.5	66.8	58.6	61.5	69.8	81.3	**67.2**

Precipitation was characterized with extreme fluctuations between monthly rainfall sums in season 2024. While May was dry with -20.2 mm less rain than climate norm, in June was listed a rain surplus of +28.2 mm. These warm and rainy weather conditions during the vegetative phase of soybean were

optimal for growth and development. In July and, moreover, in August 2024, dry and hot weather controlled the experimental site. In comparison to climate norm, rain deficits of -40.7 mm in July and -44.1 mm in August, which represent 53.6% and 44.9%, respectively, of normal.

In sharp contrast, September 2024 was extraordinary wet with 447.2 mm due to an extreme rain event and following floods in the region. The experimental site was not affected, the soil has absorbed all precipitations. Furthermore, soybean varieties were less influenced by this heavy rainings, because early genotypes in trial 1 and 2 and 4 were mainly matured and had left their leaves. Late varieties in trial 3 were even affected in growth and maturing time.

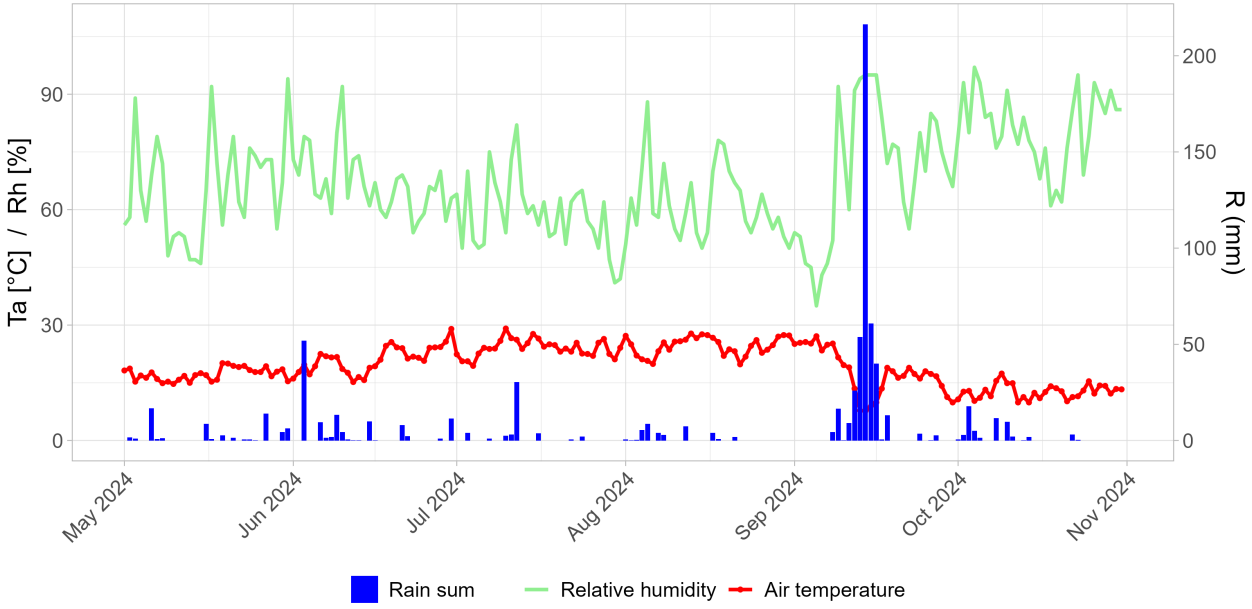

Figure 8: Daily chart in growing season 2024 between 1. May and 31. October; selected weather values: relative humidity (rH) in %, rain sum (R) in mm and air temperature (T_a) in ℃.

Relative humidity (rH) was in spring 2024 similar to long-term climate. In contrast, summer months July, August and September 2024 (monthly average of 58.6%, 61.5% and 69.8%) had much less rH than the long-term mean with 63.7% , 66.5% and 73.0%, respectively. Finally, October was even more humid than the climate norm and influenced only ripening of late genotypes.

Figure 8 displays the daily course of T_a, rH and R during the whole season between May and October 2024. In the second half of July and second half of August there were two periods with high air temperatures and very low summarized precipitation events.

2.2 Experimental design and genotypes

The whole experimental setup consists of 205 genotypes with different maturity time, thus they were separated in four variety trials according to their maturity group (MG) and food purpose, respectively, as shown in table 2. Trial 1 (Y1) consists of 60 early ripening genotypes from maturity group (MG) 000 and earlier. Trial 2 (Y2) contains 45 mid ripening genotypes according to MG 00. In trial 3 (Y3), 30 late

maturing genotypes have grown and are counted to MG 0 and I. Trial 4 (Food) includes 70 genotypes of all MGs which are used in trials Y1, Y2 and Y3, but the focus lays on nutritional and product properties for food use. Individual variety names are listed as supplementary information in figure S3a for Y1, figure S3b for Y2, figure S3c for Y3 and figure S3d for Food trial.

Table 2: Overview of experimental setup, departed in four trials with maturity group, plot number and accompanying α-lattice design.

Trial No.	Trial name	Abbr.	Maturity group	Plots	Rep	Plot No.	α-lattice design
1	Yield 1	Y1	000 and earlier	60	2	101 - 160	10x6
2	Yield 2	Y2	00	45	2	201 - 245	15x3
3	Yield 3	Y3	0 and I	30	2	301 - 330	10x3
4	Food	Food	000 – I	70	2	401 - 470	10x7

For variety trials with low replicate and high plot numbers, alpha-lattice designs were chosen to achieve low experimental error between plots (Mathews and Crossa, 2022). Alpha-lattice designs are Balanced Incomplete Block Designs (BIBD) and can be adapted to the number of varieties in each trial. The BIBD for trials Y1, Y2, Y3 and Food were realized as 10x6, 15x3, 10x3 and 10x7 alpha-lattice (genotypes x blocks), respectively. In field trials used genotypes are both in Europe certified varieties and breeding lines, which represents seven European soybean breeding institutions and companies, namely WBF Agroscope (short: AGS), Danko Hodow Roslin (DANKO) from Poland, Lidea Seeds (LIDEA) and RAGT Seeds (RAGT) from France, Saatzucht Gleisdorf (SZG) and BOKU University (BOKU) from Austria and University of Hohenheim (UHOH) from Germany (see table S2).

AGS, LIDEA, RAGT and SZG contribute own genotypes for all four trials and UHOH has genotypes for trials Y1, Y2 and Food. While DANKO's genotypes are represented in trials Y1 and Food, BOKU solely brings breeding lines in for trial Food. Two check varieties were included in all trials as a reference, namely: 'RGT STUMPA' (RAGT) and 'CH22172 Obélix' (AGS). In summary, 205 varieties were tested in a coherent area with about 600 m^2 for their performance, especially their behaviour in drought phases.

Soybean seeds were sown in 2.5 m long single-row plots with a row spacing of 50 cm and about 50 seeds per row at 10. May 2024 (doy: 131). In the first month after sowing, weed control was done either by manual work and mechanically by rotary hoes. Due to sufficient precipitation patterns and warm air temperature during summer months, no artificial irrigation was needed. Soybean plots of trial Y1, Y2 and Food were harvested at 30. September (doy: 274), only trial Y3 with late maturing genotypes was harvested 17 days later at 16. October 2024 (doy: 291).

In the framework of the EU-project 'Legume Generation', similar experimental setups with the same varieties were carried out at different locations across Europe by 8 project partners during summer season 2024.

(a)

row	rep 1						Yield 1					
30	119	152	112	159	125	133	131	152	128	105	108	142
29	135	126	118	127	156	141	117	136	133	106	154	139
28	120	131	124	139	150	101	127	140	144	143	125	160
27	146	137	117	109	114	102	156	124	115	145	113	146
26	136	108	147	116	145	130	153	122	135	107	102	104
25	106	113	155	132	104	160	149	112	103	130	120	114
24	149	134	128	107	111	144	157	155	151	141	147	109
23	153	151	143	142	129	148	116	110	159	138	150	137
22	110	121	122	154	115	157	121	132	126	158	134	148
21	105	140	158	103	138	123	129	101	123	118	119	111
col	1	2	3	4	5	6	7	8	9	10	11	12

(b)

row	rep 1			Yield 2			rep 2		
30	232	233	223	223	227	238	201	243	228
29	236	239	238	212	208	214	202	234	244
28	203	245	225	233	216	231	210	239	232
27	215	228	212	229	207	230	225	213	205
26	210	237	222	224	219	235	218	209	215
25	231	227	242	220	216	221	220	211	245
24	219	230	244	207	224	214	204	237	226
23	217	243	218	202	229	204	206	236	222
22	209	240	213	201	235	208	242	241	221
21	205	241	211	226	234	206	240	217	203
col	13	14	15	16	17	18	19	20	21

(c)

row	rep 1			Yield 3		rep 2
30	308	310	311	304	314	309
29	312	306	324	302	317	318
28	319	316	328	323	305	312
27	301	303	317	303	315	324
26	323	325	326	310	330	307
25	313	320	321	329	322	301
24	330	314	302	327	328	311
23	322	315	305	321	319	308
22	304	327	307	325	313	316
21	318	329	309	326	320	306
col	22	23	24	25	26	27

(d)

row	rep 1							Food			rep 2			
30	461	413	437	469	420	447	406	448	402	412	467	419	414	445
29	441	458	453	452	433	419	466	438	454	463	422	421	455	449
28	465	456	439	448	446	449	432	469	423	460	403	409	452	439
27	450	412	457	431	460	462	438	416	432	468	410	401	407	450
26	422	459	428	444	423	435	427	408	433	406	436	415	444	417
25	443	405	445	468	408	403	426	429	427	466	470	447	442	440
24	417	440	451	434	409	455	401	418	411	430	451	428	420	456
23	418	402	424	454	442	410	415	462	459	443	434	458	424	437
22	436	467	470	416	411	463	425	461	441	431	464	426	465	425
21	421	429	464	407	414	404	430	405	446	457	404	435	413	453
col	28	29	30	31	32	33	34	35	36	37	38	39	40	41

Figure 9: Experimental setup departed in 4 field trials in alpha-lattice design, departed in four trials with two replicates (rep) in each: (a) Yield 1, 60 genotypes with 10x6 lattice; (b) Yield 2, 45 genotypes with 15x3 lattice; (c) Yield 3, 30 genotypes with 10x3 lattice; (d) Food, 70 genotypes with 10x7 lattice.

2.3 Methods

2.3.1 Eye-visual phenotyping / scoring

Classical eye-visual phenotyping method is related to visually observable properties on plant and plant organs which were scored by breeder. Commonly, the observation of many eye-visual traits is related to soybean life-cycle according to the description of soybean development stages from Fehr et al. (1971), as listed in table 3.

Table 3: Description of vegetative (V) and reproductive (R) stages according to Fehr et al. (1971).

Stage	Abbreviated stage title	Description
VE	Emergence	Cotyledons above the soil surface
VC	Cotyledon	Unifoliate leaves unrolled sufficiently so the leaf edges are not touching
V1	First-node	Fully developed leaves at unifoliolate node
V2	Second-node	Fully developed trifoliolate leaf at node above unifoliolate node
V3	Third-node	Three nodes on the main stem with fully developed leaves beginning with the unifololate nodes
Vn	n^{th}-node	n number of nodes on the main stem with fully developed leaves beginning with the unifoliolate nodes.
R1	Beginning bloom	One open flower at any node on the main stem
R2	Full bloom	Open flower at one of the two uppermost nodes on the main stem with a fully developed leaf
R3	Beginning pod	Pod 3/16 inch long at one of the four uppermost nodes on the main stem with a fully developed leaf
R4	Full pod	Pod 3/4 inch long at one of the four uppermost nodes on the main stem with a fully developed leaf
R5	Beginning seed	Seed 1/8 inch long in a pod at one of the four uppermost nodes on the main stem with a fully developed leaf
R6	Full seed	Pod containing a green seed that fill the pod cavity at one of the four uppermost nodes on the main stem with a fully developed leaf
R7	Beginning maturity	One normal pod on the main stem that has reached its mature pod color
R8	Full maturity	95% of the pods have reached their mature pod color; 5-10 days of drying weather are required after R8 before the soybeans have less than 15% moisture

Therefore, phenotyping traits were scored in a certain timepoint or within a certain period of time to detect the developmental stage itself or the performance during one phase of development. An overview of all traits over the whole growing phase is displayed in table S4.

In VE stage, 'Field emergence' was scored by estimating the percentage of emerged plants in a plot on a scale between 1 (very low emergence) and 9 (very dense emergence). Mid of June, soybean plants

have grown for five weeks and the early vegetative development (V2/V3 stage) were scored between 1 (low) and 5 (high) as 'development score'. Figure S1a shows the soybean field in a RGB photograph.

Moreover, the reproductive phase is of great interest to breeder. The timepoint/day when soybean begins flowering (R1) is noted as 'time to flower' (ttf) in days of the year (doy). The day of full maturity (R8) is determined as 'time to maturity' (ttm) in analogous way. In consequence, the difference between ttm and ttf is equal to the reproductive period of time, called as 't-reprod'. Some performance traits, namely 'lodging', 'pod set' and 'pod shattering', were gradually scored on a scale from 1 to 5: low scores indicate no or little markedness, high scores represent strong shaping according to each trait.

Further traits are not feasible to be scored visually by eye because the phenotypic shades are rather a continuum and is more likely to measure with assistance of devices. One simple device is a measuring stick which is used to determine plant height of soybean plots. The mean height of erected plants in a single row is measured between soil surface and uppermost pods, after full maturity (R8) has been reached. Bias through too exact and time-intensive measurements was prevented by determining plant height in 5 cm clusters, e.g. 65 cm, 70 cm, 75 cm etc.

Yield measurement was similarly done with an 100 cm tall stick during manual soybean harvest. Measurement stick was put to the ground next to a single-row plot. Only plants along this 100 cm section were harvested for representative grain yield. Harvested seeds of each plot were stored in separate paper bags and dried for minimum 4 weeks at room temperature. Before seeds were purified, bags were weighed by a precision scale (model: FX-i3000, manufacturer: A&D Company, Ltd.) and determined to gramm weight exclusive paper bag tare. Yielded area of a single-row plot is equal to 0.5 m^2, in consequence, for a conversion to unit dt/ha the factor 0.2 is needed.

2.3.2 Destructive phenotyping: measuring

Leaf sampling was done for some phenotypic traits which can optimally be determined in laboratory. As selection criterion of comparable leaf samples, the middle leaflet of a fully developed trifoliate leaf was chosen. Picked leaves may have neither damages nor any distortions.

Selected leaves were located in the upper canopy, mostly at the third node below the uppermost node. Sampling time was in the morning between 8:00 and 11:00 a.m. under sunny weather and dry canopy, but without wilting leaves. Leaf samples were collected for 'Leaf size' and 'SPAD value' in all trials. The trait 'stomatal density' was only evaluated in sampled leaflets from trial 2, as descripted below.

Leaf size

Leaf size determination was done based on a sample of five central leaflets of different plants of one plot. These leaflets were put on a red cloth. RGB-camera was installed in a pre-set distance to the cloth and took one photo for each plot. Additionally as a reference, 1 cm^2 pieces of green leaf area were photographed for further calculation.

All photos were automatically processed by computer software 'SigmaScan Pro' Vers. 5.0 (SPSS, Inc. Chicago, IL, USA) to get the percentage of green pixels out of red pixels. Leaf area was calculated

by the conversion from pixels to square millimeters (cm^2) using reference photos. Leaf size of one plot was received as an average of five leaflets.

SPAD value

Matured leaves were sampled in mid of July, departed on the trial Y1 at 16. July, trials Y2 and Y3 at 17. July, and trial Food at 18. July. All leaves were evaluated to SPAD value using a chlorophyll meter (type: SPAD-502, producer: Konica Minolta Sensing, Inc.). Mean of 30 measurements at 5 leaflets results in non-dimensional SPAD value.

Stomatal density

Stomatal density (SD) was determined only in soybean varieties of trial Y2 during full flowering (R2) stage. Under dry conditions, three fully emerged leaflets at the uppermost node of several plants were collected in each line-plot before midday.

These leaflets were put in transparent folders and transported to a cooler environment either in a cold room at about 4 ℃, to prevent water loss and wilting leaflets. In the following, the nail-polish-imprint method was applied according to Millstead et al. (2020), but modified to available equipment. Figure 10 shows graphically the workflow of this method.

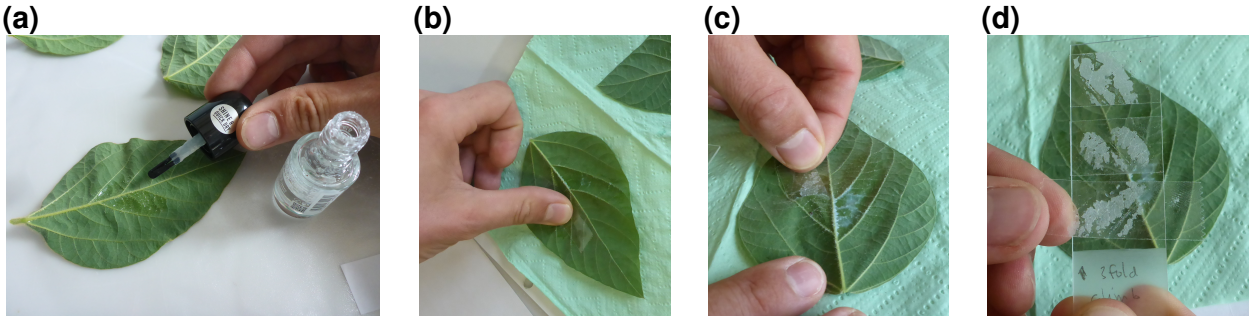

Figure 10: Workflow of Nail-polish-blottom method with most important steps: (a) nail polish is spread on abaxial leaf surface; (b) transparent adhesive tape is pressed to the dried leaf area; (c) tape with impression is removed from the leaf surface; (d) in total, three impressions from each sampled plot are fixed on a microscopic slide.

1. Transparent nail polish (producer: essence cosmetics, 8 ml) is spread on the abaxial side of leaf surface between main leaf vein and two side veins. Especially for soybean, leaf surface is hairy and needs a stronger coating with nail polish to get effectively in contact with epidermis over the spread area. The leaf area with nail polish expands a length of approximately 30 mm and a width about 10 mm (see figure 10a).

2. For nail polished leaflets a drying time of approximately 3 minutes is necessary. Dried nail polish appears as a glossy surface.

3. One piece of transparent adhesive tape (producer: Tesa, 11 mm width) with more than 20 mm length is pressed for some seconds to the dried area within central vein and two side veins (see figure 10b).

4. The tape is removed from the leaf along the central vein (figure 10c) and a transparent impression of the lower leaf epidermis is created.

This impression was stuck with adhesive side to a microscopic slide with 21 mm width and 75,5 mm length. Each microscopic slide was coated by three impressions, which were made from all three collected leaflets of one field plot. In total, 90 microscopic slides with abaxial leaf impressions were collected.

Leaf imprints on microslides were observed by a digital imaging microscope (producer: Olympus, type: DSX1000, with Universal Zoom Head DSX10), as depicted in figure 11a. In the accompanied

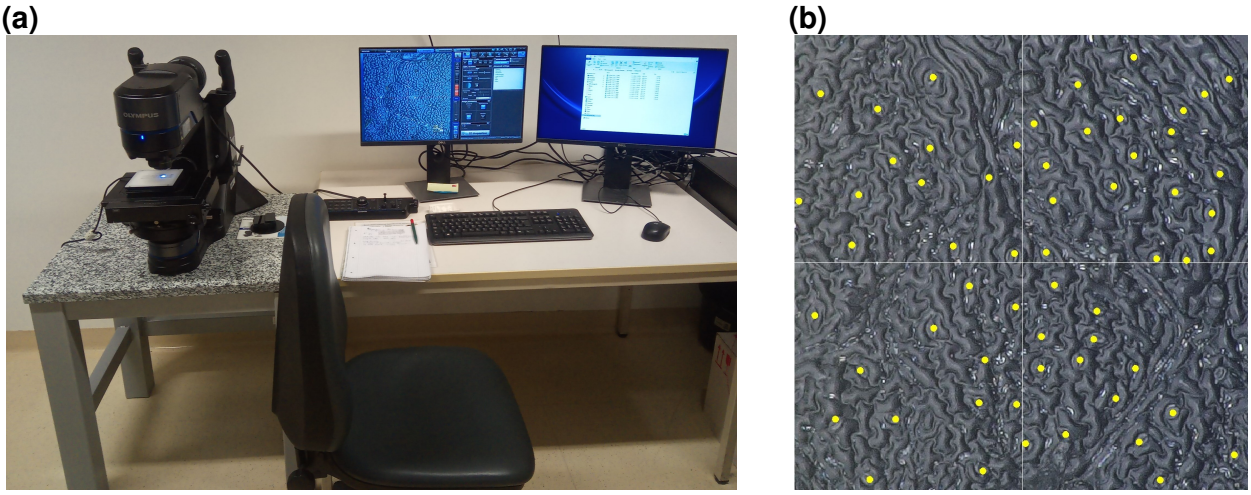

Figure 11: (a) Generation of microsopic images from leaf impressions with a digital imaging microscope; (b) Micrograph (800x800px) of abaxial leaf surface with highlighted stomata (yellow).

DSX1000 software, the reflected light microscope was set on a magnification scale of 400x. For sharp micrographs, observation mode 'OBQ' (Brightness_ Epi: 5115, Brightness_ Trans: 0) was selected, furthermore image processing settings 'depth focus' and 'HDR texture' were set to 'ON'.

In microscopic view, leaf hairs, air bubbles within tape and leaf and rough surface as well limit regions to representive and coherent areas. Appropriate microscopic extracts were used to create graphical images (size: 1200x1200 px), also called micrographs. In total, for each microscopic slide 15 micrographs were chosen, and digitally saved.

All micrographs were cropped centrally to a smaller size of 800x800 pixels with image processing software 'IrfanView', resulting in a compromise between a valid number of stomata and counting time for each micrograph. The observed leaf area is determined to 0.2031 mm^2. Stomata number of cropped micrographs was manually counted, supported by software 'DotDotGoose'. Mean stomata number of 15 micrographs per field plot was calculated.

2.3.3 Hyperspectral reflectance

Hyperspectral reflectance camera (type: FieldSpec HandHeld 2, manufactured by ASD Inc., Boulder, CO, USA) was used to detect a visible and near infrared radiation wavelength range between 325 nm and 1075 nm for spectral reflectance. Data collection in the field was adapted to the technique described in detail by Vollmann et al. (2022). Figure 12a shows the ground-based screening technique by a hand-held device.
Collected spectral data was transformed to a reflectance curve. Based on the environmental conditions, the reflectance curve varies according to abiotic or biotic stress factors, as shown in the model curve in figure 12b. Furthermore, this figure indicates the bandwidths for Blue, Green, Red, Red Edge and Near infrared reflectance at approximate wavelengths of 480 nm, 550 nm, 680 nm, 710 nm and 840 nm, respectively.

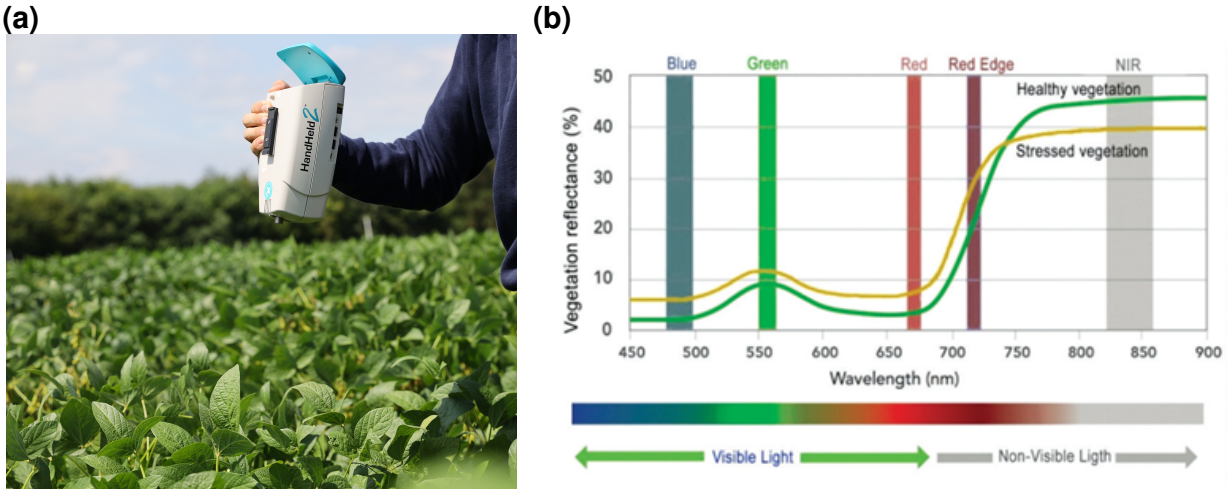

Figure 12: (a) Hyperspectral plot screening by a hand-held device (own photo); (b) Resulting spectral reflectance curve, limited to the range of 450 to 900 nm; important bandwidths are colored; published by Roman and Ursu (2016)).

Measurements were started, when canopy of soybeans had fully covered soil, and were stopped after first yellowing leaves in trial Y1 had shown beginning of senescence. As descripted in table 7, all plots of each trial were evaluated five times between mid of July and mid of August 2024, which represents the reproductive development stages from R1 (begin of flowering) to R5 (seed filling stage). Most measurements were done in a time set of 2 hours under cloudless weather conditions during midday which is the period of highest sun position on sky. Daytime varies between 11:00 and 14:00h of Central Europe Summer Time (CEST).
Summarized hyperspectral data was used to calculate 16 indices according table 4. Water indices detect the reflectance bands of water in plant leaves in simple ratios (WI) or in normalized ratios (NWI). High index values in water stress indices explain high water content and low water stressed plants. Other reflectance indices are related to vegetation status (NDVI, MA1-R), chlorophyll content (PSSRa,

PSSRb, CI) and nitrogen content (NRI, REIP), that indicate plant vigor within genotypes of the same growth stage (table 4).

Table 4: Spectral reflectance indices, arranged for water content indication (WI group, NWI group), for vegetation photosynthetic activity (NDVI, MA1-R), for chlorophyll (PSSRa, PSSRb, CI) and nitrogen (NRI, REIP) content; following wavelengths were defined as Green = 550 nm, Red = 680 nm, Red Edge (RE) = 710 nm and NIR = 840 nm.

Abbr.	Index name	Index formula	Reference
Water indices			
WI	Reflectance water index	$\frac{R_{970}}{R_{900}}$	Peñuelas et al. (1993)
NWI-1	Norm. water index 1	$\frac{R_{970}-R_{900}}{R_{970}+R_{900}}$	Babar et al. (2006)
NWI-2	Norm. water index 2	$\frac{R_{970}-R_{850}}{R_{970}+R_{850}}$	Babar et al. (2006)
NWI-3	Norm. water index 3	$\frac{R_{970}-R_{920}}{R_{970}+R_{920}}$	Prasad et al. (2007)
NWI-4	Norm. water index 4	$\frac{R_{970}-R_{880}}{R_{970}+R_{880}}$	Prasad et al. (2007)
NWI-5	Norm. water index 5	$\frac{R_{970}-R_{930}}{R_{970}+R_{930}}$	Prey et al. (2020)
WI-1	Water index 1	$\frac{R_{940}}{R_{915}}$	Christenson et al. (2016)
WI-2	Water index 2	$\frac{R_{990}}{R_{915}}$	Christenson et al. (2016)
WI-3	Water index 3	$\frac{R_{990}}{R_{940}}$	Christenson et al. (2016)
Vegetation, chlorophyll and nitrogen indices			
NDVI	Normalized difference vegetation index	$\frac{R_{\text{NIR}}-R_{\text{Red}}}{R_{\text{NIR}}+R_{\text{Red}}}$	Rouse et al. (1973)
MA1-R	RVI, Ratio vegetation index (for soybean)	$\frac{R_{638}}{R_{674}}$	Zhang et al. (2019)
PSSRa	Pigment specific simple ratio (chloroph. a)	$\frac{R_{\text{NIR}}}{R_{675}}$	Blackburn (1998)
PSSRb	Pigment specific simple ratio (chloroph. b)	$\frac{R_{\text{NIR}}}{R_{650}}$	Blackburn (1998)
CI	Chlorophyll index (red edge)	$\frac{R_{\text{NIR}}}{R_{\text{RE}}} - 1$	Gitelson et al. (2005)
NRI	Nitrogen reflectance index	$\frac{R_{\text{NIR}}}{R_{\text{Green}}}$	Cao et al. (2015)
REIP	Red edge inflection point (N-content)	$R_{700} + 40 * \frac{\frac{R_{670}+R_{780}}{2}-R_{700}}{R_{740}-R_{700}}$	Prey et al. (2020)

2.3.4 Thermal imaging

Evaluation of canopy temperature (T_c) was measured for 11 genotypes in trial Y2. All thermal measurements were done by thermal imaging camera (Model B335, produced by FLIR systems), which records thermographs in a sensitivity lower than 50 mK and with a resolution of 240x360 pixels. Each pixel of one thermograph possesses a measured temperature value in a range between -20 °C and +120 °C. Observation period for TIR was during the development stages R3 to R6 in August 2024. Thermal imaging started with fully soil covering canopy and stopped with begin of senescence when leaves in the canopy had become yellow. Two screening daytimes were chosen for method evaluation: the period around solar noon between 12:00 and 13:00h of Central Europe Summer Time (CEST) and on the afternoon between 15:00 and 16:00h (CEST) with warmest air temperatures.

Achieving consistent measurements, application of following method was realized in the same manner for each timepoint: The operating person was located in the spacings between two plots and with sunlight in the front, which may avoid shadows during measurements on the canopy. Thermal camera

was held above the canopy in a constant distance of approximately 0.3 m with both hands. In consequence, real camera height from soil was adjusted to average plant height of each plot by lifting and sinking arms.

Camera's vertical perspective may detect mainly plant canopy, while caution is advised to soil, clothes or shoes in the edge of camera's view. For a plot line, 5 thermal images, so-called thermographs, were collected by moving along a 2.5 m line in sidesteps. All 22 lines (11 genotypes, 2 replications) were measured within a time period of 30 minutes. Data evaluation was conducted with thermal imaging soft-

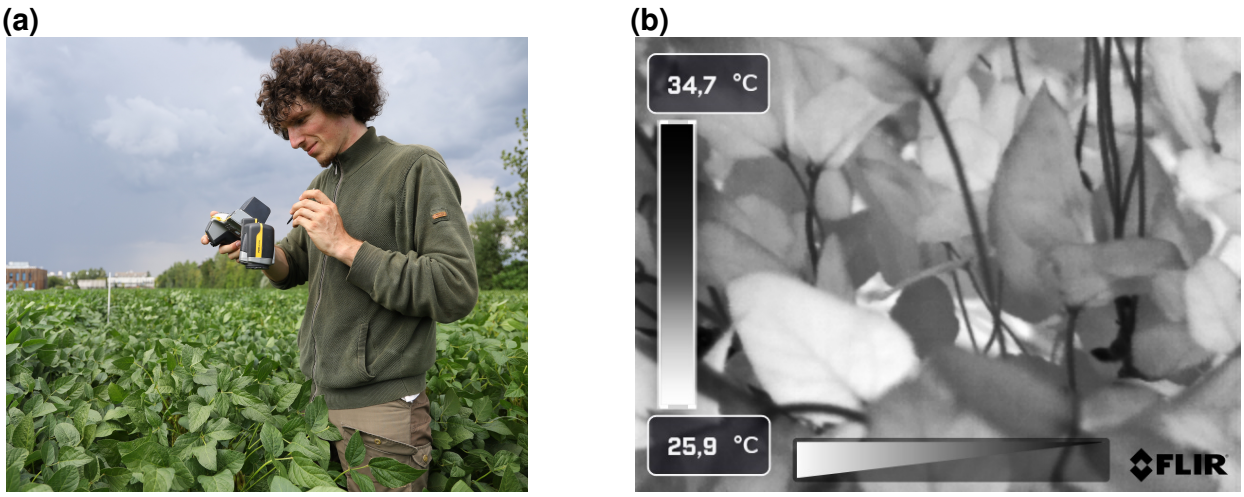

Figure 13: Thermal imaging method: (a) ground-based technique applied with a hand-held camera; five thermographs per plot were captured; (b) thermal image with highest and lowest temperature value on the display; mean temperature is calculated from values of all pixels.

ware 'FLIR Thermal Studio' to receive the mean temperature value of all pixels in a thermograph. Raw data collection includes not only mean temperature, but also minimum temperature (pixel with lowest value) and maximum temperature (pixel with highest value) of each thermograph. Average genotype mean temperature (T_c), average genotype minimum temperature (T_{min}) and average genotype maximum temperature were calculated (T_{max}) out of 10 thermographs for each genotype at one timepoint.

2.3.5 Normalizing thermal data

Weather data was included to set the thermal data in relation to environmental fluctuations.

Canopy temperature differential

A simple normalizing parameter is canopy temperature differential (dT_c), where canopy temperature (T_c) was substracted by corresponding air temperature (T_a). The calculation of dT_c is shown in following equation:

$$dT_c = T_c - T_a \tag{6}$$

Simplified Crop Water Stress Index

Another index to measure drought stress and drought stress differences between trials is Crop Water Stress Index (CWSI) as shown in formula 5. A simplified version of CWSI was developed by Bian et al. (2019) and called siCWSI. The simplification is made by a replacement of T_{wet} and T_{dry} by T_{min} and T_{max}. These modifications of formula 5 are shown in equation 7.

$$siCWSI = \frac{T_c - T_{min}}{T_{max} - T_{min}} \tag{7}$$

The calculation of siCWSI was done for each genotype in one timepoint, based on T_{min}, T_{max} and T_c.

Vapor pressure deficit

Vapor pressure deficit (VPD) is another parameter which indicates meteorological drought stress to plants. VPD is based on air temperature and relative humidity at a certain timepoint of measurement. VPD is calculated to formulas 2 and 3 and results in a range between 0 and 3 kPa in temperate climate region of Lower Austria.

According to the measured VPD for different timepoints, drought stress levels were introduced. 'Low' drought stress is suggested for VPD values below 1.5 kPa, while 'Mid' drought stress is defined for VPD between 1.5 and 2.0 kPa, while a VPD above or equal to 2.0 kPa is named as 'High' drought stress.

2.4 Statistical analysis

Data analysis was primarily done by the software program PLABSTAT, which is able to consider block effects in a lattice design (Utz, 2005). Analysis of variance (ANOVA) was conducted for all traits using an "intra-block analysis". F-test of components of variance are based on following error probability (p) levels:

\+ significant at the p = 10% level

* significant at the p = 5% level

** significant at the p = 1% level

For variety comparisons in trials, least significant difference at 5% probability level (LSD5) was determined for each trial to recognize significant yield differences between varieties.

Furthermore, coefficients of correlation (r) were calculated between all traits of the trial based on adjusted mean values. Calculated weighed mean values of block effect were returned by PLABSTAT. Pearson's correlation values are in a range of -1 to +1. Negative values ($r < 0$) indicate negative correlation, while $r > 0$ show positive linkage. In general, no clear correlation is within a range between $-0.3 < r < +0.3$, while significant correlation ($p < 0.05$) was mainly found for a magnitude $r > |0.3|$. Correlation strength was dependent on number of genotypes measured for one trait.

Mean values were used to further analysis between trials by statistical program 'RStudio' (Team, 2015). Get into knowledge, whether a trait is a parametric or non-parametric variable, Shapiro-Wilk-test was used to test normalization of distribution. After that Levene-Test determined homogeneity of variance between trials.

Parametric traits were analyzed by ANOVA (F-Test) with p = 0.05 and, in case of significant differences of means, significant groups were determined by HSD-Tukey-Test and labeled by letters. Non-parametric traits were analyzed by Kruskal-Wallis rank sum test (H-Test) and the following Dunn's test (with Bonferroni adjustment) labeled significant different groups according to median.

Thermal imaging data was analyzed with 'RStudio' because only 11 genotypes in trial 2 were measured. Low sample number and non-parametric data distribution leaded to use H-Test (Kruskal-Wallis) for analysis of variances between varieties, and Spearman's rank correlation coefficient for correlation analysis between siCWSI and several agronomic characteristics.

3 Results

3.1 Eye-visual phenotyping traits

Traits which are observed by breeder's eyes are mainly phenological traits, which have influence on agronomic traits. Table 5 shows following scored traits: emergence (emerg), vegetative development (devscore), time to flowering (ttf) and time to maturing (ttm), reproductive phase (t-reprod), pod shattering (podshat) and lodging as well as pod set.

Emergence of soybean varieties (VE stage) was similar over all trials with mean scores between 7.44 in trial Y2 and 7.71 in trial Food. Vegetative development during V2/V3 stages shows also similar mean scores between 3.19 in trial Y2 and 3.44 in trial Food.

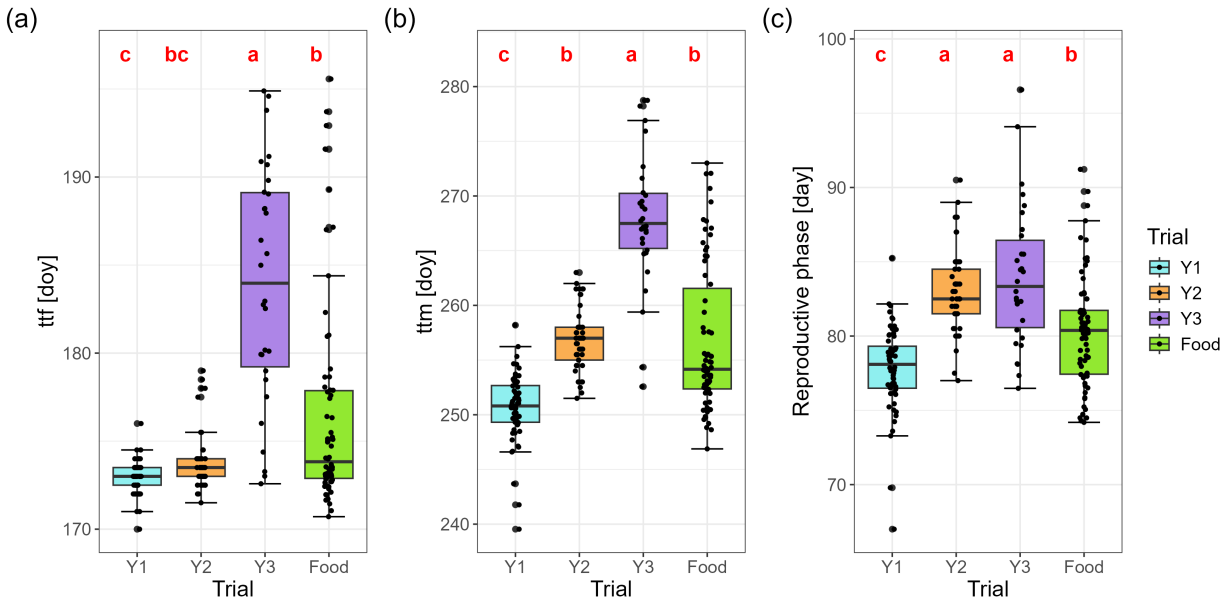

Figure 14: Boxplots with phenological variety values grouped in trials Y1, Y2, Y3 and Food: (a) timepoint when flowering phase (R1) has started; (b) timepoint when full maturity has reached (R8); (c) reproductive period of time between R1 and R8 in days; red letters show significant different groups with p<0.05; doy = day of year.

Both traits ttf (R1) and ttm (R8) varied between trials significantly. On average, **time to flowering** in trial Y1 (172.9±0.97 doy) started 0.9 days earlier than in trial Y2 (173.8±1.75 doy), 3.6 days earlier than in trial Food (176.5±6.1) and 11.1 days earlier than in trial Y3 (184.0±6.7 doy). Variance of ttf is lowest in trial Y1 and Y2 (C.V. = 0.6% and 0.5%, respectively), while Y3 show a big variance for ttf. The range for ttf in trial Y1 is with 6 days difference remarkably short, range in Y2 with 7 days lasts almost similar period. In trial Y3, ttf ranged from 173 to 196 doy over a period of 24 days. Remarkably, few varieties in trial Y3 and many varieties in trial Y2 started flowering in the same time than very early genotypes in trial Y1. Food trial showed even longest period of flowering. Figure 14a illustrates the distribution with boxplots; significant groups were labeled over all four trials.

Table 5: Overview of traits with focus on phenology in all trials (Y1, Y2, Y3, Food): emergence status (emerg) at VE stage, development score (devsc) at V2 stage, time to flowering (ttf, R1), time to mature (ttf, R8), both scored in days of the year (doy), time of reproductive phase (t-reprod, R1-R8) in days, estimated pod shattering (podshat), lodging and pod set at V8 stage; each trait with mean value (Mean), standard deviation (St.Dev.), coefficient of variance (C.V. %) and F-value to determine differences between genotypes with following significance levels (Sign.): $+$: p$<$0.1; $*$: p$<$0.05; $**$: p$<$0.01; ns: not significant.

Trait	emerg	devscore	ttf	ttm	t-reprod	podshat	lodging	pod set
Unit	[-]	[-]	[doy]	[doy]	[day]	[-]	[-]	[-]
Y1								
Range	4.9-8.5	2.0-4.5	170-176	239-258	67-85	1.0-5.0	1.0-4.5	1.0-4.1
Mean	7.53	3.27	172.87c	250.68c	77.82c	1.48	2.17a	2.71
St.Dev.	0.65	0.56	0.97	3.15	2.89	0.88	0.85	0.68
C.V.%	8.5	19.4	0.6	1.0	3.6	30.0	33.8	21.1
F-value	1.95	1.22	1.58	3.29	2.23	7.34	2.35	2.66
Sign.	$*$	ns	+	$**$	$**$	$**$	$**$	$**$
Y2								
Range	2.5–7	2.2-4.6	172-179	252-263	77-91	1.0-3.0	1.0-3.5	1.5–4.0
Mean	7.44	3.19	173.84bc	256.9b	83.06a	1.07	1.57b	2.71
St.Dev.	1.02	0.56	1.75	2.89	2.77	0.31	0.68	0.69
C.V.%	7.9	18.3	0.5	0.9	2.8	13.6	38.5	26.1
F-value	6.56	2.37	6.40	2.26	1.31	8.05	2.93	1.33
Sign.	$**$	$*$	$**$	$*$	ns	$**$	$*$	ns
Y3								
Range	5.0-9.0	1.7-4.9	173-195	253-279	76-97	1.0-2.0	1.0-4.0	1.0-4.0
Mean	7.63	3.37	183.93a	267.92a	83.98a	1.2	2.15a	2.7
St.Dev.	0.92	0.73	6.71	6.27	4.77	-	0.8	-
C.V.%	11.9	18.5	1.4	0.9	3.7	-	30.4	-
F-value	1.25	2.97	12.71	9.51	3.45	0	2.12	0
Sign.	ns	$*$	$**$	$**$	$*$	ns	+	ns
Food								
Range	6.0-9.0	1.9-4.7	171-196	247-273	74-91	1.0-5.0	1.0-5.0	1.4-4.7
Mean	7.71	3.44	176.48b	256.8b	80.32b	1.44	2.33a	2.88
St.Dev.	0.66	0.59	6.03	6.73	3.77	0.82	1.02	0.71
C.V.%	8.2	20.0	1.0	0.8	3.0	24.4	24.0	17.3
F-value	1.82	1.51	21.59	20.68	5.18	9.44	7.07	4.27
Sign.	$*$	+	$**$	$**$	$**$	$**$	$**$	$**$
H-Test (Kruskal-Wallis), trials								
p-value	0.318	0.135	<0.01**	<0.01**	<0.01**	0.059+	<0.01**	0.546

Time to maturity (R8) was reached in trial Y1 after 250.7±1.0 doy, in trial Y2 after 256.9±2.9 doy, in trial Y3 after 268.0±6.27 doy and in the food trial after 256.8±6.73 doy. Coefficients of variance of ttm was similar within trials with C.V. of 0.8 in trial Food to 1.0 in trial Y1.

In figure 14b, time to maturity is depicted in boxplots with grouped trials. Differences between trials Y1, Y2 and Y3 are significant and represent ttm of maturity groups as expected. Trial Food shows highest range in ttm due to containing varieties from different maturity groups. Although, some outliers in Y1 and Y3 indicate that some varieties may be in the wrong maturity group.

Reproductive time (t-reprod) shows significant differences in trial Y1 (77.8±2.9 days) in comparison to trials Y2 (83.1±2.8 days), Y3 (84.0±4.77 days), while Food trial (80.3±3.8 days) forms an own significant group in between. In contrast to other trials, Y2 trial has no significant differences between genotypes in reproductive time. Figure 14c shows varieties distribution of reproductive time within trials. Two outliers in trial Y1 are recognized to varieties with extraordinarily short period between ttf and ttm.

Pod shattering (podshat) was highest in Y1 (mean = 1.48) and Food (mean = 1.44). Lowest mean score for 'podshat' was found in trial Y2, but some significantly different varieties with tendency to pod shattering. In trial Y3 no pod shattering was observable.

Lodging affected varieties was found in all trials. Highest mean score for lodging was in trial Food (2.33±1.02), followed by trial Y1 (2.17±0.85) and trial Y3 (2.15±0.8). Lodging score in trial Y2 was lowest with 1.57±0.68 on average. Nevertheless, significant variety differences still exist in each trial.

Mean scores for **pod set** were similar to all trials in a range of 2.70 to 2.88. In Y1 and Food trials were significant differences between genotypes in pod set, while in genotypes of trial Y2 no significant differences were found. F-Test was not done in trial Y3 due to missing values. In summary, all trials show high average plant emergence and good vegetative development. Reproductive phase show significant differences between all trials , while flowering time (ttf), time to full maturity (ttm) are significant according to their maturity groups. Lodging and pod shattering were generally lowest in trial Y2. Mean score of pod set shows no differences between trials. Results from phenological traits are shown in table 5.

3.2 Physiological-agronomic traits

Mean **spad value** (SPAD1) was lowest in trial Y2 (mean: 41.87±1.84) and highest in trial Y3 (mean: 43.15±1.95), while trial Y1 and Food were in between. Significantly different groups were formed by Y2 and trials Y1,Y3 and Food. Boxplots in figure 15a illustrate location and distribution of varieties within trials, significantly different groups are labeled by letters. Overall, Spad value was rather more different between varieties within trials than between trials.

Second measured chlorophyll content (SPAD2) was done only in trial Y2 at 8.August. In comparison to SPAD1, SPAD2 had an increased mean value with 46.23±1.56, while no significant differences between genotypes were found.

Leaf size had lowest mean value in trials Y1 (50.89±7.4 cm²) and Y2 (49.8±9.1 cm²), which were significantly different to trials Y3 (60.87±8.37 cm²) and Food (57.8±11.35 cm²). Furthermore, significant differences between genotypes within trials were recognized. Biggest range was shown in Food (31.6-84.7 cm²). At least one plot in trial Y2 had even higher leaf size values than in Y3. This issue shows big inhomogeneity within Y2 for this trait. The distribution and significantly different groups of leaf size in varieties were shown in figure 15b.

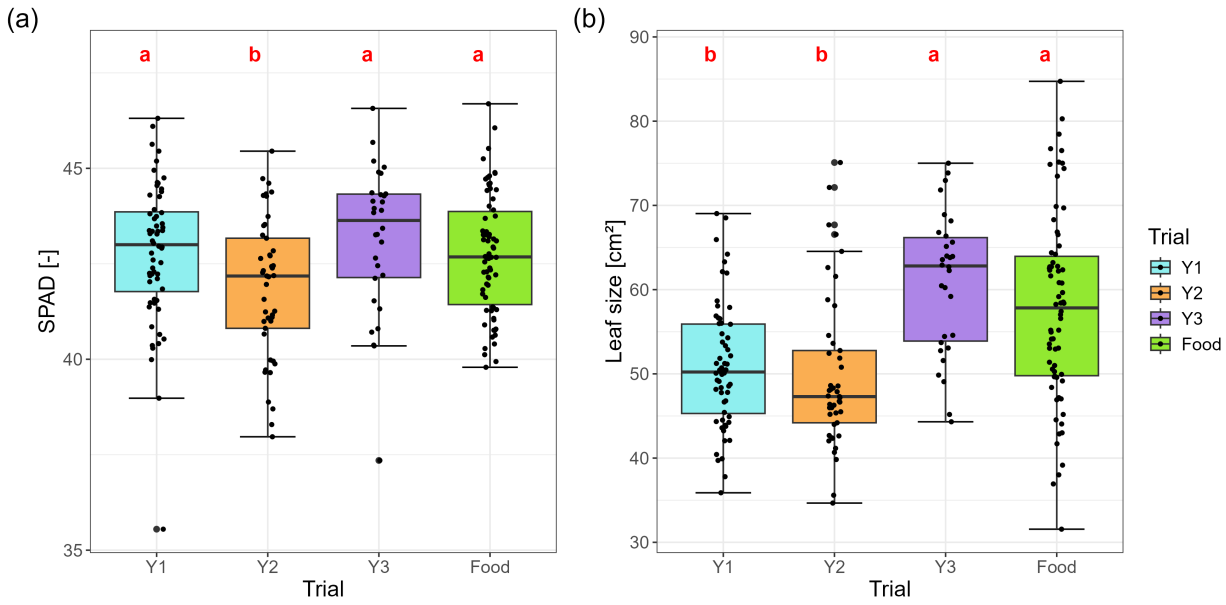

Figure 15: Boxplots with measured variety values grouped in trials Y1, Y2, Y3 and Food: (a) Spad value (SPAD1) was measured in R2/R3 stage, (b) leaf area in cm²; red letters show significant different groups with p<0.05.

Plant height was highly significant between trials and was separated in a lowest group with trial Y1 (74.38±10.64 cm), a middle group with trials Y2 (84.11±11.14 cm) and Food (81.36±10.99 cm) and a highest group with trial Y3 (92.67±8.9 cm). Nevertheless, highest plant height was measured in trial Y2 with 120 cm. Within each trial, plant height was significantly different from genotype to genotype. Figure

Table 6: Measured morphological traits in all trials (Y1, Y2, Y3, Food): Spad value in green leaves (SPAD1, at 16. July & SPAD2, at 8. August), leaf size in cm^2, stomatal density (d-stom) in stomata number per mm^2, plant height in cm and yield in dt/ha; each trait with mean value (Mean), standard deviation (St.Dev.), coefficient of variance (C.V. %) and F-value to determine differences between genotypes with following significance levels (Sign.): $+$: p$<$0.1; $*$: p$<$0.05; $**$: p$<$0.01; ns: not significant.

Trait	SPAD1	SPAD2	Leaf size	d-stom	height	yield
Unit	[-]	[-]	[cm²]	[1/mm²]	[cm]	[dt/ha]
Y1						
Range	35.6-41.8	-	35.9-69.0	-	47-102	10.8-40.4
Mean	42.8a	-	50.89b	-	74.38c	31.74ab
St.Dev.	1.85	-	7.4	-	10.64	5.9
C.V.%	5.3	-	9.6	-	8	17.7
F-value	1.35	-	4.40	-	4.77	2.48
Sign.	ns	-	$**$	-	$**$	$**$
Y2						
Range	38.0-45.5	41.6-49.1	34.7-75.1	203.4-322.2	65-112	23.8-47.1
Mean	41.87b	46.23	49.8b	251.45	84.11b	34.05a
St.Dev.	1.84	1.56	9.12	26.63	11.14	5.26
C.V.%	3.2	4.5	8	11	7	15
F-value	4.02	1.29	8.34	1.81	4.91	2.47
Sign.	$**$	ns	$**$	+	$**$	$*$
Y3						
Range	37.4-46.6	-	44.3-75.0	-	65-110	20.1-41.2
Mean	43.15a	-	60.87a	-	92.67a	30.25bc
St.Dev.	1.95	-	8.37	-	8.90	5.23
C.V.%	3.8	-	7.1	-	5.1	15.5
F-value	2.15	-	5.47	-	3.39	2.54
Sign.	+	-	$**$	-	$*$	+
Food						
Range	39.8-46.7	-	31.6-84.7	-	56-106	14.3-38.7
Mean	42.75a	-	57.8a	-	81.36b	29.03c
St.Dev.	1.58	-	11.35	-	10.99	4.79
C.V.%	2.8	-	8.1	-	6.2	15
F-value	3.51	-	11.83	-	10.02	2.41
Sign.	$**$	-	$**$	-	$**$	$**$
F-Test (Anova), trials						
p-value	<0.01**	-	<0.01**	-	<0.01**	<0.01**

16a shows plant height distribution of varieties within trials as boxplots. Remarkably, plant height was well defined among trials due to MG. However, some outliers in particular and big standard deviation on the whole show big variability within maturity group for this agronomic trait.

Average values in grain **yield** showed significant differences, which divides trial Y2 (34.05±5.26 dt/ha) from trials Y3 (30.25±5.23 dt/ha) and Food (29.03±4.79 dt/ha). Mean value of Y1 (31.74±5.9 dt/ha) shows no significant differences with both trials Y2 and Y3, but only from Food trial differs significantly, as shown in figure 16b. Big ranges in yield were recognized within all trials and significantly different yielding varieties were shown in trial Y1 ($p<0.01$), Y2 ($p<0.05$) and Food ($p<0.01$), while trial Y3 shows less different varieties due to yield ($p<0.1$).

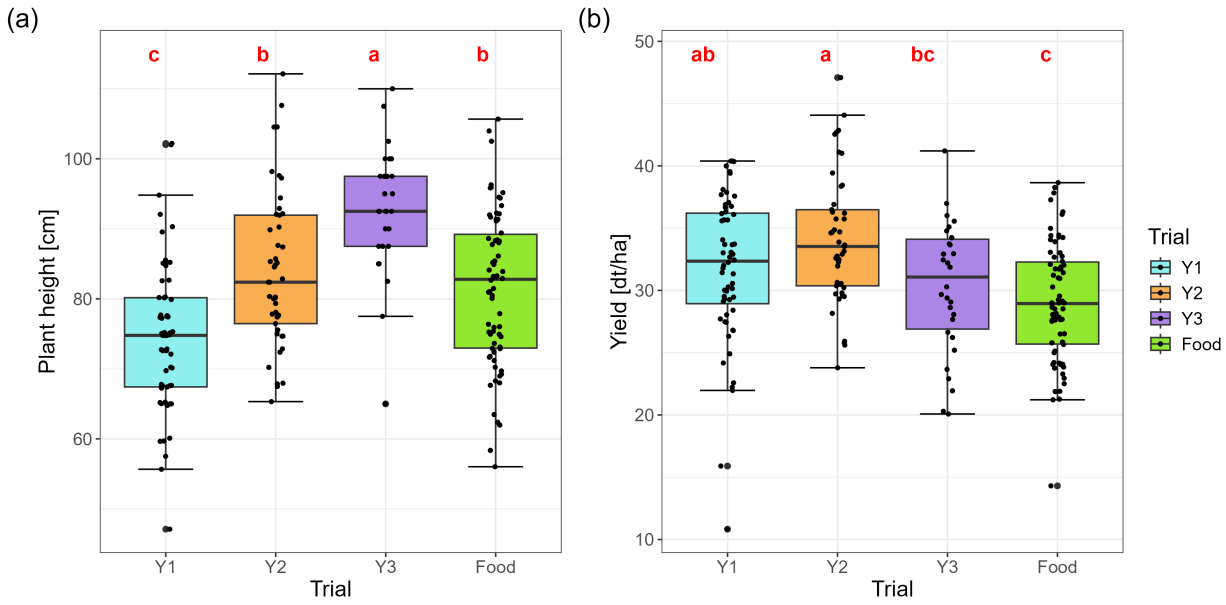

Figure 16: Boxplots with measured variety values grouped in trials Y1, Y2, Y3 and Food: (a) plant height in cm, measured in R8 stage, (b) grain yield of 0.5 m² plot area, transformed in dt/ha; red letters show significant different groups with $p<0.05$.

Summarizing these results of physiological-agronomic traits, SPAD1 values were similar between trials, but increased SPAD values were found in a second measurement three weeks later. Trial Y2 showed ordinary leaf size and plant height and highest yield. Y1 was trial with lowest mean plant height, but showed even high yield. In contrast, Y3 had highest mean leaf size and mean plant height, but significantly lower grain yield than Y2. In table 6, all results of measured morphological traits are listed.

3.3 Variety comparisons for grain yield in each trial

Grain yield of crop plants is most important quantitative trait in many breeding programs. In the following, yields of soybean varieties, grouped by trials, are listed in horizontal barplots.

Variety differences for yield in trial Y1

Grain yield of all genotypes in trial Y1 (MG 000) is depicted in figure 17 with LSD5 equal to 11.34 dt/ha. No significant difference in harvested seed yield were found in the upper 75% of varieties, while lower 25% show more variability in yield.

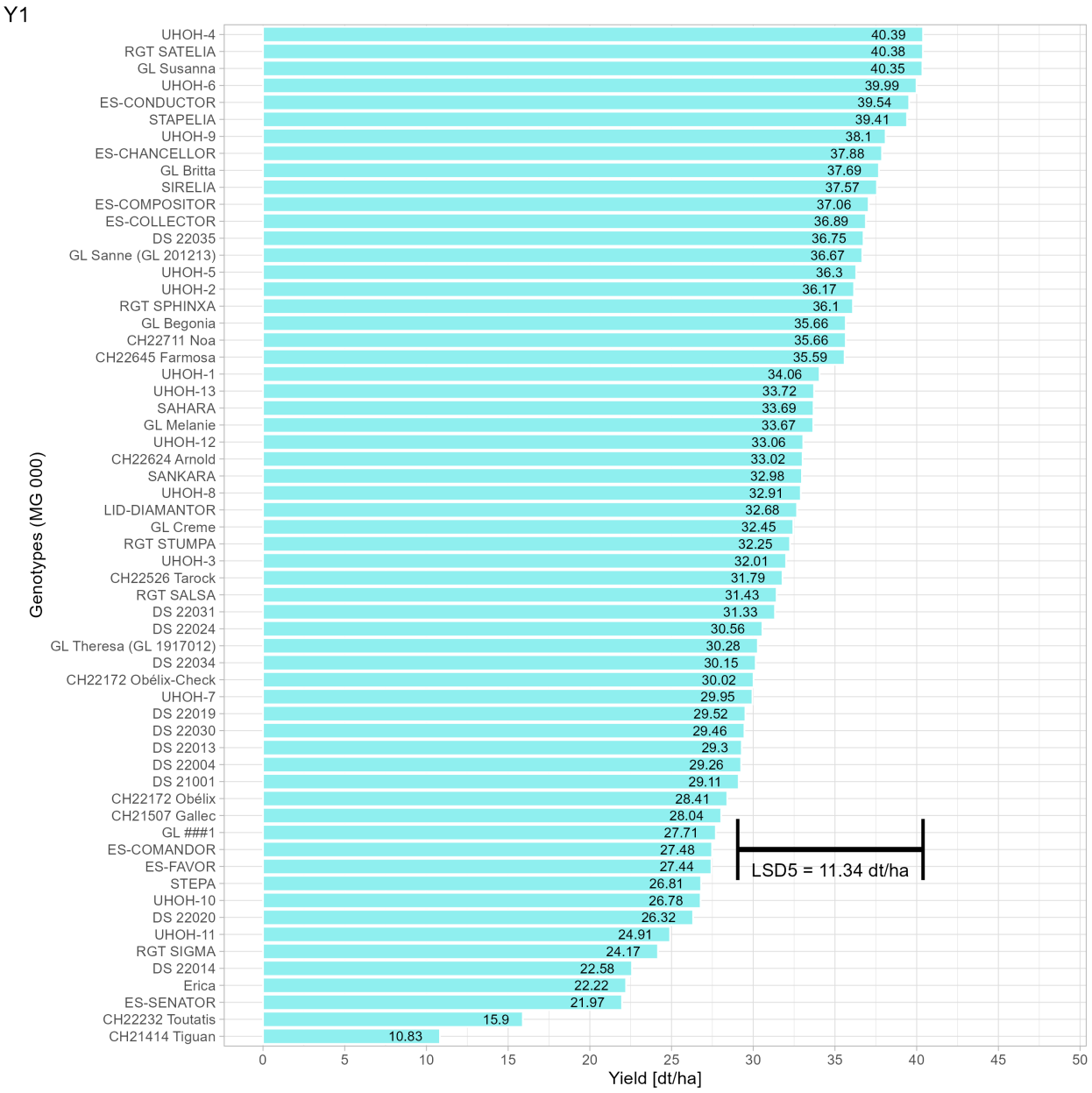

Figure 17: Yield barplot of very early varieties (MG 000) in trial Y1; least significant difference (LSD5) at a 5% probability level is added as distance bar and value.

Top three of highest-yielding lines were 'UHOH-4', 'RGT SATELIA' (RAGT) and 'GL Susanna' (SZG) at same level about 40.4 dt/ha, densely followed by three varieties 'UHOH-6', 'ES-CONDUCTOR' (LIDEA) and 'STAPELIA' (RAGT) with values about 40.0, 39.5 and 39.4 dt/ha, respectively.

Lowest-yielding variety 'CH21414 Tiguan' (AGS) resulted in 10.83 dt/ha and had, thus, significant yield difference with all other varieties trial Y1. Further low-yielding genotypes were 'CH22232 Toutatis'

(AGS) with 15.9 dt/ha, 'ES-SENATOR' (LIDEA) with 22 dt/ha, 'Erica' (DANKO) with 22.2 dt/ha and 'RGT SIGMA' (RAGT) with 22.6 dt/ha.

Variety differences for yield in trial Y2

Yield differences between varieties in trial Y2 (MG 00) are illustrated in figure 18. Significantly different yielding groups in trial Y2 can be found by LSD5 of 10.83 dt/ha.

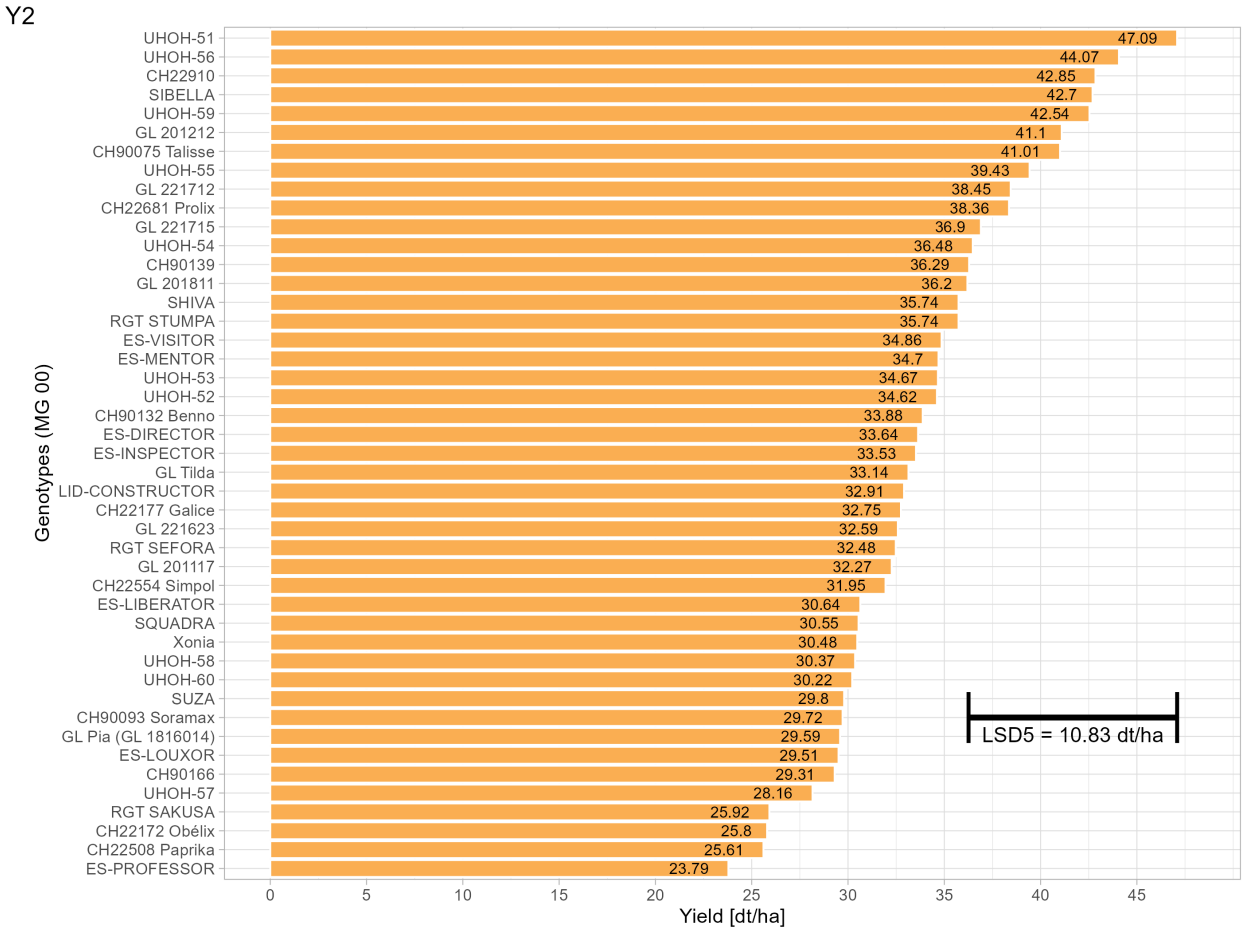

Figure 18: Yield barplot of early varieties (MG 00) in trial Y2; least significant difference (LSD5) at a 5% probability level is added as distance bar with labeled value.

Group of 13 highest-yielding varieties (28.9% of entries) was not significantly different to maximum, while 26 lowest-yielding entries showed no significant difference to the variety with minimum yield.

Variety 'UHOH-51' in trial Y2 was way ahead and resulted in a harvested seed yield of 47.1 dt/ha. Further high-yielding varieties above 41 dt/ha took places 2 to 7, with names 'UHOH-56' (44.1 dt/ha), 'CH22910' (42.9 dt/ha, AGS),'SIBELLA' (42.7 dt/ha, RAGT), 'UHOH-59' (42.5 dt/ha), 'GL201212' (41.1 dt/ha, SZG) and 'CH90075 Talisse' (41.0 dt/ha, AGS).

Lowest yield was observed for variety 'ES-PROFESSOR' (LIDEA) with 23.8 dt/ha. Similarly low yielding varieties in this experiment were 'CH22508 Paprika', 'CH22172 Obélix' (both AGS) and 'RGT

SAKUSA' (RAGT) with yields of 25.6, 25.8 and 25.9 dt/ha, respectively.

Variety differences for yield in trial Y3

Grain yield for late maturing genotypes (MG 0/I) in trial Y3 are illustrated in figure 19. LSD5 is equal to 10.31 dt/ha and shows low significant differences between varieties.

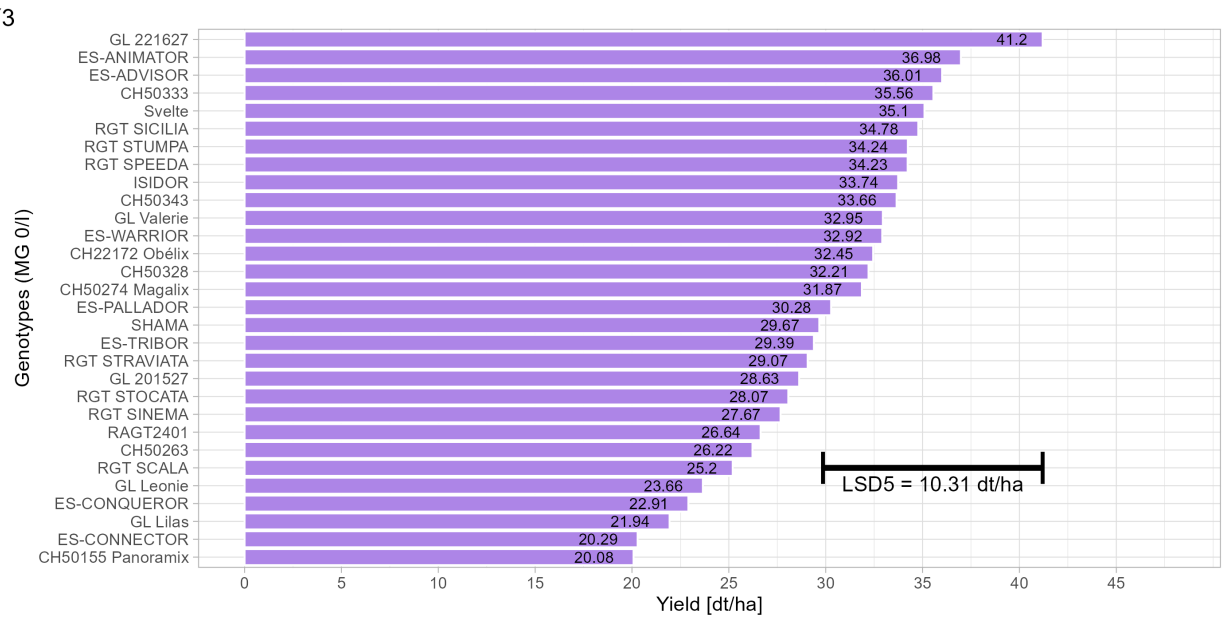

Figure 19: Yield barplot of early varieties (MG 0/I) in trial Y3; least significant difference at a 5% probability level (LSD5)is added as distance bar with labeled value.

At the top of variety table for grain yield is 'GL 221627' (SZG) with harvested 41.2 dt/ha. At following ranks another high-yielding and late ripening varieties had more than 35 dt/ha seed yield: 'ES-ANIMATOR', 'ES-ADVISOR' (both LIDEA), 'CH50333' (AGS) and 'Svelte' (SZG) resulted in 37.0, 36.0, 35.6 and 35.1 dt/ha, respectively. Upper 16 varieties (53.3% of trial Y3) had no significant difference to maximum yield.

Two lowest-yielding entries were 'CH50155 Panoramix' (AGS) with 20.1 dt/ha and 'ES-CONNECTOR' (LIDEA) with 20.29 dt/ha. Further varieties with low yields were 'GL Lilas' and 'GL Leonie' (both SZG) and 'ES-CONQUEROR' (LIDEA) with 21.9, 23.7 and 22.9 dt/ha, respectively. According to minimum yield, no significant difference was found for yields in lower 15 varieties.

Variety differences for yield in trial Food

In trial Food, significant yield differences between soybean varieties of all maturity groups (MG 000-I) were found with a LSD5 of 8.74 dt/ha, as shown in figure 20.

Top 3 of highest-yielding entries for food use were varieties 'SHIVA' (RAGT) with 38.7 dt/ha, 'ES-MENTOR' (LIDEA) with 38.3 dt/ha and breeding line 'UHOH-Food-4' with 37.8 dt/ha. Following three genotypes have reached a harvested grain yield over 36 dt/ha, namely 'RGT STUMPA' (37.8 dt/ha,

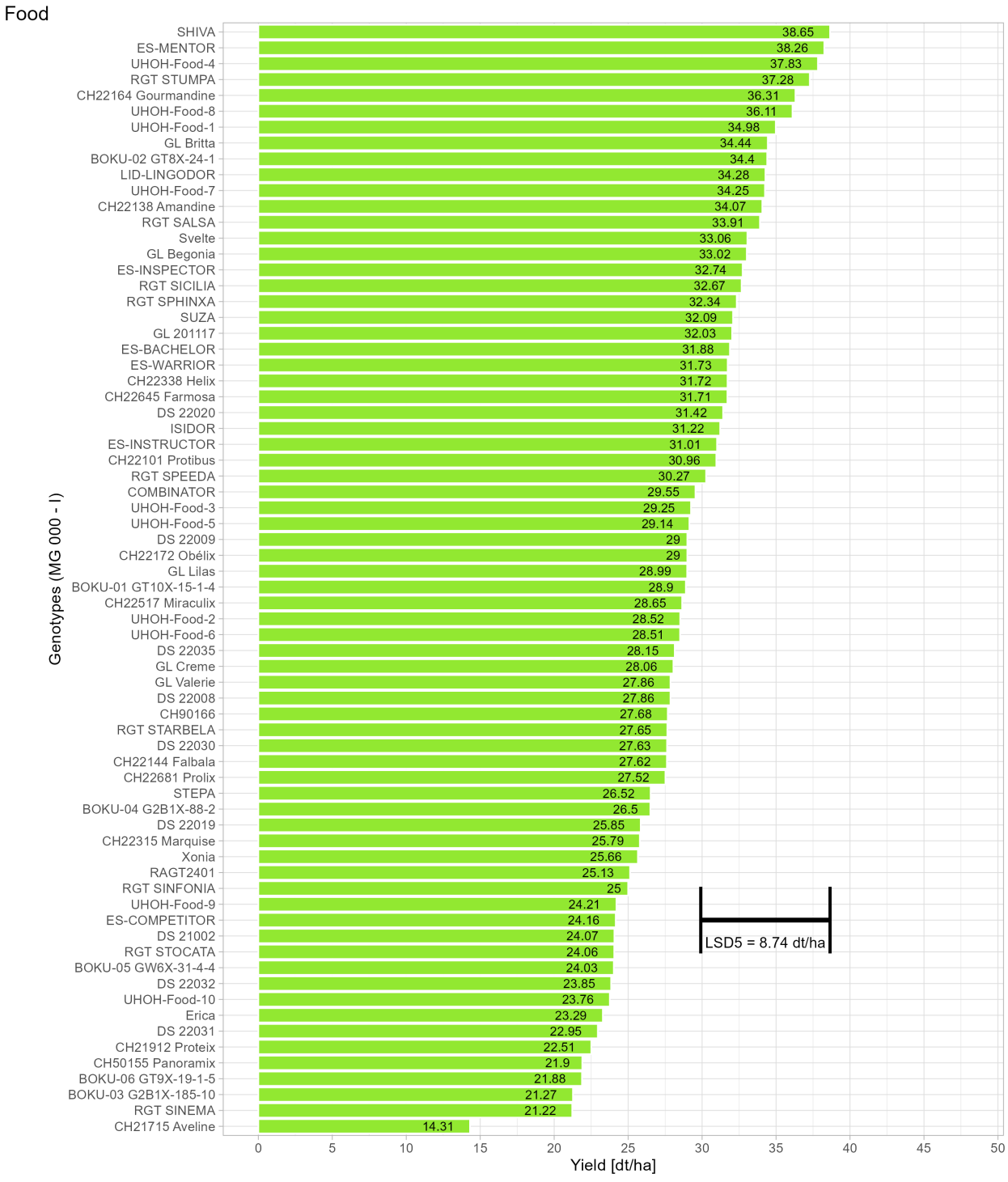

Figure 20: Yield barplot of early varieties (MGs 000-I) in trial Food; least significant difference at a 5% probability level (LSD5) is added as distance bar with labeled value.

RAGT), 'CH22164 Goumandine' (36.3 dt/ha, AGS) and 'UHOH-Food-8' with 36.1 dt/ha. Upper yielding group of 29 entries (41.4%) had no significantly different yield compared to maximum in trial Food.

Lowest-yielding variety in Food trial is 'CH21715 Aveline' (14.3 dt/ha, AGS) which is significantly different to all other entries, with exception to six varieties with a grain yield below 23 dt/ha. These low-yielding varieties were 'RGT SINEMA' (21.2 dt/ha) from RAGT; 'BOKU-03 G3B1X-185-10' (21.3 dt/ha) and 'BOKU-06 GT9X-19-1-5' (21. dt/ha), both from BOKU; 'CH50155 Panoramix' (21.9 dt/ha) and 'CH21912 Proteix' (22.5 dt/ha), both from AGS; and 'DS 22031' from DANKO with harvested seed yield of 23.0 dt/ha.

3.4 Variety comparisons for stomatal density in trial Y2

Stomatal density (SD) on abaxial leaf surface significantly differs between soybean varieties of trial Y2. Figure 21 shows these differences in a barplot with a LSD5 of 58.9 stomata per mm².

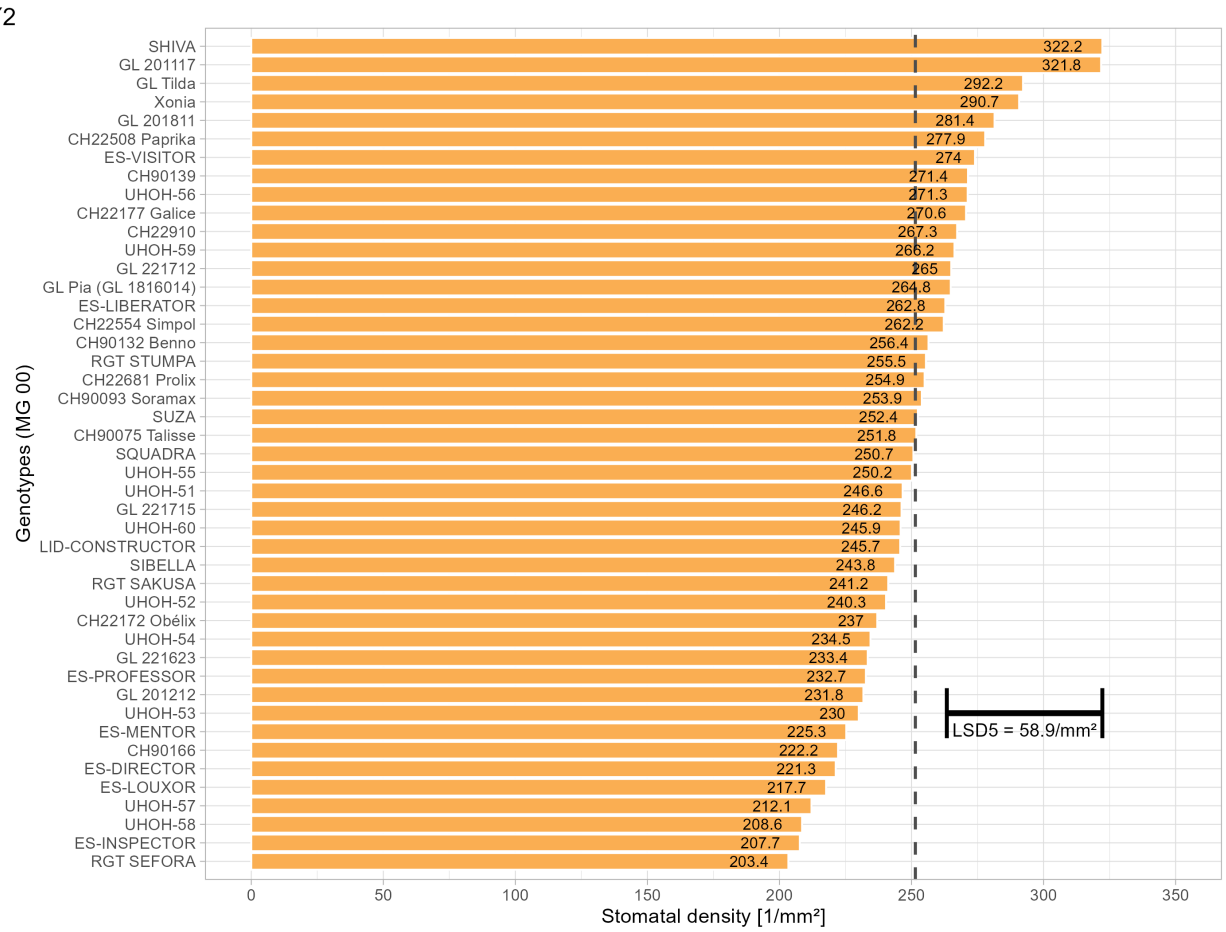

Figure 21: Barplot of stomatal density for mid early varieties (MG 00) in trial Y2; least significant difference at a 5% probability level (LSD5) is added as distance bar with labeled value; dotted line represents the overall mean = 251.45 stomata/mm².

Highest counted SD around 322 stomata per mm² were achieved by varieties 'SHIVA' (RAGT) and 'GL 201117' (SZG). Following three varieties in SD ranking were 'GL Tilda' (292/mm²) and 'Xonia' (290/mm²) and 'GL 201811' (281/mm²) that all three derived to SZG.

Varieties with lowest SD were 'RGT SEFORA' (203.4/mm², RAGT), 'ES-INSPECTOR' (207.7/mm², LIDEA) and two breeding lines from UHOH, namely 'UHOH-58' (208.6/mm²) and 'UHOH-57' (212.1/mm²). Significant differences from variety 'SHIVA' were found for the lower 69% of varieties. Lowest ranked variety for stomatal density ('RGT SEFORA') is significantly different to the upper third (33.3%)varieties of trial Y2.

3.5 Correlation between time to maturity and yield / plant height

Correlation analysis between time to maturity (ttm) and **plant height** shows positive and partly significant relationship. Lowest Pearson's correlation coefficient was found in Y1 (r = 0.24, p = 0.067). In contrast, significant correlation shows Y2 (r = 0.38, p = 0.011*) and Y3 shows even stronger relationship to plant height (r = 0.64, p<0.001**).

Yield and ttm have also a linkage, but in a different pattern within trials. Trial Y1 shows a strong positive correlation (r = 0.46, p<0.01**) between full maturity and yield. Differently to Y1, correlation in trial Y2 is not significant and seemingly positive (r = 0.21, p = 0.175). In contrast, trial Y3 is significantly correlated to maturity time (r = -0.47, p = 0.008), but in a negative way.

Scatterplots in figure 22 illustrate the correlation of ttm with plant height (a) and yield (b) with regression lines and are labeled with Pearson's correlation coefficient (r) and probability level (p) for trials Y1, Y2 and Y3. Furthermore, density plots on the side axis represent bimodal distribution of maturity time in

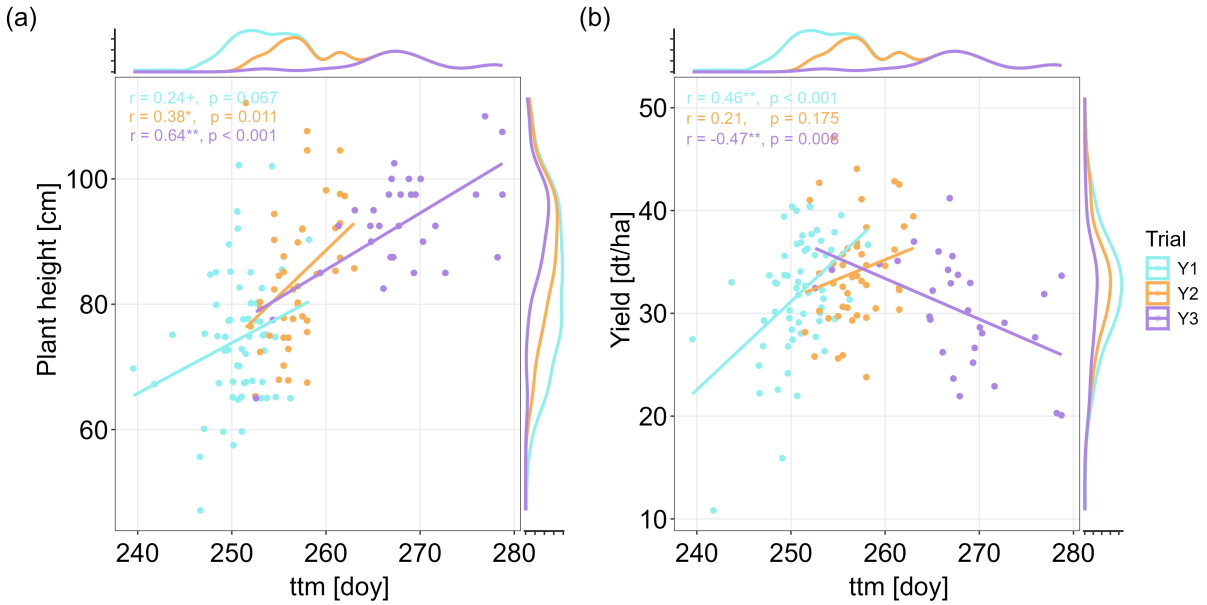

Figure 22: Scatterplots with regression line between time to full maturity (ttm) in doy and (a) plant height in cm and (b) grain yield in dt/ha, separated in trials Y1, Y2 and Y3; r = Pearson's correlation coefficient, p = significance level with **: p<0.01, *: p<0.05; +: p<0.1.

trial Y2. Plant height distribution shows a big range with even one peak, while grain yield shows normal distribution very well. In the following, correlation between ttm and yield is displayed at variety level for all four trials.

3.5.1 Time to maturity vs. yield in trial Y1

Trial Y1 is consisted of very early genotypes (MG 000 and earlier) and shows correlations in some other vegetative and reproductive traits than described above (see supplementary material, table S5). As mentioned above, the correlation of ttm and yield is positively correlated in trial Y1. Figure 23 shows the spatial distribution of all varieties between both traits and divided by trait mean values in four parts.

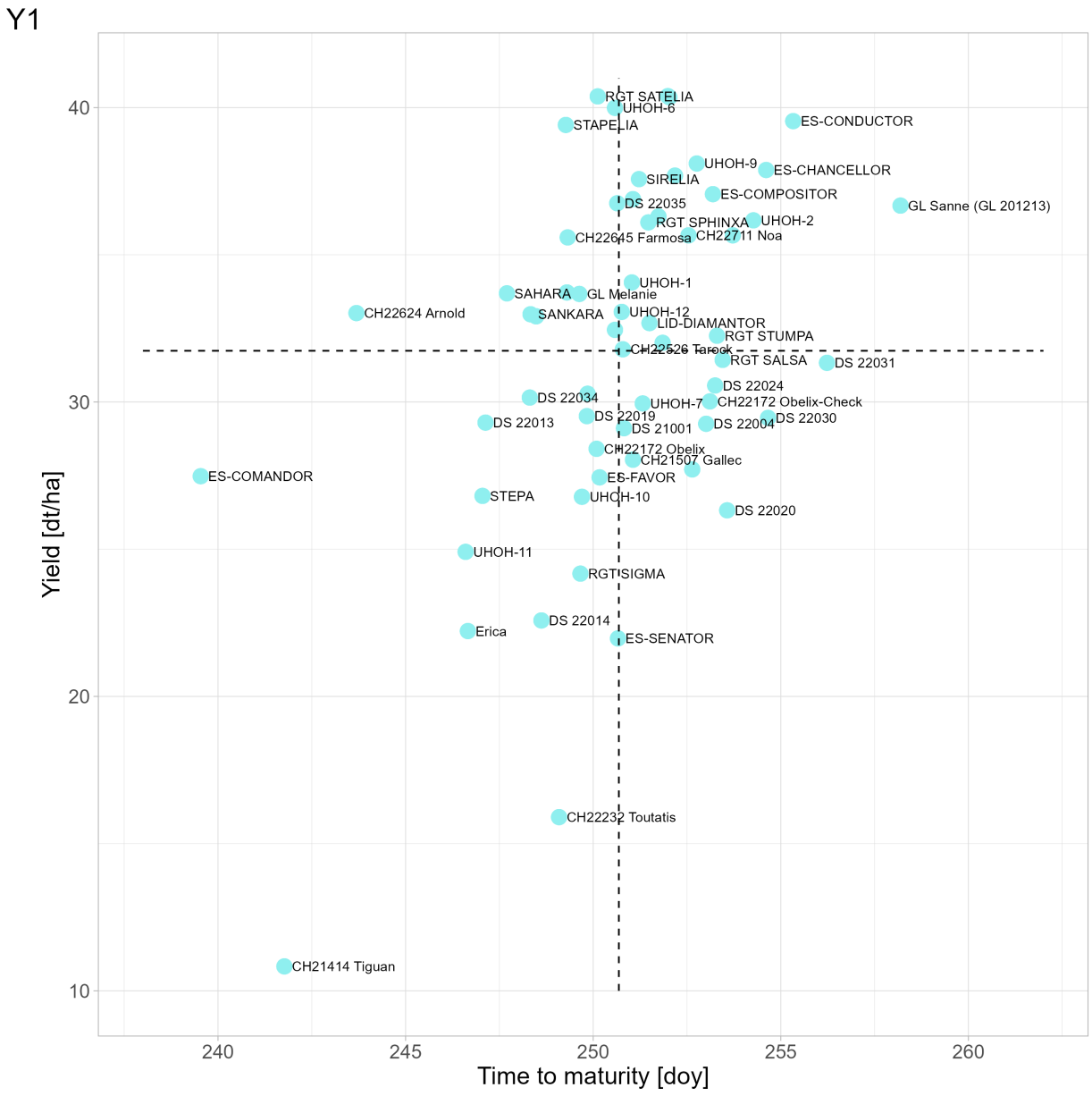

Figure 23: Scatterplot between time to maturity (ttm) and grain yield, position of most entries of trial Y1 was labeled by variety name; dashed lines show the mean values for each trait.

Very early maturing genotypes were 'ES-COMMANDOR' (LIDEA), 'CH21414 Tiguan' and 'CH22624 Arnold' (both AGS). Yield loss of 'CH21414 Tiguan' was severely affected by pod shattering, while 'ES-

COMMANDOR' and 'CH22624 Arnold' had moderate and even above-average yield, respectively. Most very early varieties in MG 000 show lower yield than the average.

Remarkably, 'SAHARA' and 'SANKARA' (both RAGT), 'UHOH-8' and 'UHOH-13' (both UHOH), and finally 'GL Melanie' (SZG) were also above-average yield and earlier matured than the mean. Highest yields combined with relatively early maturity time were achieved by varieties 'RGT SATELIA', 'STAPELIA' (both RAGT) and 'UHOH-6'.

3.5.2 Time to maturity vs. yield in trial Y2

Trial Y2 contains mid-early germplasms (MG 00) and shows cohesion between several traits (see supplementary material, table S6). Relationship between maturity time and grain yield was mentioned above with not significant correlation. Scatterplot in figure 24 shows the position of individual varieties in trial Y2 for ttm and yield, dashed lines indicate the mean of each trait and divide the plot in four regions.

The region with relatively short maturity time and high yields is dominated by varieties 'UHOH-51' (UHOH), 'SIBELLA' (LIDEA) and 'CH90075 Talisse' (AGS) with yields above 40 dt/ha and maturity time lower than 125 days.

Most early maturing varieties achieved average or lower yields. Some very low yielding and very early genotypes were 'UHOH-60' and 'UHOH-57' (both UHOH), 'CH22172 Obélix' (AGS), while lowest total yields were found in varieties with more or less mean maturity time, namely 'CH22508 Paprika' (AGS), 'RGT SAKUSA' (RAGT) and 'ES-PROFESSOR' (LIDEA). Relatively late varieties with yield below the average were 'RGT SEFORA' (RAGT), 'GL 201117' (SZG, not labeled) and 'UHOH-58' (UHOH)

In the quarter with high yields and relatively long time to maturity were the outstanding breeding lines 'CH22910' (AGS) and 'UHOH-59' (UHOH) above 40 dt/ha and maturity 130 days after sowing. Germplasms with similar ttm and above-average yields were labeled as 'UHOH-55' (UHOH), 'GL221712' and 'GL201811' (both SZG).

In summary, main varieties were located closely to average ttm and yield (dashed lines in figure 24). Only few 'outlier' varieties have positions on the edges of each quarter.

Furthermore, several scored traits were correlated with plant height. Higher plants were related to high emergence (r = 0.35), later blooming date (r = 0.375), higher scores for pod shattering (r = 0.34) and lodging (r = 0.39). Additionally, there is strong negative correlation between height and pod-set (r = -0.61).

Spad values (SPAD1, SPAD2) has no mutual correlation and no relationship with any observed trait. Similarily, stomatal density shows no relationship to other traits in trial 2.

3.5.3 Time to maturity vs. yield in trial Y3

Trial Y3 includes late varieties from MG 0 and MG I with some correlations in scored and measured traits (see supplementary material, S7). As mentioned in section 3.5, ttm is significantly correlated with grain yield in trial Y3 on a negative way, which means relatively early varieties show higher yields in most times, and vice versa.

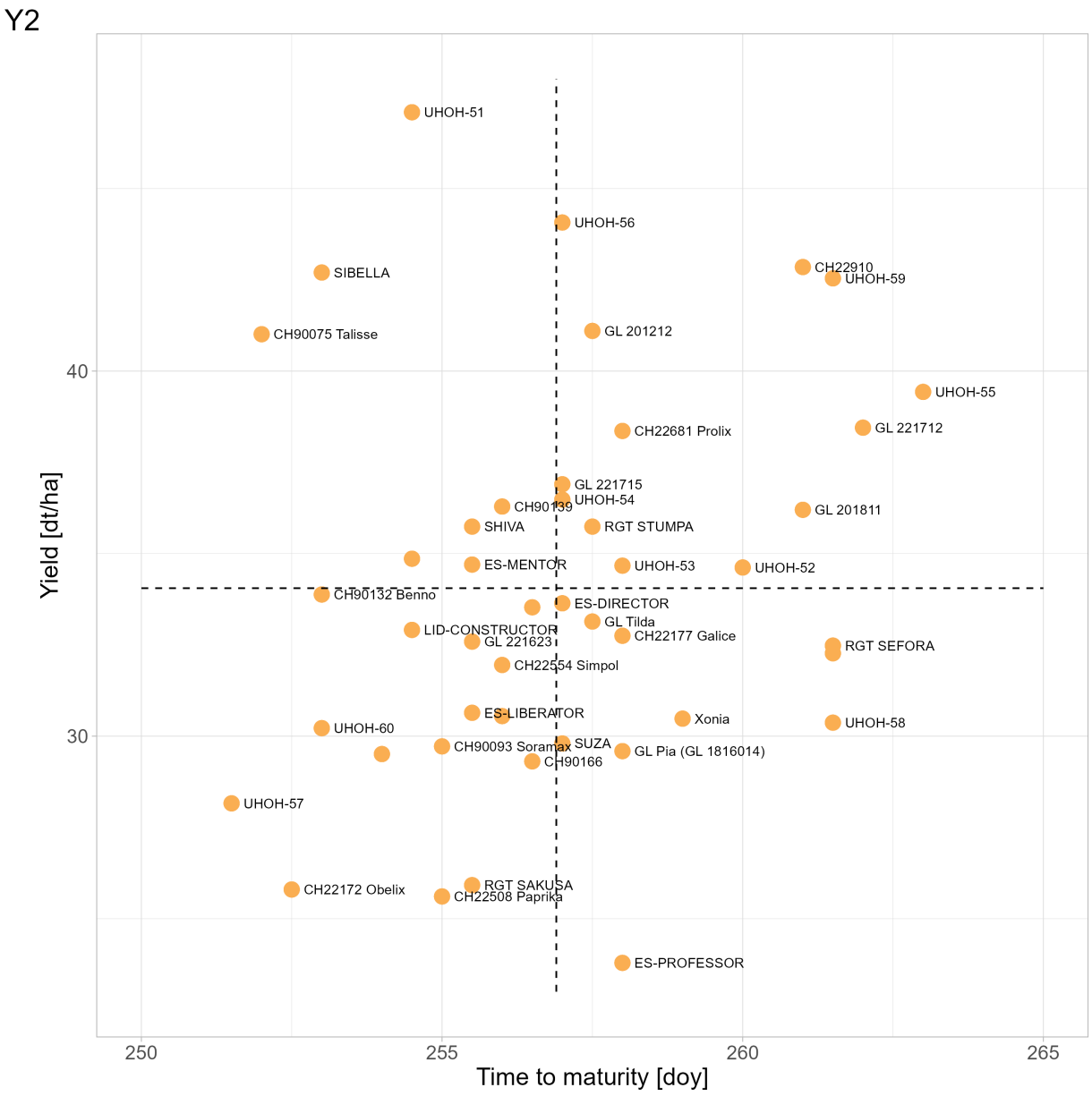

Figure 24: Scatterplot between time to maturity (ttm) and grain yield, position of most entries of trial Y2 was labeled by variety name; dashed lines show the mean values for each trait.

Figure 25 shows spatial distribution of ttm and yield in a two-dimensional matrix for all varieties of MG 0 and MG I in trial Y3.

In the corner of very late maturity time (above 145 days) and lowest yield (about 20 dt/ha) were two varieties 'CH50155 Panoramix' (AGS) and 'ES CONNECTOR' (LIDEA). Similar late ttm, but yields above average were met by varieties 'CH50343' and 'CH50274' (both AGS).

Varieties with relatively short ttm had shown only above-average yields. Earliest matured genotypes in trial Y3 were both check varieties 'CH22172 Obélix' (AGS) and 'RGT STUMPA' (RAGT), which belong

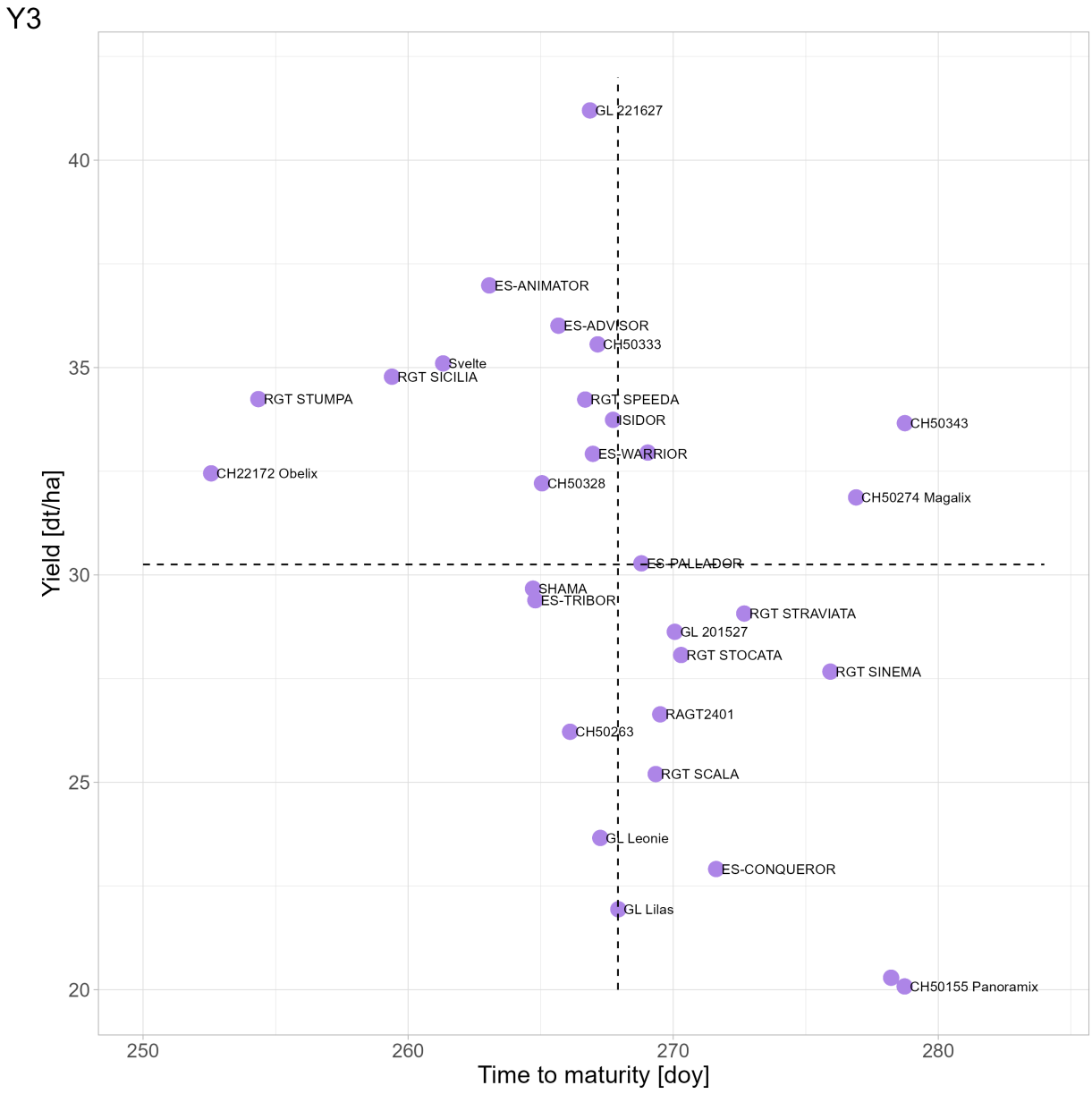

Figure 25: Scatterplot between time to maturity (ttm) and grain yield, position of most entries of trial Y3 was labeled by variety name; dashed lines show the mean values for each trait.

to MG 000 and MG 00, respectively. Further varieties of with short ttm were 'RGT SICILIA' (RAGT), 'Svelte' (SZG) and 'ES-ANIMATOR' (LIDEA) from MG 0.

3.5.4 Time to maturity vs. yield in trial Food

In trial Food, varieties have been selected for food use, but not to maturity. That's why all before mentioned mature groups (MG 000 - I) were included and examined for correlations in phenotyped plant characteristics (see supplementary material, S8).

Yield and ttm were negatively correlated in trial Food (r = -0.28**), but less strong than in trial Y3. Scatterplot with both traits for varieties in trial Food is displayed in figure 26, including means as dashed lines. In the region with very late maturing varieties (more than 140 days after sowing) and low yields (equal or below 25 dt/ha) is taken by 'RGT SINEMA' (RAGT), 'CH50155 Panoramix' (AGS). Two breeding lines of BOKU ('BOKU-03 G2B1X-185-10' and 'BOKU-06 GT9X-19-1-5) were nearly located at the same yield level, but earlier matured. Genotypes 'RGT SINFONIA' and 'RAGT2401' (both RAGT) had also very late date for full maturity, but had higher yields about 25 dt/ha.

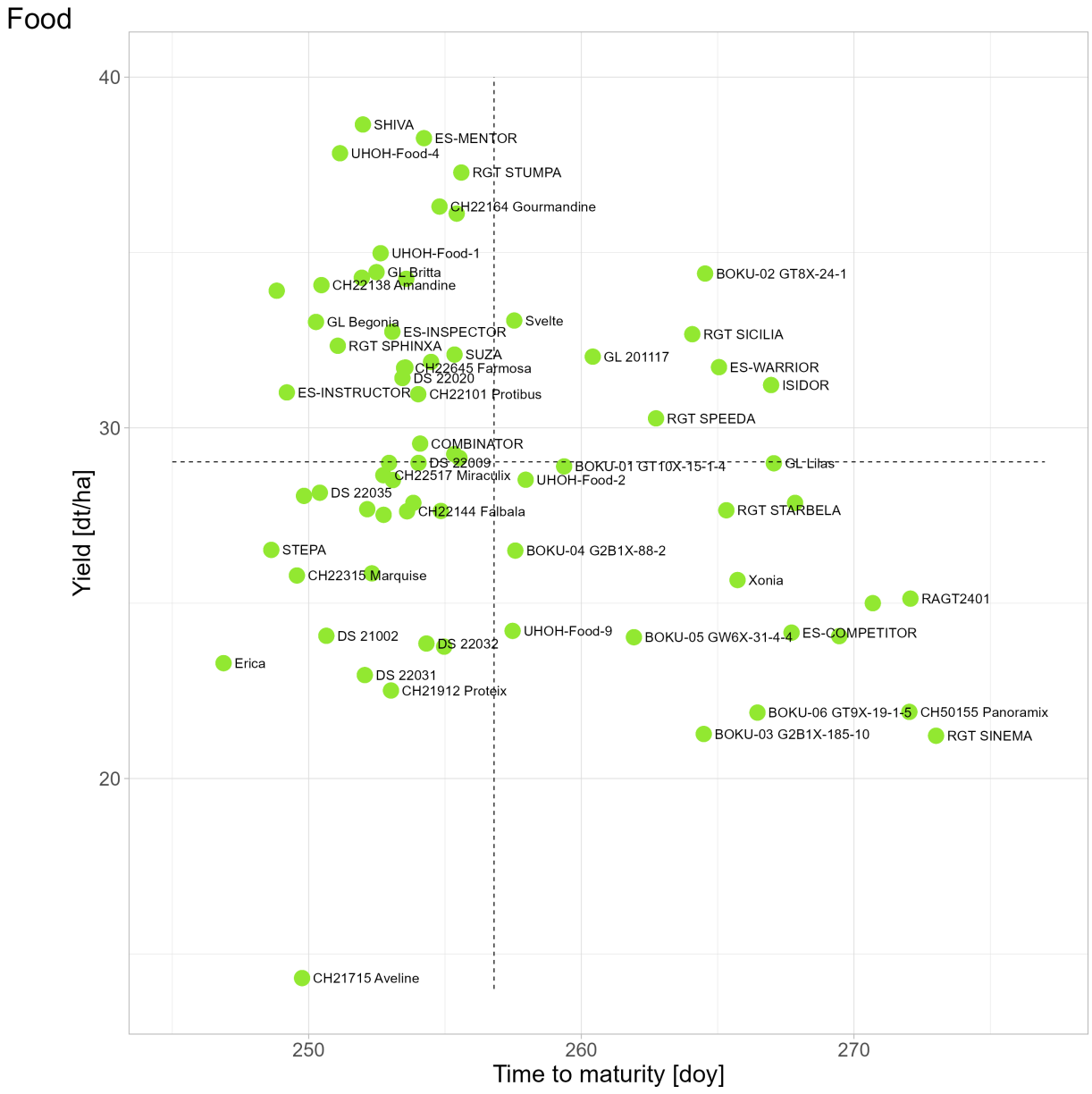

Figure 26: Scatterplot between time to maturity (ttm) and grain yield, position of most entries of trial Food was labeled by variety name; dashed lines show the mean values for each trait.

Relatively early genotypes (less than 120 days after sowing) in trial Food combined with low yields were 'CH21715 Aveline' (AGS), 'Erica' (DANKO), 'CH22315 Marquise' (AGS), 'STEPA' and 'SALSA' (both RAGT). Varieties with similar early ttm, but yields above average were achieved by 'ES-INSTRUCTOR' (LIDEA) and 'GL Begonia' (SZG) and 'RGT Salsa' (RAGT, not labeled in plot).

Highest yielding varieties were ranged in maturity time below average (less than 125 days after sowing) and called 'SHIVA' and 'RGT STUMPA' (both RAGT), 'ES-MENTOR' (LIDEA), and 'UHOH-Food-4' (UHOH).

Varieties with relatively high ttm (more than 132 days after sowing) and yields above average were located in the right upper corner of the scatterplot, which are called 'BOKU-02-GT8X-24-1' (BOKU), 'RGT SICILIA' (RAGT), 'ES-WARRIOR' and 'ISIDOR'. Leaf size (r = 0.49 and 0.54) and plant height (r = 0.65 and 0.67) are positively correlated to ttm and ttf, while yield shows negative correlation to both reproductive stages (r = -0.31 and -0.28).

3.6 Physiological traits - screening methods

Hyperspectral reflectance screenings were conducted between 11:00 and 14:00h (CEST)for all four trials at days with high solar radiation g_{rad} that indicates sunny and clear sky during all measurements. Thermal imaging was done only in trial Y2 during reproductive stages R3 - R5 on days with different environmental conditions. Furthermore, thermography screenings were done at mid-day between 12:00 and 13:00h (CEST) and in the afternoon between 15:00 and 16:00h (CEST).

3.6.1 Hyperspectral reflectance

Diverse timepoints show high global radiation above 600 W/m², while there is a remark for timepoint K, that the sky was 'slightly overcast'. The average air temperature (T_a) during measurements (11:00h - 14:00h) are highest at timepoints G (30.4℃) and K (28.9℃) for trials Y1, Y2 and Y3, while timepoints G, L (29.3℃) and B (28.6℃) were warmest for Food trial.

Vapor pressure deficit (VPD) shows highest values at timepoints D, G and K with values 1.71, 2.02 and 1.91 kPa, respectively for screening in trials Y1, Y2 and Y3. Highest VPD values for Food trials were calculated at timepoints E, G and L with values 1.75, 2.02 and 1.60 kPa, respectively.

Including breeder's remarks, 'wet' soils indicate no water-stress in plants due to previous rainfalls. Negative selection of timepoints to recorded soil conditions will provide timepoints D, E, G, K and L as appropriate dates to detect moderate water stress in soybean plants. Among all hyperspectral screening dates, these five timepoints show also highest VPD values between 1.60 and 2.02 kPa.

Table 7 summarizes all screening timepoints done with hyperspectral reflectance.

3.6.2 Correlations between agronomic traits and spectral reflectance indices

Some agronomic traits (yield, height, ttf, ttm and leaf area) were examined to find relationships with hyperspectral indices which allow to indicate chlorophyll content and water status of soybean varieties.

Table 7: Overview of hyperspectral screening dates for all subsets; prevailing air temperature and radiation are mean values between 11:00 and 14:00; T_a = air Temperature in ℃, g_rad is global radiation in W/m², rH is relative humidity in %, VPD is vapor pressure deficit in kPa.

ID	Date	Evaluated trials	T_a	g_{rad}	rH	VPD	Remarks	
			[℃]	[W/m²]	[%]	[kPa]	precipitation	soil
A	14.07.2024	Y1 - Y2 - Y3	25.4	703.6	64.0	1.20	35 mm rain, 36h ago	wet
B	15.07.2024	Food	28.6	678.5	60.9	1.57	35 mm rain, 60h ago	wet
D	18.07.2024	Y1 - Y2 - Y3	26.3	687.2	51.1	1.71	5 mm rain, 30h ago	–
E	19.07.2024	Food	27.4	707.3	53.5	1.75	5 mm rain, 54 h ago	–
G	27.07.2024	Y1 - Y2 - Y3 - Food	30.1	656.2	54.1	2.02	1 mm rain, 100 h ago	dry
J	07.08.2024	Y1 - Y2 - Y3 - Food	24.7	648.8	61.9	1.21	15 mm rain, 48 h ago	wet
K	12.08.2024	Y1 - Y2 - Y3	28.9	629.7	53.2	1.91	slightly overcast	–
L	13.08.2024	Food	29.3	671.3	61.8	1.60	7 mm rain, 10 h ago	wet

In the following, correlation of each agronomic trait is treated separately to all 16 spectral reflectance indices which were used in this work (compare to table 4). Correlation coefficient r is the average value of all 5 timepoints, when trials were screened. Each trial is solely described for r between agronomic trait and indices.

All r values for each timepoint are listed as supplementary material for trial Y1 on tables S9a, S9b and S9c; for trial Y2 on tables S10a, S10b and S10c; for trial Y3 on tables S11a, S11b and S11c; and for trial Food on tables S12a, S12b and S12c. First of all results, significant differences between varieties were evaluated. At almost all timepoints vegetation indices and chlorophyll indices showed significant varietal differences, but water indices were not significantly different for most timepoints (see supplementary material).

Correlation of yield and hyperspectral indices

Figure 27 illustrates the correlations between soybean yield and hyperspectral indices for all trials as line plot. Over all trials, very early matured genotypes in Y1 had shown highest correlation values for yield, while mid-early matured varieties in Y2 showed second highest r values, following by Food trial. No relationship between yield and hyperspectral indices was found in late maturing genotypes of trial Y3.

Highest positive correlation in Y1 (r = 0.46**) and Y2 (r = 0.33*) was found between yield and Red Edge Inflection Point (REIP) which indicates nitrogen content. In analogous way, chlorophyll indices CI (r = 0.41**), PSSRa (r = 0.33*)and PSSRb (r = 0.36**) and vegetation index NDVI (r = 0.34**) had high positive correlation with yield for trial Y1. Vegetation index MA1-R shows significantly negative correlation with yield in trial Y1 (r(MA1-R) = -0.29*), while other trials are not significant for this index.

Among 9 tested water indices, only WI is positively correlated for trial Y1 (r = 0.28*), while WI-1 was negatively correlated to for trial Y1 (r = -0.41**). Water indices NWI-2 and NWI-4 showed significant

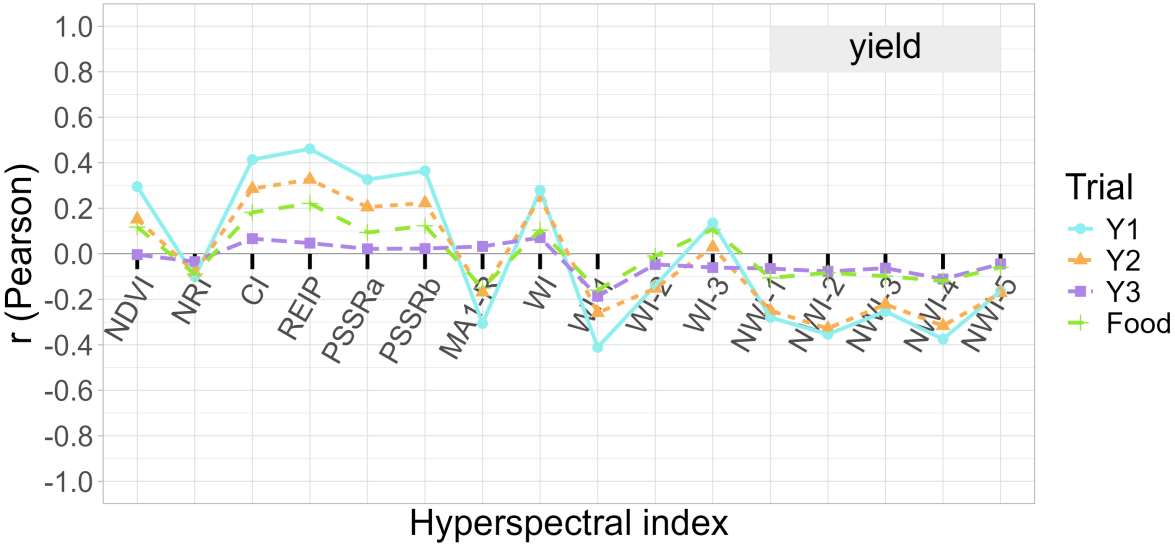

Figure 27: Correlation coefficients (r) for the relationship between soybean yield and spectral reflectance indices, grouped in trials with different maturity groups, averaged across all five timepoints.

correlation with trial Y1 (r(NWI-2) = -0.35** and r(NWI-4) = -0.375**) and trial Y2 (r(NWI-2) = -0.33* and r(NWI-4) = -0.30*)).

Summarizing, there are some chlorophyll indices and also water indices with significantly high correlations for seed yield in soybean varieties, especially in field trials with early maturing MG because of advanced development stage during screening period.

Correlation of plant height and hyperspectral indices

Plant height shows significant correlation for some hyperspectral indices, as shown in figure 28.

In **trial Y1** (MG 000), significant relationship with plant height was found only in water indices. WI is positively correlated (r = 0.35**), while other water indices are negatively correlated with lowest r values for WI-1 (r = -0.52**), NWI-2 (r = -0.48**) and NWI-4 (r = -0.48**).

Varieties of **trial Y2** (MG 00) show significant correlation for height and a lot of indices. Negative relationship was calculated for vegetation index NDVI (r = -0.31*), and chlorophyll indices PSSRa (r = -0.30*) and PSSRb (r = -0.33*) and plant height. Furthermore, Water indices WI-1 (r = -0.45**), WI-3 (r = 0.39**), NWI-2 (r = -0.39**) and NWI-4 (r = -0.36*) show significant correlation coefficients with plant height in trial Y2.

Plant height was not significantly correlated with hyperspectral indices in **trial Y3**, except water index NWI-2 (r = -0.386*). In **trial Food**, correlation between height and indices show the same pattern as in trial Y1: water indices WI (r = 0.33**) was positively correlated, while other indices with lowest r values were found for WI-1 (r = -0.45**), NWI-2 (r = -0.48**) and NWI-4 (r = -0.43**).

In summary, Water indices WI, WI-1, NWI-2 and NWI-4 have best correlations with plant height over all soybean trials. Furthermore, only trial Y2 has remarkably strong correlation between plant height

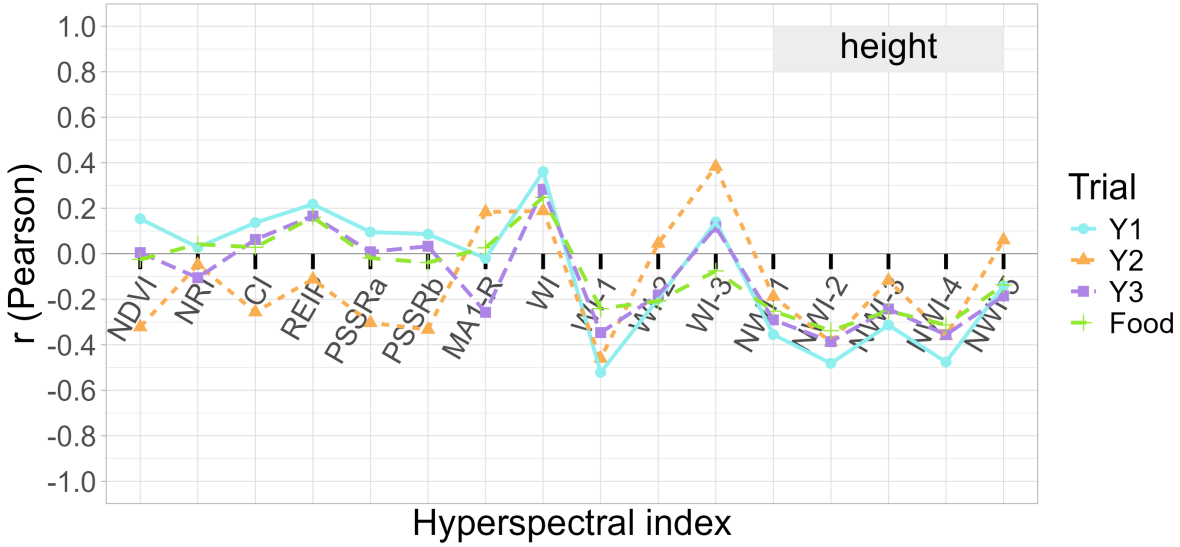

Figure 28: Correlation coefficients (r) for the relationship between plant height and spectral reflectance indices, grouped in trials with different maturity groups, averaged r values across all five timepoints.

and NDVI, PSSRa and PSSRb.

Correlation of time to flowering (ttf) and hyperspectral indices

Time to flowering (ttf) has no significant correlation between any hyperspectral index in any trial. Figure 29 illustrates the correlation patterns between (ttf) over 16 indices for each trial.

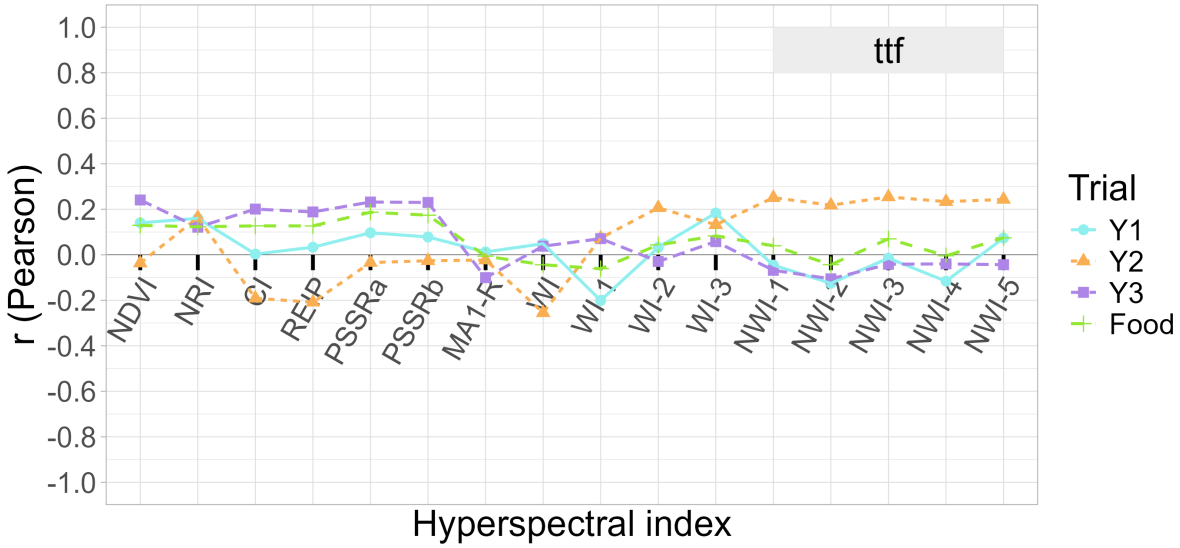

Figure 29: Correlation coefficients (r) for the relationship between flowering time (ttf) and spectral reflectance indices, grouped in trials with different maturity groups, averaged r values across all five timepoints.

Even if there is no strong correlation, varieties of **trial Y2** show a different relationship to most indices compared to trials Y1, Y3 and Food. Water indices NWI-1, NWI-2 and NWI-5 show relative high correlation coefficients around r = 0.25 for ttf in trial Y2.

Correlation of time to maturity (ttm) and hyperspectral indices

Relationship between ttm and hyperspectral indices is presented in figure 30 for all four trials as Pearson's correlation coefficients (r).

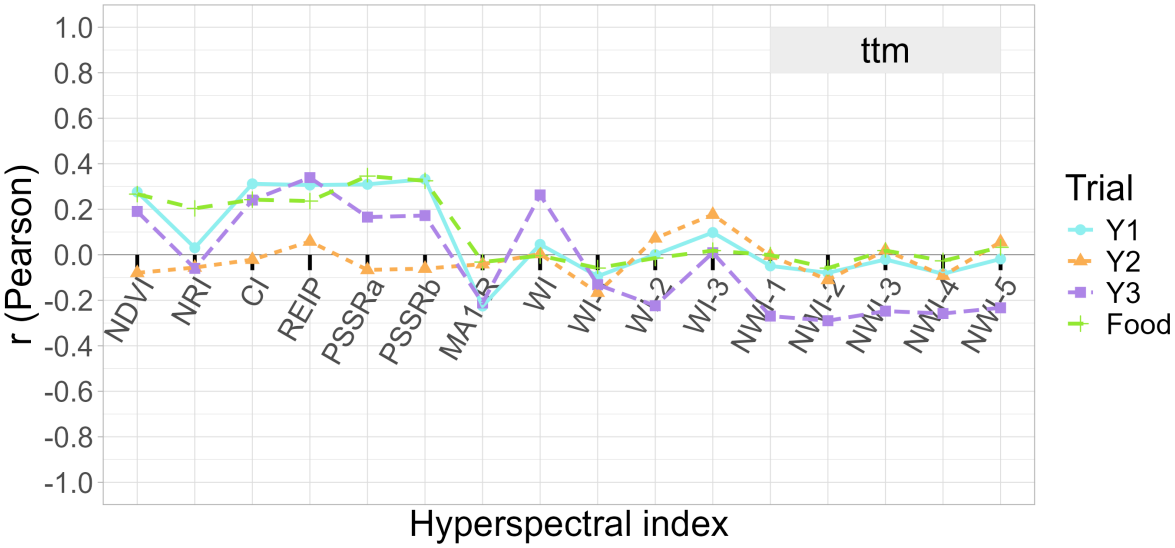

Figure 30: Correlation coefficients (r) for the relationship between maturity time (ttm) and spectral reflectance indices, grouped in trials with different maturity groups, averaged r values across all five timepoints.

Only vegetation and chlorophyll indices show significant correlation with ttm, while water indices were not significantly correlated to ttm. Varieties in **trial Y1** show significant relationship between ttm and NDVI (r = 0.32*), CI, REIP and PSSRa (all three r = 0.31*), and PSSRb (r = 0.33*), respectively. In **trial Y2**, ttm of varieties has no correlation with any hyperspectral index. **Trial Y3** shows a similar correlation pattern for vegetation indices and ttm, and relative high negative correlations for water indices and ttm, but all r values are not significant. Highest r value with ttm was found for nitrogen index REIP (r = 0.34) and water index NWI-2 (r = -0.29).

Trial Food shows significant correlation for ttm and vegetation index NDVI (r = 0.29*). Furthermore, ttm and either PSSRa (r = 0.35**) and PSSRb (r = 0.33**) is significantly correlated in trial Food.

Correlation of leaf size and hyperspectral indices

Leaf size is a vegetative trait which is correlated with some hyperspectral indices in different maturity groups, as depicted in figure 31.

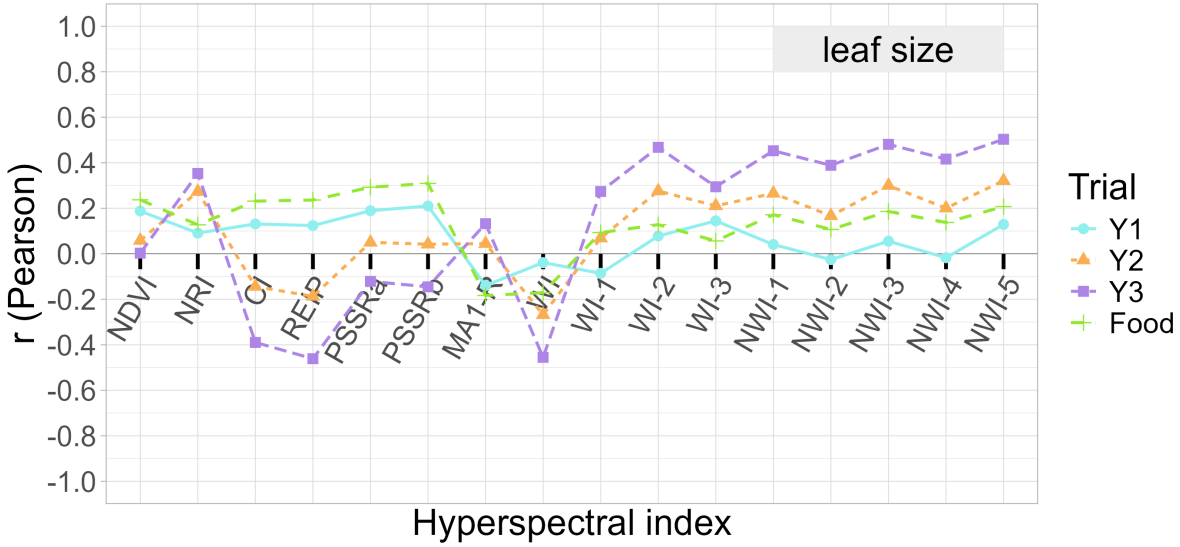

Figure 31: Correlation coefficients(r) for the relationship between soybean leaf area and spectral reflectance indices, grouped in trials with different maturity groups, averaged r values across all five timepoints.

Trial Y1 has no significant correlation between leaf size and hyperspectral indices. In contrast, **trial Y2** shows significant correlation between leaf size and water indices NWI-3 (r = 0.30*) and NWI-5 (r = 0.32**).

Best correlations between leaf size and hyperspectral indices were found in **trial Y3**: chlorophyll index CI (r = -0.39*) and REIP (r = -0.46*) and water index WI (r = -0.45*) show highest negative correlation, while all other water indices have high positive correlation with leaf size. Indices WI-2 (r = 0.46**), NWI-3 (r = 0.48**) and NWI-5 (r = 0.5**) show best correlations for leaf size in varieties of trial Y3.

LA of genotypes in **trial Food** is only significantly correlated with NDVI (r = 0.26*), PSSRa (r = 0.29*) and PSSRb (r = 0.31**), respectively. In summary, leaf size vs. indices correlations were especially high for late ripening varieties in trial Y3 which were screened during vegetative development phase. Remarkably, that soybean emergence (emerg) has shown significant correlations for all water indices (except WI-3) in trial Y3 averaged over all timepoints (see table S11b and S11c in the appendix). Trial Y1 is also significantly correlated with this trait for all water indices (with exception to WI-1, NWI-2 and NWI-4), shown in table S9b and S9c.

3.6.3 Thermal imaging

Midday timepoints

Timepoints for thermal imaging on midday were exposed to varying environmental conditions. An overview to measured and calculated parameters to all 10 timepoints at 12:00h is listed in table 8.

Table 8: Overview of timepoints for thermal imaging at midday (12:00h); measured parameters by thermal imaging: canopy temperature (T_c); meteorological parameters obtained by weather station: relative humidity (rH), air temperature (T_a) and days after last rain (daP); calculated parameter: canopy and air temperature differential (Tc-Ta), simplified Crop Water Stress Index (siCWSI), vapor pressure deficit (VPD) and drought stress level (dstress) for soybean; significance levels (Sign.): $+$: p<0.1; $*$: p<0.05; $**$: p<0.01; ns: not significant.

ID	date	T_c			rH	T_a	daP	$T_c - T_a$	siCWSI	VPD	dstress
12:00h		[°C]	Chi-value	Sign.	[%]	[°C]	[day]	[K]	[-]	[kPa]	
C.t	9.8.24	27.4	13.0	ns	65.0	24.0	1	3.44	0.32	1.06	low
E.t	12.8.24	34.6	33.3	***	52.7	28.5	4	6.08	0.34	1.89	mid
G.t	13.8.24	30.6	19.8	*	62.0	28.9	0	1.72	0.31	1.55	mid
I.t	14.8.24	31.7	38.5	***	51.5	30.4	1	1.34	0.34	2.17	high
K.t	19.8.24	25.9	20.2	*	71.2	21.6	1	4.33	0.31	0.76	low
M.t	20.8.24	27.3	24.0	**	73.3	22.9	2	4.42	0.33	0.76	low
Q.t	23.8.24	31.1	23.4	**	61.7	24.9	2	6.16	0.33	1.23	low
S.t	24.8.24	35.0	19.4	*	54.0	28.3	3	6.71	0.35	1.82	mid
V.t	27.8.24	30.2	33.4	***	68.3	23.3	6	6.89	0.31	0.92	low
X.t	28.8.24	38.1	36.1	***	51.3	29.4	7	8.66	0.33	2.05	high

Average **canopy temperature** T_c over all genotypes was highest on timepoints E.t, S.t and X.t with 34.6, 35.0 and 38.1°C, respectively, while lowest mean canopy temperatures were measured at timepoints C, K and M with 27.4, 25.9 and 27.3°C, respectively. Significant T_c differences between genotypes were found in all timepoints with exception of timepoint C.t.

In contrast, **canopy air temperature differential** ($T_c - T_a$) was lowest at timepoints G.t and I.t with 1.72 and 1.34 K, respectively, while timepoints C.t, K.t and M.t show high $T_c - T_a$ of +3.44, +4.33 and +4.42 K above air temperature. All other timepoints show high canopy air differences in a range between +6.08 and +8.66 K, where timepoint X has the highest value. Furthermore, the days after last precipitation event (daP) can be grouped in 0 (timepoint G.t) and 1 day (C.t, I.t and K.t), 2 days (M.t and Q.t), 3 to 4 days (S.t and E.t) and above 5 days (V.t and X.t).

The range of **siCWSI** over all timepoints is between 0.31 and 0.35 and had highest values at timepoint S (0.35) and, respectively, E.t and I.t (0.34). **Vapor pressure deficit** (VPD) shows a range between 0.76 and 2.17 kPa. Timepoints with VPD values under 1.5 kPa were grouped 'low' drought stress, such as timepoints K.t and M.t (0.76 kPa, both) and V.t (0.92 kPa) as well. 'High' drought stress level was determined for high VPD at timepoints X.t (2.05 kPa) and I.t (2.17 kPa). Timepoints E.t (1.89 kPa) and S.t (1.82 kPa were grouped to 'mid' drought stress level, In summary, timepoints X.t, E.t and S.t show high values to drought-related parameter ($T_c - T_a$, VPD), while timepoints C.t, M.t and K.t show similarly

low values in different parameters (T_c, $T_c - T_a$, VPD).

Afternoon timepoints

Thermography screening in the afternoon around 15:00h was conducted under different weather conditions in August 2024 at 15 dates. Mean values for each timepoint are shown in table 9.

Table 9: Overview of timepoints for thermal imaging in the afternoon (15:00h); measured parameters by thermal imaging: canopy temperature (T_c); meteorological parameters obtained by weather station: relative humidity (rH), air temperature (T_a) and days after last rain (daP); calculated parameters: canopy and air temperature differential (Tc-Ta), simplified Crop Water Stress Index (siCWSI), vapor pressure deficit (VPD) and drought stress level (dstress) for soybean; significance levels (Sign.): $+$: p$<$0.1; $*$: p$<$0.05; $**$: p$<$0.01; ns: not significant.

ID	date	T_c			rH	T_a	daP	$T_c - T_a$	siCWSI	VPD	dstress
15:00h		[℃]	Chi-value	Sign.	[%]	[℃]	[day]	[K]	[-]	[kPa]	
A.t	7.8.24	30.5	45.0	***	49.0	29.3	2	1.18	0.37	2.14	high
B.t	8.8.24	28.6	43.6	***	53.5	27.8	3	0.79	0.41	1.78	mid
D.t	9.8.24	28.1	28.5	**	52.3	26.8	1	1.34	0.32	1.72	mid
F.t	12.8.24	35.7	39.3	***	51.0	32.5	4	3.22	0.36	2.48	high
H.t	13.8.24	32.0	41.1	***	48.0	33.1	0	-1.09	0.34	2.72	high
J.t	14.8.24	28.9	55.0	***	56.5	29.7	1	-0.80	0.46	1.87	mid
L.t	19.8.24	21.0	34.1	***	84.0	19.3	1	1.74	0.34	0.36	low
N.t	20.8.24	29.3	26.6	**	65.7	26.3	2	3.02	0.31	1.20	low
O.t	21.8.24	26.2	43.2	***	65.0	24.5	3	1.66	0.34	1.10	low
P.t	22.8.24	25.9	35.9	***	53.5	23.5	1	2.39	0.39	1.37	low
R.t	23.8.24	33.7	50.7	***	46.0	29.5	2	4.18	0.40	2.29	high
T.t	24.8.24	37.7	38.3	***	42.5	32.9	3	4.77	0.42	2.98	high
U.t	26.8.24	31.7	19.1	+	57.0	26.0	5	5.70	0.28	1.48	low
W.t	27.8.24	35.7	34.0	***	51.0	27.3	6	8.39	0.31	1.82	mid
Y.t	28.8.24	37.8	26.7	**	44.7	32.0	7	5.80	0.33	2.72	high

Canopy temperature (T_c) was highest at timepoints F.t (35.7℃), T.t (37.7℃), W.t (35.7℃) and Y.t (37.8℃). Lowest T_c was observed at timepoint L.t with 21.0℃ warm leaves. All timepoints show significant T_c differences between varieties (Sign.) at probability levels p<0.1 (+), p<0.05 (*), p<0.01 (**) and p<0.001 (***).

Air temperature (T_a) ranges from highest at timepoint H.t (33.1℃), T.t (32.9℃), F.t (32.5℃) and Y.t (32.0℃) to lowest at L.t (19.3℃). Relative humidity (rH) was in a range from 44.7% at timepoint Y.t, which occured 7 days after last rain event, and 84% at timepoint L.t, that was only 1 day after precipitation (daP).

Timepoints can be divided in daP groups of 0-1 days (D.t, H.t, J.t, L.t and P.t), 2-3 days (A.t, B.t, N.t, O.t, R.t, T.t) and 4 days or higher (F.t, U.t, W.t, Y.t). **Canopy air temperature differential** ($T_c - T_a$) was highest at timepoints in high daP group, such as U.t (5.70 K), Y.t (5.80 K) and W.t (8.39 K), where last

rain event was far away. Remarkably, at timepoints H.t and J.t the temperature differential $T_c - T_a$ was negative with -1.09 and -0.80 K, which indicates high transpiration capacity of plant's canopy.

Mean siCWSI for each timepoint was in a range between 0.28 and 0.46, but there is no relationship found with daP and $T_c - T_a$. High T_a is mainly negatively correlated with low rH and resulted in high VPD, which indicates high meteorological drought stress for plants. VPD shows minimum value at timepoint L.t (0.36 kPa) and highest value at timepoints H.t and Y.t (both 2.72 kPa). 'High' drought stress level was determined for timepoints A.t, F.t, H.t, R.t, T.t and Y.t, while 'low' stress level is found in timepoints L.t, N.t, O.t and T.t. Some timepoints had calculated high VPDs and plants have apparently high drought stress level driven by atmosphere, nevertheless, measured low $T_c - T_a$ indicates no common plant stress for this timepoint.

In summary, timepoints Y.t and T.t and W.t have highest canopy temperatures and high VPD values, which strongly indicate high water stress to plants.

3.6.4 Correlation of siCWSI and agronomic traits

Correlation between siCWSI and agronomic traits were calculated with Spearman's rank correlation coefficient (r) due to low sample number. Correlation coefficients were calculated for timepoints at midday (12:00h, n = 10) and in the afternoon (15:00h, n = 15) as 'average' values. Furthermore, timepoints were departed in drought stress levels 'low', 'mid' and 'high' for each daytime (mid-day and afternoon). All r- and p-values for correlation of siCWSI and agronomic traits are summarized in table S13 as supplementary data. Figure 32 shows relationship between siCWSI and several agronomic traits, differently coloured for timepoints at 12:00h and 15:00h.

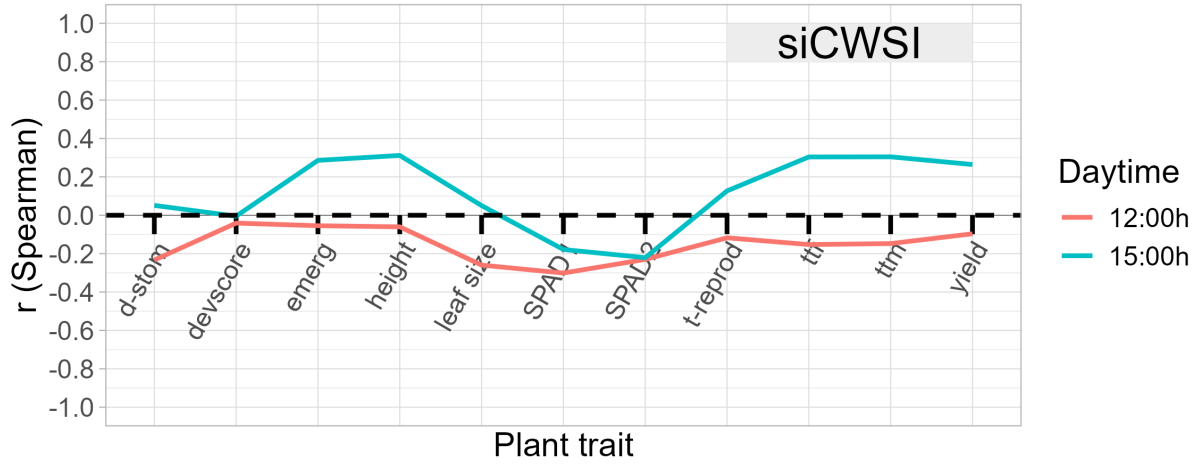

Figure 32: Spearman's rank correlation coefficient r for siCWSI and agronomic traits, grouped for timepoints at midday (12:00h) and afternoon (15:00h).

At midday significant correlation was found for SPAD1 (r = -0.30**) and SPAD2 (r = -0.23*) and stomatal density (r = -0.23*). All other traits had no significant correlation with timepoints at 12am. In

contrast, thermal measurements in the evening (15:00h) show significant correlation between siCWSI and most agronomic traits. Main agronomic traits were positively correlated according to siCWSI during the afternoon, namely: ttf (r = 0.30**), ttm (r = 0.31**), height (r = 0.31**) and grain yield (r = 0.26**). Physiological traits SPAD1 (r = -0.18*), SPAD2 (r = -0.22**) were negatively correlated with siCWSI in the evening. Phenological traits like plant emergence (r = 0.29**) and lodging (r = 0.17*) have positive and significant correlation, while pod set (r = -0.23**) and pod shattering (r = -0.16*) show negative relationship to siCWSI at thermal screenings around 15:00h.

In summary, measured timepoints in the afternoon (15:00h) show low, but significant correlations between calculated siCWSI and agronomic traits. Comparisons to timepoints at 12:00h, siCWSI shows no clear relationship to plant traits in varieties. Apparently, variability in crop water stress was higher in the afternoon than on midday.

Figure 33 shows Spearman's rank correlation coefficients for siCWSI and agronomic traits in all timepoints ('average') in the evening and grouped by drought stress levels 'low' (VPD < 1.5 kPa), 'mid' (1.5 < VPD < 2.0 kPa) and 'high' (VPD > 2.0 kPa).

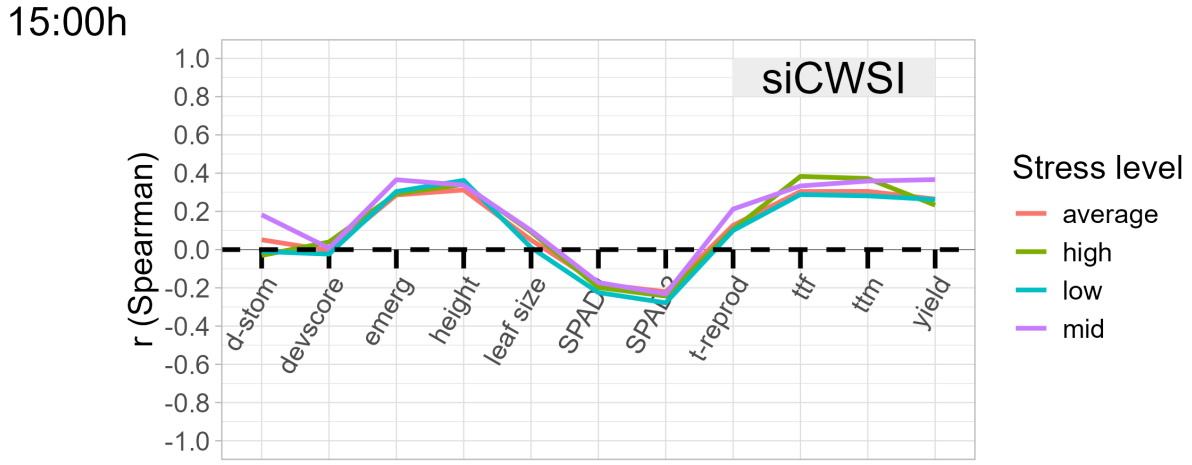

Figure 33: Spearman's rank correlation coefficient r for siCWSI and agronomic traits, grouped for stress level at 15:00h, with 'low' stress at VPD =< 1.5 kPa, mid stress at 1.5<VPD=<2.0 kPa, and 'high' stress for VPD>2.0 kPa; 'average' stress includes mean values over all timepoints.

Timepoints at all three drought stress levels show similar relationship between siCWSI and individual agronomic traits. No stress level had shown superior correlations over all examined traits and siCWSI.

4 Discussion

The present work was focused on phenotyping phenological and agronomic traits of European soybean varieties of different maturity groups (MG), grown in a temperate climate region in Tulln (Austria). Further objective of this work was detection of water stress in soybean varieties by screening approaches and selection of reliable indices.

Warm air temperatures around 20℃ and regular precipitations in May and June 2024 provided optimal growing conditions for soybean in the vegetative phase. Therefore, both phenological stages emergence (VE) and vegetative development (V2/V3) had high scores.Generally, season 2024 in Austria was humid and had only short periods (maximum 1 week) without precipitation. Average drought stress over the whole growing season was low. Only in second half of August, hot and dry weather has shortened reproductive phases after flowering.

Phenological traits, like time to flowering (ttf) and time to maturity (ttm), in soybean are crucial for plant breeders, because those development stages indicate transitions in plant's physiology.

In the reproductive phase, expected pattern for ttm were fulfilled, while ttf had shown different pattern. Beginning of flowering was very similar in varieties of trial Y1 (MG 000) and trial Y2 (MG00) that started flowering almost simultaneously. Additionally, some varieties in trial Y3 flowered at similar time as in trial Y1 or Y2, which was partly expected due to early check varieties 'Obélix' and 'STUMPA'. Apparently, all late soybean varieties (MG 0/I), which were provided by Saatzucht Gleisdorf (SZG) to trial Y3, flowered as early as varieties in trial Y1 and Y2, but had average maturity time.

Maturity time (R8) plays a big role in soybean's agronomy because farmer's harvesting date is determined to fully ripening stage. Expected differentiation between very early, mid-early and late cultivars were found in trials Y1, Y2 and Y3, while maturity in Food trial ranged over all three groups (see figure 14b).

The results for ttm show that most varieties are correctly classified according to maturity group. Only some outliers in trial Y1 are too early, so these varieties will belong to even earlier maturity group, called MG 0000 Jia et al. (2014). The reproductive phase (R1-R8) in soybean trials shows an interesting aspect: MG 00 genotypes in trial Y2 took similar time for seed formation than cultivars of MGs 0/I in trial Y3. This implicates that MG classification is less dependent on flowering time and rather affected by the reproductive period.

Flowering initiation for European soybean varieties (MG 000-I) is mainly determined on daylength (Jia et al., 2014) and accumulated temperature (Yao and Zhang, 2024). In soybean, light and thermal requirements are associated with a complex interplay of several E-genes (*E1–E4*) and other putative quantitative trait loci (QTLs), such as *Dt2* locus (Vollmann and Škrabišová, 2023).

Plant height was positively correlated with time to maturity, as expected. The longer ttm, the taller plant varieties were grown. This relationship is valid within and between maturity groups of trials Y1, Y2 and Y3 (see figure 22a).

Time to maturity and yield

Soybean variety trials in Tulln (Austria) showed a big variation in yield because there is a relationship to maturity time. Correlation analysis between yield and time to maturity (ttm) showed in this work, that there is an optimum time window for maturity to achieve highest yields, as shown in figure 22b. Top-yielding varieties (above 35 dt/ha) across different MG had similar ttm with an optimum range between 250 and 265 doy, which can be transformed to 119-134 days after sowing date (das). Varieties with ttm lower 119 das and higher 134 das showed grain yields below average (mean = 32.18 dt/ha) for the experimental site in Tulln. Comparable yield data of field experiments in Serbia, Germany and Poland across soybean MG II - 0000 was obtained by Nendel et al. (2023):

In Backa Tobala (Serbia) several soybean varieties of MG 0, MG I and MG II were grown in different seasons between 2006 and 2017. Time to maturity and yield showed no relationship for late cultivars in MG I and MG II (ttm range: 122 to 160 das; yield range: 19.9 to 42.2 dt/ha). In contrast, varieties in MG 0 showed a tendency to higher yields (yield range: 21.2 to 31.4 dt/ha) when ttm increased from 134 to 155 das. These results may show that varieties of MG I and MG II are adapted very well to this region in Serbia, while earlier varieties of MG 0 need longer vegetation periods with warm temperatures in autumn to achieve relative high yields.

In Müncheberg (Germany) very early cultivars 'Merlin' and 'Sultana' (MG 000) were grown over three seasons between 2015 and 2017. Maturity was reached 100 days after sowing (season 2015), 116 das (season 2016) and 133 das (season 2017). Harvested yield was positively correlated with time to maturity. Yield on average was measured on a range from 12 dt/ha (season 2015) to 35.5 dt/ha (season 2017). In Krakow (Poland) very early cultivars 'Lissabon' (MG 000), 'Augusta' and 'Erica' (both MG 0000) were grown in two seasons 2017 and 2018. Time to maturity strongly differed between season 2017 (154 and 140 das) and season 2018 (108 and 83 das) for MG 000 and MG 0000, respectively. Seed yield was comparatively higher in MG 000 than in MG 0000 either in season 2017 (33.7 and 31.7 dt/ha) and in season 2018 (48.9 and 29.7 dt/ha). Both field experiments in Müncheberg and Krakow demonstrated that later time to maturity had positive effect to grain yield of very early varieties of MG 000 and MG 0000, respectively. Later maturing soybean varieties from MG 00 or even MG 0 are less adapted to these locations at high latitudes. Unfortunately, this issue makes the dataset of Nendel et al. (2023) less comparable with results in Tulln, Austria.

For better comparisons between soybean growing regions in Europe, Kurasch et al. (2017) suggested to cluster Europe in six megaenvironments (MEV 1-6), where Tulln is on the edge between MEV 2 and MEV 3. As a reference, mean ttm values from early (MG 0), mid-early (MG 00) and very early (MG 000) genotypes in MEV 2 and MEV 3, respectively, are noted in the following: MG 0 (163.1 and 149.1 das), MG 00 (159.6 and 139.9 das) and MG 000 (149.1 and 128.8 das). In comparison to results in the present work, mean values for ttm were 136.9 das (Y3, MG 0/I), 125.9 das (Y2, MG 00) and 119.7 das (Y1, MG 000) which are 10-14 days earlier than reference values in MEV2 and 30-35 days earlier than in MEV3. These big ttm differences of 2 weeks and 4 weeks, respectively show a clear contrast between findings of Kurasch et al. (2017) and results in this work.

Another insight made by Kurasch et al. (2017) is the very large phenotypic variation of ttf and ttm in MG 00 compared to all other observed maturity groups in Europe. Therefore, varieties of MG 00 were divided into an early group, which is more similar to MG 000, and a late group, which was clustered together with MG 0 varieties. Genotyping for maturity loci *E1*, *E2*, *E3* and *E4* confirmed similarities in ttm: early cultivars of MG 00 and MG 000 carried the *e1-nl* allele, while varieties of MG 0 and late MG 00 carried the *e1-as* allele.

This knowledge about genotypic background of MG 00 genotypes may explain no correlation between ttm and yield in trial Y2 of the present work: genetic variation in *E*-alleles within MG 00 has brought best adaptations to region of Middle Europe belonging to MEV2 and MEV3. Top-yielding varieties of MG 00 were distributed over the whole period of ttm from 250-265 doy (119 to 134 das). In conclusion, soybean varieties of MG 00 have the best results due to harvested yield in Tulln (Austria) and were almost independent from time to maturity.

Differences in stomatal density

The examination of European soybean cultivars (MG 00) to differences in stomatal density (SD) has not been published before. In this work, SD of 45 European soybean varieties were measured and shown the first time, with a range of 203.3 to 322.2 stomata/mm² and a LSD5 of 58.9/mm², as shown in figure 21.

Highest average of SD were counted at varieties 'SHIVA' from RAGT and four genotypes of SZG, namely 'GL 201117', 'GL Tilda', 'Xonia' and 'GL 201811'. Apparently, many varieties of Austrian breeder SZG had high SD (above 281 stomata/mm²) in comparison to variety sets of other breeders. Moreover, six of eight varieties from breeder LIDEA were shown a density less than 246 stomata/mm². This means that most varieties of LIDEA had relative low SD compared to the variety sets of other breeders. The origin of breeding germplasms may explain phenotypic differences to climatic conditions in temperature and moisture. Varieties of each breeder show adaptations for SD due to their breeding region in Europe.

In scientific literature, only soybean germplasms grown in United States and Asian countries were investigated to stomatal characteristics. The survey of Tanaka et al. (2010) showed a variation of SD ranging from 148 to 334 stomata/mm² for US and Japanese varieties, while the mean SD of US (n = 26) and Japanese cultivars (n=20) were 229 and 221 stomata/mm², respectively. Mano et al. (2023) examined SD for North American variety 'IA3023' (Iowa State University, MG III) at different water contents (30, 50, 75 and 100%). High and mid water contents (50, 75 and 100%) showed SD between 250 and 300 stomata/mm², while drought stressed soybean plants at 30% water content had always higher values for SD. Another field experiment with 43 soybean cultivars (Minnesota, USA) was conducted by Ciha and Brun (1975) and showed a SD range of 242 to 385 stomata/mm². In the same work, researchers found out that mean SD was significantly increased in water stressed plants compared to non-water stressed plants.

All three studies above mainly agree with SD range evaluated in the present work at European soybean variety set of MG 00. The issue of increased SD under drought stress can be explained by a decreasing leaf size, which is negatively correlated with SD (Ciha and Brun, 1975).

Drought stress affects plant's response during the growing period, but in drought-prone regions adaptations of stomatal characteristics are hereditary and can improve drought tolerance in genotypes. In a study of Khazaei et al. (2013) two sets of faba bean accessions, one from drought-prone and another from non-drought-prone environments, were tested to differences in stomatal characteristics. It was found, that under well-watered conditions, the dry-adapted set had bigger stomata, higher relative water content and cooler leaves, but similar level of stomatal density compared to wet-adapted set. When drought was imposed, the stomatal size was reduced in both sets, while the dry set significantly increased in SD by 17%.

Beside the varietal results, the methodology for SD detection work flow is a relevant aspect to get reliable data. The sampling date according to the development stage of soybean plants is a variable factor. Research group around Sultana et al. (2024) sampled in greenhouse growing soybean leaflets at different vegetative stages (VE, V1, V2, V3, V4) and measured SD for each sampling date. The findings of this survey showed a tendency for increasing stomatal density across growth stages (from VE to V4), with exception of V2 and V3 stages. In contrast, stomatal density was often counted on field-grown soybeans. Soybean leaflet collection in field experiments was done at beginning flowering stage (R1) (Ciha and Brun, 1975; Sakoda et al., 2019), at beginning pod stage (R3) (Tanaka et al., 2010; Sakoda et al., 2019) and over different stages (V5, R2, R4 and R6) (Casado-García et al., 2020). The sampling date in the present work was around 61 days after sowing, thus, full flowering stage (R2) or beginning pod stage (R3) was already reached.

After sampling, a decisive choice is the examined area of the leaflets for SD evaluation. In this work, only stomata on abaxial (bottom) leaf surface were observed. Moreover, SD on the adaxial (upper) side of leaves was examined in several studies (Sultana et al. (2024), Mano et al. (2023) and Julia et al. (2019)). Adaxial leaf side of soybean show less, but considerable amount of stomata. The abaxial:adaxial ratio ranges between 3 and 4 under well-watered conditions and around 5 at drought stress (water content of 30%) (Mano et al., 2023). There was also found a strong positive relationship between abaxial and adaxial SD (Julia et al., 2019).

Furthermore, a study of Sultana et al. (2024) found differences in SD dependent on the sampling position at one leaflet: number of stomata/mm² was highest at the tip of leaflet and decreased in direction to bottom of leaflet.

Especially for soybean, the issue of hairy leaves has to be recognized. Meeus et al. (2020) applied the nail polish method on dried leaves of different species to detect stomata. Although, impression generation failed in species with hairy or velvety leaf surfaces. In contrast, the findings of Julia et al. (2019) in a set of 10 Indonesian soybean lines were showing a negative relationship between abaxial stomata number and abaxial trichome length.

Another aspect is the choice of glue to make leaf imprints. Transparent nail polish is used in the majority of papers because this adhesive product dries very fast and can shorten waiting time. Other studies used adhesives like gelatine (Julia et al., 2019), cyanoacrylate glue (Casado-García et al., 2020), nitrocellulose spray laquer (Gitz and Baker, 2009) or clearing solvents based upon combinations of ethanol and sodium hypochlorite (NaOCl) (Sultana et al., 2021). In some papers (Sakoda et al. (2019),

Tanaka et al. (2010)) so-called 'Suzuki's Universal Method of Printing' (short: SUMP) was reported as an established approach for making imprints of plant leaves. SUMP is based on pressing abaxial leaf surface on a SUMP plate with a SUMP liquid containing amyl acetate which became solid.

Furthermore, microscopic extracts from leaf imprints were commonly created by using a transmission light or bright field microscope. This microscope type is widely used for stomata detection due to high contrast in micrographs (Gitz and Baker (2009); Sultana et al. (2024); Casado-García et al. (2020)). In the present work, micrographs were done by means of reflected light microscope, which has the disadvantage of less sharp contrast between cell borders in micrographs. In the following, stomata counting was difficult at micrographs and some stomata could not be recognized due to low image quality caused by microscope type.

Finally, stomata counting approach has limits to accuracy. In this work, all micrographs were manually counted for stomata by two persons. This counting approach is a time-consuming and error-prone process. In the recent decade, automated stomata evaluation applications were established as a fast and software-based approach with deep learning networks. A selection of these developed stomata analysing programs use deep learning network types, departed in object detection or semantic methods (Gibbs and Burgess, 2024). However, the availability of most software applications is restricted.

In summary, methodology for stomata detection is prone to many potential error sources. Nevertheless, results in this work showed significant differences in SD between European soybean cultivars of MG 00. Range of SD resulted in similar values compared to other studies with soybean varieties.

Hyperspectral indices and agronomic traits

Hyperspectral measurement is a promising phenotyping technique assisting breeders to predict yield and other agronomic traits under drought stress. This work shows that prediction of grain yield, plant height or ttm is only possible when development stage of soybean trial is considered. It's clear, development stages of soybean varieties differed across and within trials during hyperspectral screening period between 14. July and 13. August 2024. In detail, very early varieties of trial Y1 has gone through reproductive stages R3 to R7, while late varieties of trial Y3 were observed at stages R1 to R5. Prey et al. (2020) has optimized prediction of grain yield and dry matter formation in wheat with hyperspectral canopy measurements. Several screening dates during development stages were examined: most reliable measurements were done at late anthesis. Within all tested hyperspectral indices, best correlations with grain yield were found in water index NWI-2.

In the present work, some hyperspectral indices showed significant correlations with yield, namely Chlorophyll Index (CI) and Red Edge Inflection Point (REIP) as well as water indices WI-1, NWI-2 and NWI-4. It's suggested that these indices can be used more likely to predict plot-yield than other tested indices. The study of Christenson et al. (2016) was conducted on soybean variety trials of MG III and MG IV and demonstrated strong relationship ($p < 0.01$) between yield and spectral indices WI-1 and WI-2.

However, late varieties of trial Y3 showed no correlation between yield and any spectral index. This issue can be explained by hyperspectral screenings that were done in a period of time while most varieties of trial Y3 were observed at the full flowering stage (R1/R2).

This explanation is proved by a study of Zhang et al. (2019), who used a hyperspectral remote-sensing system on an unmanned aerial vehicle to test soybean breeding lines to the linkage of plot yield and canopy spectral reflectance at reproductive stages R2, R4, R5 and R6. The research group around Zhang observed only VIS and NIR region (450-950 nm) and compared 10 most popular vegetation indices related to yield prediction. The results of the study show that hyperspectral measurements have best relationship to yield at growth stage R5 using two indices NDVI and RVI. The researchers proposed an optimized RVI and NDVI for soybean using the wavelengths 638 nm and 674 nm which were defined as MA1-R and MA1-N, respectively.

Compared to NDVI correlations in this work, only varieties in trial Y1 showed significant relationship with yield. MA1-R was also tested for yield prediction, but showed even less correlation to yield than NDVI. Other spectral indices like CI and REIP had higher correlation values with yield than NDVI and MA1-R. One explanation for different results may be the screening method: hand-held screening approach differs from remote sensing technique with spatial resolution and temporal accuracy. However, some studies found high correlations for NDVI done by airborne measurements and ground-based screenings (Xie and Yang, 2020).

Thermal infrared imaging

In addition, this work had the objective to evaluate the approach of thermal infrared imaging (TIR) for putative selection to drought tolerance. The focus was laid on the screening daytime and the drought stress level according to vapor pressure deficit (VPD). Pineda et al. (2021) stated, that thermography is a widely used phenotyping approach for farmers and breeders detecting abiotic and biotic stresses in plants. Especially for plant breeders, TIR is a valuable tool to screen for mutants and breeding lines with enhanced performance upon certain stress conditions, such as drought tolerance. However, the use of TIR on field experiments is exposed to variable ambient conditions, which has to be recognized to get reliable data.

First evaluated criterion was daytime: Anda et al. (2021) suggested thermal measurements at high solar angles between 11:00h and 15:00h, while other authors measured 'around midday' (Crusiol et al., 2020) and 'during solar noon' (Poudel et al., 2024). However, TIR observation period over 4 hours according to high noon is uncertain because canopy temperature (CT) generally changes during this long timeframe. Plant's temperature is strongly influenced by air temperature and relative humidity, and especially, the course of the day.

In the present work, thermography measurements were done separately at midday (12:00h) and on the afternoon (15:00h), respectively. Almost all screening timepoints, except timepoint C.t, showed significant CT differences between eleven varieties, which means that high sensitivity of TIR camera can detect variability in field experiments at most timepoints. Furthermore, calculated siCWSI showed

significantly positive relationship with yield, ttf and ttm at afternoon (15:00h), while correlations for timepoints measured at 12:00h were not significant (see figure 32 and table S13)

Another evaluated parameter was ambient drought stress level, that plants were exposed during TIR screenings. The calculated siCWSI has similar correlation patterns with agronomic traits for low, mid and high drought stress levels, as shown in figure 33. This data shows that ambient conditions to drought stress can be neglected for timepoint selection. However, siCWSI is positively correlated with yield, height and ttm at timepoints around 15:00h, while Anda et al. (2021) found a negative relationship for soybean varieties. There is no clear explanation about the contrary issue.

Some researches argued, that CWSI has it's best potential as indicator for water stress in arid and semi-arid regions and, respectively, under hot and dry weather conditions (Maes and Steppe, 2012; Idso et al., 1981). Another, but similar hypothesis for erratic correlations between CWSI and yield is the narrow range of VPD between 0.4 and 3.0 kPa, which soybean varieties were exposed in the field experiment in Tulln. Anda et al. (2021) has considered that in arid regions a range of 1-6 kPa is suitable for an extended use of CWSI. Therefore, humid and temperate weather conditions are less appropriate for application of CWSI.

Furthermore, the technical side of thermal image acquisition has to be discussed. Similar to hyperspectral measurements, thermal infrared screenings can be done by either ground-based or airborne sensor systems. In the present work, hand-held approach was done per plot with approximately 50 cm distance to plant canopy. Five thermographs was taken for a single-row. This time-consuming method is not practical for big breeding programs with some hundreds of breeding lines. Higher speed in imaging acquisition process can be managed with multiplot screening. In a survey of Zia et al. (2013) thermographs were taken from a movable platform which was mounted on a tractor and was positioned eight meters above canopy, thus, one thermal image contain ten single-rows with 0.75 m row spacing. Field experiments with larger plots have not necessity to capture thermographs from a vertical perspective. Melandri et al. (2020) conducted thermal measurements covering 50 m² field area at a camera height of 3.5 m with a camera angle of approximately 20° from the ground. An unfavourable issue of this method is spatial distortion of plots in the resulting image caused by this side perspective. Recent innovations for high-throughput thermal imaging are aerial unmanned vehicles (UAV) which decrease screening time to a minimum. Crusiol et al. (2020) described that octocopter has moved to a height of 125 m above ground and has captured one thermal image of all plots of the experimental setup in a vertical perspective. Thermal screening by UAV has the advantage to exclude error sources like temporal changes in surface temperature and weather conditions.

Summarizing, thermography screening shows significant CT differences at almost all timepoints. Correlations with other traits and calculated siCWSI demonstrated higher values in the afternoon than at midday. Different VPD levels had no measurable effect for the relationship between siCWSI and agronomic traits because of too narrow VPD range. Handheld methodology is not useful for big scales in plant breeding. Faster image acquisition is enabled by airborne systems like UAVs which are used in plant breeding experiments. In future, high-throughput phenotyping approaches will broadly use visual sensors mounted on UAVs to screen large field experiments.

5 Conclusion

Soybean variety field trials under rainfed conditions were examined for drought-related stress traits in growing season 2024 in Tulln, Austria. However, drought stress for soybean was absent or low because of regular and sufficient precipitation from May until Mid of July. Transient drought stress may be found in August, but post-anthesis stages were less affected by water-deficit. Nevertheless, phenotypic variability between varieties was measured for ttf, ttm, leaflet area, plant height and grain yield in all four observed trials. Between maturity groups, grain yield varied highest in very early genotypes (MG 000). Mid-early (MG 00) and late varieties (MG 0/I) had less variation in yield.

One of the most important agronomic traits in soybean breeding is the timepoint when full maturity has reached. Time to maturity (ttm) has strongly influenced grain yield within MGs in a certain growing region. Very early varieties of MG 000 had highest grain yield in the later ripening germplasms. In contrast, late variety set (MG 0/I) had a tendency of top-yield for relatively early ripening varieties. In conclusion, optimum ttm for high yields in Lower Austria has shown for MG 00 and yield reduction for both earlier (MG 000) and later (MG 0/I) soybean genotypes. Reproductive time (t-reprod) is the critical period of crop development between flowering (R1) and full maturity (R8). T-reprod was significantly shorter in very early genotypes of MG 000 than in trials of MG 00 and MG 0/I.

First time results about stomatal density was published for European soybean varieties of MG 00. This data shows similar findings with surveys on other continents. Time-consuming sampling and counting for stomatal density is not applicable for experimental setups with hundreds of plots. The methodology has to be revised for future measurements. Hyperspectral imaging received good correlations between some water indices and yield. Water indices WI-1, NWI-2 and NWI-4 showed best agreement with yield, especially in MG 000 and MG 00. Seed filling stage and later were appropriate to find relationship between hyperspectral indices and harvested yield.

In this work, temperature based siCWSI show best correlation with yield at afternoon around 15:00h, while drought stress level had less influence to siCWSI vs. yield linkage. The use of handheld thermography in plant breeding is limited due to time-consuming screening technique. High-throughput phenotyping with thermal IR cameras can be realized on airborne systems like drones. Summarizing, European soybean varieties have broad phenotypic variability in drought-related traits, although drought stress was low.

In future, deeper insights in plant's responses to drought stress will come through the scientific and technological progress in physiological and genetic understanding. The development of 'OMICs'-based approaches plays a major role to identify connections and interactions between genes, metabolites, proteins and to explain their functions related to drought resistance.
In a bigger framework, field trials with same varieties were conducted at more than seven other locations in Europe during season 2024. Soybean varieties will grow at the same locations again in season 2025. The findings of the present work might be helpful as a reference for results in other environments due to drought tolerance and maturity time. Further research is needed to find traits which are strongly related to drought tolerance in soybean.

References

Abebe, A. M., Kim, Y., Kim, J., Kim, S. L., and Baek, J. (2023). Image-Based High-Throughput Phenotyping in Horticultural Crops. Plants, 12(10):2061.

Abou-Elwafa, S. F. and Shehzad, T. (2021). Genetic diversity, GWAS and prediction for drought and terminal heat stress tolerance in bread wheat (Triticum aestivum L.). Genet Resour Crop Evol, 68(2):711–728.

Al-Tamimi, N., Langan, P., Bernád, V., Walsh, J., Mangina, E., and Negrão, S. (2022). Capturing crop adaptation to abiotic stress using image-based technologies. Open Biol., 12(6):210353.

Anda, A., Simon-Gáspár, B., and Soós, G. (2021). The application of a self-organizing model for the estimation of crop water stress index (CWSI) in soybean with different watering levels. Water, 13(22):3306.

Anderson, D. B. (1936). Relative Humidity or Vapor Pressure Deficit. Ecology, 17(2):277–282.

Apel, K. and Hirt, H. (2004). REACTIVE OXYGEN SPECIES: Metabolism, Oxidative Stress, and Signal Transduction. Annual Review of Plant Biology, 55(1):373–399.

Araus, J., Casadesus, J., and Bort, J. (2001). Recent tools for the screening of physiological traits determining yield. In Application of Physiology in Wheat Breeding Mexico, DF: CIMMYT, pages 59–77.

Babar, M. A., Reynolds, M. P., van Ginkel, M., Klatt, A. R., Raun, W. R., and Stone, M. L. (2006). Spectral Reflectance Indices as a Potential Indirect Selection Criteria for Wheat Yield under Irrigation. Crop Science, 46(2):578–588.

Bai, G., Ge, Y., Scoby, D., Leavitt, B., Stoerger, V., Kirchgessner, N., Irmak, S., Graef, G., Schnable, J., and Awada, T. (2019). NU-Spidercam: A large-scale, cable-driven, integrated sensing and robotic system for advanced phenotyping, remote sensing, and agronomic research. Computers and Electronics in Agriculture, 160:71–81.

Bandurska, H. (2022). Drought Stress Responses: Coping Strategy and Resistance. Plants, 11(7):922.

Becker, H. (2011). Pflanzenzüchtung. Number 1744 in UTB. UTB GmbH, Stuttgart, 2. edition.

Bian, J., Zhang, Z., Chen, J., Chen, H., Cui, C., Li, X., Chen, S., and Fu, Q. (2019). Simplified Evaluation of Cotton Water Stress Using High Resolution Unmanned Aerial Vehicle Thermal Imagery. Remote Sensing, 11(3):267.

Bista, D. R., Heckathorn, S. A., Jayawardena, D. M., Mishra, S., and Boldt, J. K. (2018). Effects of Drought on Nutrient Uptake and the Levels of Nutrient-Uptake Proteins in Roots of Drought-Sensitive and -Tolerant Grasses. Plants, 7(2):28.

REFERENCES

Biswas, D., Coulman, B., Biligetu, B., and Fu, Y.-B. (2020). Advancing Bromegrass Breeding Through Imaging Phenotyping and Genomic Selection: A Review. Frontiers in Plant Science, 10:1673.

Blackburn, G. A. (1998). Spectral indices for estimating photosynthetic pigment concentrations: A test using senescent tree leaves. International Journal of Remote Sensing, 19(4):657–675.

Blum, A. (2011). Plant Breeding for Water-Limited Environments. Springer New York, New York, NY.

Blum, A., Mayer, J., and Gozlan, G. (1982). Infrared thermal sensing of plant canopies as a screening technique for dehydration avoidance in wheat. Field Crops Research, 5:137–146.

Boerema, A., Peeters, A., Swolfs, S., Vandevenne, F., Jacobs, S., Staes, J., and Meire, P. (2016). Soybean Trade: Balancing Environmental and Socio-Economic Impacts of an Intercontinental Market. PLoS ONE, 11(5):e0155222.

Braga, P., Crusiol, L., Nanni, M., Caranhato, A., Fuhrmann, M., Nepomuceno, A., Neumaier, N., Farias, J., Koltun, A., Gonçalves, L., and Mertz-Henning, L. (2021). Vegetation indices and NIR-SWIR spectral bands as a phenotyping tool for water status determination in soybean. Precision Agriculture, 22(1):249–266.

Brevedan, R. E. and Egli, D. B. (2003). Short Periods of Water Stress during Seed Filling, Leaf Senescence, and Yield of Soybean. Crop Science, 43(6):2083–2088.

Cao, Z., Wang, Q., and Zheng, C. (2015). Best hyperspectral indices for tracing leaf water status as determined from leaf dehydration experiments. Ecological Indicators, 54:96–107.

Casado-García, A., del Canto, A., Sanz-Saez, A., Pérez-López, U., Bilbao-Kareaga, A., Fritschi, F. B., Miranda-Apodaca, J., Muñoz-Rueda, A., Sillero-Martínez, A., Yoldi-Achalandabaso, A., Lacuesta, M., and Heras, J. (2020). LabelStoma: A tool for stomata detection based on the YOLO algorithm. Computers and Electronics in Agriculture, 178:105751.

Christenson, B. S., Schapaugh, W. T., An, N., Price, K. P., Prasad, V., and Fritz, A. K. (2016). Predicting Soybean Relative Maturity and Seed Yield Using Canopy Reflectance. Crop Science, 56(2):625–643.

Ciha, A. J. and Brun, W. A. (1975). Stomatal Size and Frequency in Soybeans. Crop Science, 15(3):309–313.

Commision, E. (2020). A Farm to Fork Strategy for a fair, healthy and environmentally-friendly food system. URL: https://eur-lex.europa.eu/legal-content/EN/TXT/?uri=CELEX:52020DC0381; accessed: 5. March 2025.

Commission, E. (2024). EU feed protein balance sheet. URL: https://data.europa.eu/data/datasets/eu-feed-protein-balance-sheet?locale=en; accessed: 5. March 2025.

Crusiol, L., Nanni, M., Furlanetto, R., Sibaldelli, R., Cezar, E., Mertz-Henning, L., Nepomuceno, A., Neumaier, N., and Farias, J. (2020). UAV-based thermal imaging in the assessment of water status of soybean plants. International Journal of Remote Sensing, 41(9):3243–3265.

Deery, D., Rebetzke, G., Jimenez-Berni, J., James, R., Condon, A., Bovill, W., Hutchinson, P., Scarrow, J., Davy, R., and Furbank, R. (2016). Methodology for high-throughput field phenotyping of canopy temperature using airborne thermography. Frontiers in Plant Science, 7:1808.

Dogan, E., Kirnak, H., and Copur, O. (2007). Effect of seasonal water stress on soybean and site specific evaluation of CROPGRO-Soybean model under semi-arid climatic conditions. Agricultural Water Management, 90(1):56–62.

Doughty, C. E., Field, C. B., and McMillan, A. M. S. (2011). Can crop albedo be increased through the modification of leaf trichomes, and could this cool regional climate?: A letter. Climatic Change, 104(2):379–387.

Ergo, V. V., Lascano, R., Vega, C. R. C., Parola, R., and Carrera, C. S. (2018). Heat and water stressed field-grown soybean: A multivariate study on the relationship between physiological-biochemical traits and yield. Environmental and Experimental Botany, 148:1–11.

Fahad, S., Bajwa, A. A., Nazir, U., Anjum, S. A., Farooq, A., Zohaib, A., Sadia, S., Nasim, W., Adkins, S., Saud, S., Ihsan, M. Z., Alharby, H., Wu, C., Wang, D., and Huang, J. (2017). Crop Production under Drought and Heat Stress: Plant Responses and Management Options. Front. Plant Sci., 8:1147.

FAOSTAT (2024). Data for crops and livestock products. URL: https://www.fao.org/faostat/en/#data/QCL; accessed: 9. February 2025.

Farooq, M., Gogoi, N., Barthakur, S., Baroowa, B., Bharadwaj, N., Alghamdi, S. S., and Siddique, K. H. M. (2017). Drought Stress in Grain Legumes during Reproduction and Grain Filling. Journal of Agronomy and Crop Science, 203(2):81–102.

Farooq, M., Wahid, A., Kobayashi, N., Fujita, D., and Basra, S. M. A. (2009). Plant drought stress: effects, mechanisms and management. Agron. Sustain. Dev., 29(1):185–212.

Fehr, W. R., Caviness, C. E., Burmood, D. T., and Pennington, J. S. (1971). Stage of Development Descriptions for Soybeans, *Glycine Max* (L.) Merrill. Crop Science, 11(6):929–931.

Fletcher, A. L., Sinclair, T. R., and Allen, L. H. (2007). Transpiration responses to vapor pressure deficit in well watered 'slow-wilting' and commercial soybean. Environmental and Experimental Botany, 61(2):145–151.

Gao, B.-c. (1996). NDWI—A normalized difference water index for remote sensing of vegetation liquid water from space. Remote Sensing of Environment, 58(3):257–266.

Gates, D. M. (1968). Transpiration and Leaf Temperature. Annual Review of Plant Biology, 19(Volume 19, 1968):211–238.

GeoSphere Austria (2024). https://data.hub.geosphere.at/dataset/klima-v2-1d. Accessed: 19. January 2025.

Gibbs, J. A. and Burgess, A. J. (2024). Application of deep learning for the analysis of stomata: a review of current methods and future directions. Journal of Experimental Botany, 75(21):6704–6718.

Gitelson, A. A., Viña, A., Ciganda, V., Rundquist, D. C., and Arkebauer, T. J. (2005). Remote estimation of canopy chlorophyll content in crops. Geophysical Research Letters, 32:L08403.

Gitz, D. C. and Baker, J. T. (2009). Methods for Creating Stomatal Impressions Directly onto Archivable Slides. Agronomy Journal, 101(1):232–236.

Grossiord, C., Buckley, T. N., Cernusak, L. A., Novick, K. A., Poulter, B., Siegwolf, R. T. W., Sperry, J. S., and McDowell, N. G. (2020). Plant responses to rising vapor pressure deficit. New Phytologist, 226(6):1550–1566.

Harris, D., Pacovsky, R. S., and Paul, E. A. (1985). Carbon Economy of Soybean–Rhizobium–Glomus Associations. New Phytologist, 101(3):427–440.

Hatfield, J. L., Boote, K. J., Kimball, B. A., Ziska, L. H., Izaurralde, R. C., Ort, D., Thomson, A. M., and Wolfe, D. (2011). Climate Impacts on Agriculture: Implications for Crop Production. Agronomy Journal, 103(2):351–370.

Helms, T. C., Deckard, E. L., and Gregoire, P. A. (1997). Corn, Sunflower, and Soybean Emergence Influenced by Soil Temperature and Soil Water Content. Agronomy Journal, 89(1):59–63.

Hesketh, J. D., Myhre, D. L., and Willey, C. R. (1973). Temperature Control of Time Intervals Between Vegetative and Reproductive Events in Soybeans. Crop Science, 13(2):250–254.

Hossain, M. M., Liu, X., Qi, X., Lam, H.-M., and Zhang, J. (2014). Differences between soybean genotypes in physiological response to sequential soil drying and rewetting. The Crop Journal, 2(6):366–380.

Idso, S. B., Jackson, R. D., Pinter, P. J., Reginato, R. J., and Hatfield, J. L. (1981). Normalizing the stress-degree-day parameter for environmental variability. Agricultural Meteorology, 24:45–55.

Jackson, P., Robertson, M., Cooper, M., and Hammer, G. (1996). The role of physiological understanding in plant breeding; from a breeding perspective. Field Crops Research, 49(1):11–37.

Jia, H., Jiang, B., Wu, C., Lu, W., Hou, W., Sun, S., Yan, H., and Han, T. (2014). Maturity Group Classification and Maturity Locus Genotyping of Early-Maturing Soybean Varieties from High-Latitude Cold Regions. PLOS ONE, 9(4):e94139.

Jones, H. G. (1999). Use of infrared thermometry for estimation of stomatal conductance as a possible aid to irrigation scheduling. Agricultural and Forest Meteorology, 95(3):139–149.

Joshi, S., Chinnusamy, V., and Joshi, R. (2022). Root System Architecture and Omics Approaches for Belowground Abiotic Stress Tolerance in Plants. AGRICULTURE-BASEL, 12(10):1677.

Julia, N., Zubaidah, S., and Kuswantoro, H. (2019). Morphological and Anatomical Characteristics of leaves of Ten Soybean (*Glycine max* L. Merill) Lines. IOP Conf. Ser.: Earth Environ. Sci., 276(1):012027.

Jumrani, K. and Bhatia, V. (2019). Identification of drought tolerant genotypes using physiological traits in soybean. Physiology and Molecular Biology of Plants, 25(3):697–711.

Khatun, M., Sarkar, S., Era, F. M., Islam, A. K. M. M., Anwar, M. P., Fahad, S., Datta, R., and Islam, A. K. M. A. (2021). Drought Stress in Grain Legumes: Effects, Tolerance Mechanisms and Management. Agronomy, 11(12):2374.

Khazaei, H., Street, K., Santanen, A., Bari, A., and Stoddard, F. L. (2013). Do faba bean (Vicia faba L.) accessions from environments with contrasting seasonal moisture availabilities differ in stomatal characteristics and related traits? Genet Resour Crop Evol, 60(8):2343–2357.

Kim, M., Lee, C., Hong, S., Kim, S. L., Baek, J.-H., and Kim, K.-H. (2021). High-Throughput Phenotyping Methods for Breeding Drought-Tolerant Crops. International Journal of Molecular Sciences, 22(15):8266.

Kumudini, S. (2010). Soybean growth and development. In The soybean: botany, production and uses, Botany, Production and Uses, pages 48–73. Wallingford, UK.

Kurasch, A. K., Hahn, V., Leiser, W. L., Vollmann, J., Schori, A., Bétrix, C.-A., Mayr, B., Winkler, J., Mechtler, K., Aper, J., Sudaric, A., Pejic, I., Sarcevic, H., Jeanson, P., Balko, C., Signor, M., Miceli, F., Strijk, P., Rietman, H., Muresanu, E., Djordjevic, V., Pospišil, A., Barion, G., Weigold, P., Streng, S., Krön, M., and Würschum, T. (2017). Identification of mega-environments in Europe and effect of allelic variation at maturity E loci on adaptation of European soybean. Plant, Cell & Environment, 40(5):765–778.

Leinonen, I. and Jones, H. G. (2004). Combining thermal and visible imagery for estimating canopy temperature and identifying plant stress. Journal of Experimental Botany, 55(401):1423–1431.

Lumactud, R. A., Dollete, D., Liyanage, D. K., Szczyglowski, K., Hill, B., and Thilakarathna, M. S. (2023). The effect of drought stress on nodulation, plant growth, and nitrogen fixation in soybean during early plant growth. Journal of Agronomy and Crop Science, 209(3):345–354.

Luo, Q. (2011). Temperature thresholds and crop production: a review. Climatic Change, 109(3):583–598.

Maes, W. H. and Steppe, K. (2012). Estimating evapotranspiration and drought stress with ground-based thermal remote sensing in agriculture: a review. Journal of Experimental Botany, 63(13):4671–4712.

Manavalan, L. P., Guttikonda, S. K., Phan Tran, L.-S., and Nguyen, H. T. (2009). Physiological and Molecular Approaches to Improve Drought Resistance in Soybean. Plant and Cell Physiology, 50(7):1260–1276.

Mannan, M., Rima, I., Karim, A., Mannan, M., Rima, I., and Karim, A. (2022). Physiological and Biochemical Basis of Stress Tolerance in Soybean. In Soybean - Recent Advances in Research and Applications, pages 1–11. IntechOpen, published online.

Mano, N., Madore, B., and Mickelbart, M. (2023). Different Leaf Anatomical Responses to Water Deficit in Maize and Soybean. Life, 13(2):290.

Matei, G., Woyann, L. G., Milioli, A. S., De Bem Oliveira, I., Zdziarski, A. D., Zanella, R., Coelho, A. S. G., Finatto, T., and Benin, G. (2018). Genomic selection in soybean: accuracy and time gain in relation to phenotypic selection. Mol Breeding, 38(9):117.

Mathews, K. L. and Crossa, J. (2022). Experimental Design for Plant Improvement. In Reynolds, M. P. and Braun, H.-J., editors, Wheat Improvement: Food Security in a Changing Climate, pages 215–235. Springer International Publishing, Cham.

Meeus, S., Van den Bulcke, J., and Wyffels, F. (2020). From leaf to label: A robust automated workflow for stomata detection. Ecology and Evolution, 10(17):9178–9191.

Melandri, G., Prashar, A., McCouch, S., Van Der Linden, G., Jones, H., Kadam, N., Jagadish, K., Bouwmeester, H., and Ruyter-Spira, C. (2020). Association mapping and genetic dissection of drought-induced canopy temperature differences in rice. Journal of Experimental Botany, 71(4):1614–1627.

Miladinović, J. and Djordjević, V. (2011). Soybean morphology and stages of development. Soybean, pages 45–71. Publisher: Novi Sad: Institute of Field and Vegetable Crops.

Millstead, L., Jayakody, H., Patel, H., Kaura, V., Petrie, P. R., Tomasetig, F., and Whitty, M. (2020). Accelerating Automated Stomata Analysis Through Simplified Sample Collection and Imaging Techniques. Front. Plant Sci., 11:580389.

Mishra, P., Asaari, M. S. M., Herrero-Langreo, A., Lohumi, S., Diezma, B., and Scheunders, P. (2017). Close range hyperspectral imaging of plants: A review. Biosystems Engineering, 164:49–67.

Monnens, D., López, J. R., McCoy, E., Tamang, B. G., Lorenz, A. J., and Sadok, W. (2024). High-throughput phenotyping of soybean (*Glycine max*) transpiration response curves to rising atmospheric drying in a mapping population. Funct Plant Biol, 51(12).

Nadeem, M., Li, J., Yahya, M., Sher, A., Ma, C., Wang, X., and Qiu, L. (2019). Research Progress and Perspective on Drought Stress in Legumes: A Review. IJMS, 20(10):2541.

Nendel, C., Reckling, M., Debaeke, P., Schulz, S., Berg-Mohnicke, M., Constantin, J., Fronzek, S., Hoffmann, M., Jakšić, S., Kersebaum, K.-C., Klimek-Kopyra, A., Raynal, H., Schoving, C., Stella, T., and Battisti, R. (2023). Future area expansion outweighs increasing drought risk for soybean in Europe. Global Change Biology, 29(5):1340–1358.

Pask, A. (2012). Physiological Breeding: A field guide to wheat phenotyping. II. CIMMYT.

Peñuelas, J., Filella, I., Biel, C., Serrano, L., and Savé, R. (1993). The reflectance at the 950–970 nm region as an indicator of plant water status. International Journal of Remote Sensing, 14(10):1887–1905.

Pineda, M., Barón, M., and Pérez-Bueno, M.-L. (2021). Thermal Imaging for Plant Stress Detection and Phenotyping. Remote Sensing, 13(1):68.

Poudel, S., Adhikari, B., Dhillon, J., Reddy, K., Stetina, S., and Bheemanahalli, R. (2023a). Quantifying the physiological, yield, and quality plasticity of Southern USA soybeans under heat stress. Plant Stress, 9:100195.

Poudel, S., Vennam, R., Sankarapillai, L., Liu, J., Reddy, K., Wijewardane, N., Mukhtar, M., and Bheemanahalli, R. (2024). Negative synergistic effects of drought and heat during flowering and seed setting in soybean. Environmental and Experimental Botany, 222:105769.

Poudel, S., Vennam, R., Shrestha, A., Reddy, K., Wijewardane, N., Reddy, K., and Bheemanahalli, R. (2023b). Resilience of soybean cultivars to drought stress during flowering and early-seed setting stages. Scientific Reports, 13(1):1277.

Prasad, B., Carver, B. F., Stone, M. L., Babar, M. A., Raun, W. R., and Klatt, A. R. (2007). Potential Use of Spectral Reflectance Indices as a Selection Tool for Grain Yield in Winter Wheat under Great Plains Conditions. Crop Science, 47(4):1426–1440.

Prey, L., Hu, Y., and Schmidhalter, U. (2020). High-Throughput Field Phenotyping Traits of Grain Yield Formation and Nitrogen Use Efficiency: Optimizing the Selection of Vegetation Indices and Growth Stages. Front. Plant Sci., 10:1672.

Reynolds, M. P. (2012). Physiological breeding I: interdisciplinary approaches to improve crop adaption. CIMMYT, Mexiko, D.F.

Römer, C., Wahabzada, M., Ballvora, A., Pinto, F., Rossini, M., Panigada, C., Behmann, J., Léon, J., Thurau, C., Bauckhage, C., Kersting, K., Rascher, U., and Plümer, L. (2012). Early drought stress detection in cereals: simplex volume maximisation for hyperspectral image analysis. Functional Plant Biol., 39(11):878–890.

Rolbiecki, S., Kasperska-Wołowicz, W., Jagosz, B., Sadan, H. A., Rolbiecki, R., Szczepanek, M., Kanecka-Geszke, E., and Łangowski, A. (2023). Water and Irrigation Requirements of *Glycine max* (L.) Merr. in 1981–2020 in Central Poland, Central Europe. Agronomy, 13(9):2429.

Roman, A. and Ursu, T. (2016). Multispectral satellite imagery and airborne laser scanning techniques for the detection of archaeological vegetation marks. In LANDSCAPES OF THE NORTH-WESTERN LIMES OF ROMAN DACIA, pages 141–152. Cluj-Napoca, Romania.

Rotundo, J. L., Marshall, R., McCormick, R., Truong, S. K., Styles, D., Gerde, J. A., Gonzalez-Escobar, E., Carmo-Silva, E., Janes-Bassett, V., Logue, J., Annicchiarico, P., de Visser, C., Dind, A., Dodd, I. C., Dye, L., Long, S. P., Lopes, M. S., Pannecoucque, J., Reckling, M., Rushton, J., Schmid, N., Shield, I., Signor, M., Messina, C. D., and Rufino, M. C. (2024). European soybean to benefit people and the environment. Sci Rep, 14(1):7612.

Rouse, J., Haas, R. H., Schell, J. A., and Deering, D. (1973). Monitoring vegetation systems in the great plains with ERTS. In Proceedings of the Third Earth Resources Technology Satellite-1 Symposium-Volume I: Technical Presentations., pages 309 – 317.

Sakoda, K., Watanabe, T., Sukemura, S., Kobayashi, S., Nagasaki, Y., Tanaka, Y., and Shiraiwa, T. (2019). Genetic Diversity in Stomatal Density among Soybeans Elucidated Using High-throughput Technique Based on an Algorithm for Object Detection. Scientific Reports, 9(1):7610.

Samarah, N. H., Mullen, R. E., Cianzio, S. R., and Scott, P. (2006). Dehydrin-Like Proteins in Soybean Seeds in Response to Drought Stress during Seed Filling. Crop Science, 46(5):2141–2150.

Serraj, R., Sinclair, T. R., and Purcell, L. C. (1999). Symbiotic N2 fixation response to drought. Journal of Experimental Botany, 50(331):143–155.

Sinclair, T., Messina, C., Beatty, A., and Samples, M. (2010). Assessment across the united states of the benefits of altered soybean drought traits. Agronomy Journal, 102(2):475–482.

Sinclair, T. and Serraj, R. (1995). Legume nitrogen fixation and drought. Nature, 378(6555):344.

Staniak, M., Czopek, K., Stępień-Warda, A., Kocira, A., and Przybyś, M. (2021a). Cold Stress during Flowering Alters Plant Structure, Yield and Seed Quality of Different Soybean Genotypes. Agronomy, 11(10):2059.

Staniak, M., Stępień-Warda, A., Czopek, K., Kocira, A., and Baca, E. (2021b). Seeds Quality and Quantity of Soybean [*Glycine max* (L.) Merr.] Cultivars in Response to Cold Stress. Agronomy, 11(3):520.

Staniak, M., Szpunar-Krok, E., and Kocira, A. (2023). Responses of Soybean to Selected Abiotic Stresses—Photoperiod, Temperature and Water. Agriculture, 13(1):146.

Struthers, R., Ivanova, A., Tits, L., Swennen, R., and Coppin, P. (2015). Thermal infrared imaging of the temporal variability in stomatal conductance for fruit trees. International Journal of Applied Earth Observation and Geoinformation, 39:9–17.

Sultana, S., Park, H., Choi, S., Jo, H., Song, J., Lee, J.-D., and Kang, Y. (2021). Optimizing the experimental method for stomata-profiling automation of soybean leaves based on deep learning. Plants, 10(12):2714.

Sultana, S. N., Jo, H., Song, J. T., Kim, K., and Lee, J.-D. (2024). Stomatal Density Variation Within and Among Different Soybean Cultivars Across Various Growth Stages. Agriculture, 14(11):2028.

Taiz, L., Zeiger, E., Amasino, R., Bernasconi, P., Blankenship, R. E., Bloom, A. J., Bressan, R. A., Buchanan, B. B., Cosgrove, D. J., Davies, P. J., and others (2010). Plant physiology.

Tanaka, Y., Fujii, K., and Shiraiwa, T. (2010). Variability of Leaf Morphology and Stomatal Conductance in Soybean [*Glycine max* (L.) Merr.] Cultivars. Crop Science, 50(6):2525–2532.

Team, R. C. (2015). R: A Language and Environment for Statistical Computing. R Foundation for Statistical Computing, Vienna, Austria. URL: https://cran.r-project.org/doc/FAQ/R-FAQ.html#Citing-R).

Toum, L., Perez-Borroto, L., Peña-Malavera, A., Luque, C., Welin, B., Berenstein, A., Fernández Do Porto, D., Vojnov, A., Castagnaro, A., and Pardo, E. (2022). Selecting putative drought-tolerance markers in two contrasting soybeans. Scientific Reports, 12(1):10872.

Turner, N. C., Wright, G. C., and Siddique, K. H. M. (2001). Adaptation of grain legumes (pulses) to water-limited environments. Advances in Agronomy, 71:193–231.

Ucak, A. B. and Arslan, H. (2023). Drought stress resistance indicators of chickpea varieties grown under deficit irrigation conditions. PeerJ, 11:e14818.

Uddling, J., Gelang-Alfredsson, J., Piikki, K., and Pleijel, H. (2007). Evaluating the relationship between leaf chlorophyll concentration and SPAD-502 chlorophyll meter readings. Photosynth Res, 91(1):37–46.

Ullah, A. and Farooq, M. (2022). The challenge of drought stress for grain legumes and options for improvement. Archives of Agronomy and Soil Science, 68(11):1601–1618.

Utz, H. (2005). PLABSTAT - Plant Breeding Statistical Program. Version 3A. Institute of Plant Breeding, Seed Science and Population Genetics, University of Hohenheim, Stuttgart, Germany.

Vollmann, J. and Škrabišová, M. (2023). Going north: adaptation of soybean to long-day environments. Journal of Experimental Botany, 74(10):2933–2936.

Vollmann, J., Rischbeck, P., Pachner, M., Đorđević, V., and Manschadi, A. M. (2022). High-throughput screening of soybean di-nitrogen fixation and seed nitrogen content using spectral sensing. Computers and Electronics in Agriculture, 199:107169.

Xie, C. and Yang, C. (2020). A review on plant high-throughput phenotyping traits using UAV-based sensors. Computers and Electronics in Agriculture, 178:105731.

REFERENCES

Yamaguchi, N., Yamazaki, H., Ohnishi, S., Suzuki, C., Hagihara, S., Miyoshi, T., and Senda, M. (2014). Method for selection of soybeans tolerant to seed cracking under chilling temperatures. Breeding Science, 64(1):103–108.

Yao, X. and Zhang, D. (2024). Genome-Wide Association Analysis of Active Accumulated Temperature versus Flowering Time in Soybean [*Glycine max* (L.) Merr.]. Agronomy, 14(4):833.

Ye, H., Song, L., Shannon, J. G., University of Missouri, USA, Chen, P., University of Missouri, USA, Nguyen, H. T., and University of Missouri, USA (2018). Advances in the drought and heat resistance of soybean. In University of Missouri, USA and Nguyen, H. T., editors, Burleigh Dodds Series in Agricultural Science, pages 171–190. Burleigh Dodds Science Publishing.

Zargar, A., Sadiq, R., Naser, B., and Khan, F. I. (2011). A review of drought indices. Environ. Rev., 19:333–349.

Zhang, X., Zhao, J., Yang, G., Liu, J., Cao, J., Li, C., Zhao, X., and Gai, J. (2019). Establishment of Plot-Yield Prediction Models in Soybean Breeding Programs Using UAV-Based Hyperspectral Remote Sensing. Remote Sensing, 11(23):2752.

Zia, S., Romano, G., Spreer, W., Sanchez, C., Cairns, J., Araus, J. L., and Müller, J. (2013). Infrared Thermal Imaging as a Rapid Tool for Identifying Water-Stress Tolerant Maize Genotypes of Different Phenology. Journal of Agronomy and Crop Science, 199(2):75–84.

7 Supplementary material

Figure S1: Single row plots of experimental setup in Tulln, Austria in growing season 2024; photographs were taken (a) at 18. June (doy: 179) during vegetative phase and (b) at 12. July (doy: 194) after canopy has fully covered soil.

Table S2: Number of genotypes represented by contributing European breeding institutions and companies for each trial.

			Trial No.			
			Y1	Y2	Y3	FD
Breeder	Abbr.	Country	Number of genotypes			
WBF Agroscope	AGS	Suisse	9	11	7	14
Danko Hodowa Roslin	DANKO	Poland	12	–	–	10
Lidea Seeds	LIDEA	France	8	8	8	9
RAGT Seeds	RAGT	France	10	7	9	13
Saatzucht Gleisdorf	SZG	Austria	8	9	6	8
University of Hohenheim	UHOH	Germany	13	10	–	10
BOKU University	BOKU	Austria	–	–	–	6
		Total	60	45	30	70

Table S3a: Experimental setup of trial Y1 with all soybean varieties of MG 000.

Yield1 early (000) - Tulln (AT) - 2024

n= 60, rep=2, 10x6 lattice

Genotype ID		rep 1						rep 2					
	30	119	152	112	**159**	125	133	131	152	128	105	108	142
	29	135	126	118	127	156	141	117	136	133	106	154	139
	28	120	131	124	139	150	101	127	140	144	143	125	**160**
	27	146	137	117	109	114	102	156	124	115	145	113	146
	26	136	108	147	116	145	130	153	122	135	107	102	104
	25	106	113	155	132	104	**160**	149	112	103	130	120	114
	24	149	134	128	107	111	144	157	155	151	141	147	109
	23	153	151	143	142	129	148	116	110	**159**	138	150	137
	22	110	121	122	154	115	157	121	132	126	158	134	148
row	21	105	140	158	103	138	123	129	101	123	118	119	111
		1	2	3	4	5	6	7	8	9	10	11	12
		column											

Varieties

AGS	101	CH21414 Tiguan	121	ES-COMANDOR	141	GL Begonia
DANKO	102	CH21507 Gallec	122	ES-SENATOR	142	GL Theresa (GL 1917012)
LIDEA	103	CH22172 Obélix	123	ES-CHANCELLOR	143	GL Sanne (GL 201213)
RAGT	104	CH22232 Toutatis	124	ES-COLLECTOR	144	GL Susanna
SZG	105	CH22526 Tarock	125	ES-FAVOR	145	GL ###1
UHOH	106	CH22624 Arnold	126	LID-DIAMANTOR	146	UHOH-1
Standard	107	CH22645 Farmosa	127	ES-CONDUCTOR	147	UHOH-2
	108	CH22711 Noa	128	ES-COMPOSITOR	148	UHOH-3
	109	Erica	129	RGT SIGMA	149	UHOH-4
	110	DS 21001	130	SANKARA	150	UHOH-5
	111	DS 22004	131	RGT SALSA	151	UHOH-6
	112	DS 22014	132	RGT SPHINXA	152	UHOH-7
	113	DS 22020	133	STEPA	153	UHOH-8
	114	DS 22031	134	SAHARA	154	UHOH-9
	115	DS 22013	135	RGT SATELIA	155	UHOH-10
	116	DS 22019	136	STAPELIA	156	UHOH-11
	117	DS 22030	137	SIRELIA	157	UHOH-12
	118	DS 22034	138	GL Creme	158	UHOH-13
	119	DS 22035	139	GL Britta	159	**CH22172 Obélix**
	120	DS 22024	140	GL Melanie	160	**RGT STUMPA**

Table S3b: Experimental setup of trial Y2 with all soybean varieties of MG 00.

Yield2 mid (00) - Tulln (AT) - 2024

n= 45, rep=2, 15x3 lattice

Genotype ID		rep 1			rep 2				
	30	232	233	223	223	227	238	201	243	228
	29	236	239	238	212	208	214	202	234	244
	28	203	**245**	225	233	216	231	210	239	232
	27	215	228	212	229	207	230	225	213	205
	26	210	237	222	224	**219**	235	218	209	215
	25	231	227	242	220	216	221	220	211	**245**
	24	**219**	230	244	207	224	214	204	237	226
	23	217	243	218	202	229	204	206	236	222
	22	209	240	213	201	235	208	242	241	221
row	21	205	241	211	226	234	206	240	217	203
		13	14	15	16	17	18	19	20	21
		column								

Varieties

AGS	**201**	CH22177 Galice	**223**	SQUADRA
LIDEA	**202**	CH22508 Paprika	**224**	SHIVA
RAGT	**203**	CH22554 Simpol	**225**	SIBELLA
SZG	**204**	CH22681 Prolix	**226**	GL Pia (GL 1816014)
UHOH	**205**	CH90075 Talisse	**227**	GL 201212
Standard	**206**	CH90093 Soramax	**228**	GL 201811
	207	CH90132 Benno	**229**	GL 201117
	208	CH90139	**230**	Xonia
	209	CH22910	**231**	GL 221712
	210	CH90166	**232**	GL 221623
	211	LID-CONSTRUCTOR	**233**	GL 221715
	212	ES-DIRECTOR	**234**	GL Tilda
	213	ES-INSPECTOR	**235**	UHOH-51
	214	ES-LIBERATOR	**236**	UHOH-52
	215	ES-LOUXOR	**237**	UHOH-53
	216	ES-MENTOR	**238**	UHOH-54
	217	ES-PROFESSOR	**239**	UHOH-55
	218	ES-VISITOR	**240**	UHOH-56
	219	**RGT STUMPA**	**241**	UHOH-57
	220	RGT SEFORA	**242**	UHOH-58
	221	RGT SAKUSA	**243**	UHOH-59
	222	SUZA	**244**	UHOH-60
			245	**CH22172 Obélix**

Table S3c: Experimental setup of trial Y2 with all soybean varieties of MG 0/I.

Yield3 late (0-I) - Tulln (AT) - 2024

n= 30, rep=2, 10x3 lattice

Genotype ID		rep 1			rep 2		
	30	308	310	311	304	314	309
	29	312	306	324	302	317	318
	28	319	316	328	323	305	312
	27	301	303	317	303	315	324
	26	323	325	326	310	**330**	307
	25	313	320	321	**329**	322	301
	24	**330**	314	302	327	328	311
	23	322	315	305	321	319	308
	22	304	327	307	325	313	316
row	21	318	**329**	309	326	320	306
		22	23	24	25	26	27
		column					

Varieties					
	301	CH50155 Panoramix	315	RGT SPEEDA
	302	CH50263	316	RGT SICILIA
	303	CH50274 Magalix	317	RGT SCALA
	304	CH50328	318	RGT STRAVIATA
AGS	305	CH50333	319	RGT STOCATA
LIDEA	306	CH50343	320	RGT SINEMA
RAGT	307	ES-ADVISOR	321	SHAMA
SZG	308	ES-ANIMATOR	322	RAGT2401
Standard	309	ES-TRIBOR	323	GL Valerie
	310	ES-WARRIOR	324	GL Leonie
	311	ES-CONQUEROR	325	GL Lilas
	312	ES-CONNECTOR	326	GL 201527
	313	ES-PALLADOR	327	Svelte
	314	ISIDOR	328	GL 221627
	329	**CH22172 Obélix**	330	**RGT STUMPA**

Table S3d: Experimental setup of trial Food with all soybean varieties for food use.

Food - Tulln (AT) - 2024

n= 70, rep=2, 10x7 lattice

Genotype ID		rep 1							rep 2						
	30	461	413	437	**469**	420	447	406	448	402	412	467	419	414	445
	29	441	458	453	452	433	419	466	438	454	463	422	421	455	449
	28	465	456	439	448	446	449	432	**469**	423	460	403	409	452	439
	27	450	412	457	431	460	462	438	416	432	468	410	401	407	450
	26	422	459	428	444	423	435	427	408	433	406	436	415	444	417
	25	443	405	445	468	408	403	426	429	427	466	**470**	447	442	440
	24	417	440	451	434	409	455	401	418	411	430	451	428	420	456
	23	418	402	424	454	442	410	415	462	459	443	434	458	424	437
	22	436	467	**470**	416	411	463	425	461	441	431	464	426	465	425
row	21	421	429	464	407	414	404	430	405	446	457	404	435	413	453
		28	29	30	31	32	33	34	35	36	37	38	39	40	41
		column													

Varieties

AGS	
DANKO	
LIDEA	
RAGT	
SZG	
UHOH	
BOKU	
Standard	

401	CH21912 Protéix
402	CH22101 Protibus
403	CH22138 Amandine
404	CH22144 Falbala
405	CH22315 Marquise
406	CH22517 Miraculix
407	CH22645 Farmosa
408	CH22681 Prolix
409	CH50155 Panoramix
410	CH90166
411	CH21715 Aveline
412	CH22164 Gourmandine
413	CH22338 Helix
414	Erica
415	DS 22020
416	DS 22031
417	DS 22019
418	DS 22030
419	DS 22035
420	DS 21002
421	DS 22032
421	DS 22032
422	DS 22008
423	DS 22009
424	ES-INSTRUCTOR
425	COMBINATOR
426	ES-BACHELOR
427	ES-INSPECTOR
428	ES-MENTOR
429	ES-WARRIOR
429	ES-WARRIOR
430	ES-COMPETITOR
431	ISIDOR
432	LID-LINGODOR
433	RGT SALSA
434	RGT SPHINXA
435	STEPA
436	SUZA
437	SHIVA
438	RGT SPEEDA
439	RGT STOCATA
440	RAGT2401
441	RGT SICILIA
442	RGT SINFONIA
443	RGT SINEMA
444	RGT STARBELA
445	GL Valerie
446	GL Lilas
447	GL Britta
448	GL Creme
449	GL Begonia
450	GL 201117
451	Xonia
452	Svelte
453	UHOH-Food-1
454	UHOH-Food-2
455	UHOH-Food-3
456	UHOH-Food-4
457	UHOH-Food-5
458	UHOH-Food-6
459	UHOH-Food-7
460	UHOH-Food-8
461	UHOH-Food-9
462	UHOH-Food-10
463	BOKU-01 GT10X-15-1-4
464	BOKU-02 GT8X-24-1
465	BOKU-03 G2B1X-185-10
466	BOKU-04 G2B1X-88-2
467	BOKU-05 GW6X-31-4-4
468	BOKU-06 GT9X-19-1-5
469	**CH22172 Obélix**
470	**RGT STUMPA**

Table S4: Overview of all evaluated traits on soybean field trials in season 2024.

Date	Trait	Remark	unit	description
10.05.	Sowing date			doy: 131
30.09./16.10.	Harvesting date	Y1+Y2+Food / Y3		doy: 274/291
24.05.	Field emergence (VE)		-	1 = very low, 9 = very dense
18.06.	Development score (V2)		-	1 = sparse, 5 = dense
18.06. - 14.07.	Time to flowering (R1)		doy	day on which 50% of plants per plot show the first flower(s) on the main stem
26.08. - 06.10.	Time to maturity (R8)		doy	day of full maturity with leaves dropped, pods brown, seeds hard
10./11.07.	Stomatal density	only Y2	N/cm²	15 images per plot; observed area: 0.2031 mm²
16.07.-18.07.	Leaf size		cm²	5 central leaflets per plot; green pixels of RGB-photo are counted
16.07.-18.07.	SPAD value 1		-	SPADmeter
08.08.	SPAD value 2	only Y2	-	SPADmeter
20./30.09.	Plant height		cm	plant height at the end of season
26.09. / 27.09.	Pod set		-	1 = low, 3 = mid, 5 = high
19.09. / 26.09.	Scores for lodging	Y1+Y2 / Y3+Food	-	1 = none, 5 = highest
19.09. / 26.09.	Pod shattering	Y1+Y2 / Y3+Food	-	1 = none, 5 = strongest
18.11.	Grain yield		dt/ha	air-dried seeds in paper bags

Table S5: Trial Y1, statistical analysis from plabstat in all scored and measured traits; Anova with F-values between unadjusted Treatments (Varieties), Replications and Blocks (adjusted); correlation matrix with all traits (Pearson): colored cells show significant correlation; following significance levels (Sign.) are valid: +: p<0.1; ∗: p<0.05; ∗∗: p<0.01; ns: not significant.

Y1	60 Genotypes; Lattice 10x6 ; 2 rep			**Software:** Plabstat		**Date:** 20.01.2025				
ANOVA							**Distribution of traits**			
Trait	**Treatments (unadj.)**		**Replications**		**Blocks (adj.)**					
	F-value	Sign.	F-value	Sign.	F-value	Sign.	**Unit**	**Mean**	**St.Dev.**	**C.V.%**	**LSD5**
emerg	**1.95**	*	7.25	**	1.14	ns	[-]	7.53	0.65	8.5	1.30
devscore	**1.22**	ns	0.75	ns	1.07	ns	[-]	3.27	0.56	19.4	1.28
ttf	**1.58**	+	2.25	ns	0.60	ns	[doy]	172.87	0.97	0.6	1.97
ttm	**3.29**	**	13.26	**	1.37	ns	[doy]	250.68	3.15	1	5.00
t-reprod	**2.23**	**	14.51	**	1.20	ns	[day]	77.82	2.89	3.6	5.59
podshat	**7.34**	**	3.37	+	1.32	ns	[-]	1.48	0.88	30	0.89
lodging	**2.35**	**	1.25	ns	0.90	ns	[-]	2.17	0.85	33.8	1.48
podset	**2.66**	**	2.01	ns	1.36	ns	[-]	2.71	0.68	21.1	1.16
SPAD	**1.35**	ns	6.85	*	1.02	ns	[-]	42.8	1.85	5.3	4.54
leaf size	**4.40**	**	1.26	ns	2.29	*	[cm²]	50.89	7.4	9.6	9.91
height	**4.77**	**	0.01	ns	1.12	ns	[cm]	74.38	10.64	8	12.06
yield	**2.48**	**	9.88	**	2.07	*	[dt/ha]	31.74	5.9	17.7	11.34

Correlation matrix - Pearson's correlation coefficient (r)

	emerg	devscore	ttf	ttm	t-reprod	podshat	lodging	podset	SPAD	leaf size	height
devscore	0.513**										
ttf	-0.201	-0.382**									
ttm	-0.011	-0.234	0.411**								
t-reprod	0.051	-0.129	0.113	0.951**							
podshat	0.07	0.08	-0.014	-0.348**	-0.372**						
lodging	-0.137	0.07	0.239	-0.061	-0.153	0.005					
podset	-0.067	-0.081	-0.049	0.09	0.121	-0.099	-0.461**				
SPAD	-0.377**	-0.058	-0.122	-0.069	-0.028	-0.035	-0.011	0.161			
leaf size	0.023	-0.189	0.410**	0.189	0.063	-0.199	0.019	0.18	-0.114		
height	-0.028	-0.032	0.488**	0.238	0.078	-0.082	0.653**	-0.294*	-0.165	0.277*	
yield	0.024	-0.021	0.234	0.459**	0.416**	-0.617**	0.270*	0.163	-0.094	0.325*	0.466**

Table S6: Trial Y2, statistical analysis from plabstat in all scored and measured traits; Anova with F-values between unadjusted Treatments (Varieties), Replications and Blocks (adjusted); correlation matrix with all traits (Pearson): colored cells show significant correlation; following significance levels (Sign.) are valid: +: p<0.1; ∗: p<0.05; ∗∗: p<0.01; ns: not significant.

Y2	45 Genotypes; Lattice 15x3 ; 2 rep			Software: Plabstat		Date: 20.01.2025				
ANOVA						**Distribution of traits**				
Trait	**Treatments (unadj.)**		**Replications**		**Blocks (adj.)**					
	F-value	Sign.	F-value	Sign.	F-value	Sign.	**Unit**	**Mean**	**St.Dev.**	**C.V.%**	**LSD5**
emerg	6.56	**	2.73	ns	1.90	+	[-]	7.44	1.02	7.9	1.25
devscore	2.37	*	3.45	+	1.78	ns	[-]	3.19	0.56	18.3	1.24
ttf	6.40	**	-	ns	0.92	ns	[doy]	173.84	1.75	0.5	1.89
ttm	2.26	*	1.49	ns	0.96	ns	[doy]	256.90	2.89	0.9	4.94
t-reprod	1.31	ns	1.45	ns	0.57	ns	[day]	83.06	2.77	2.8	5.01
podshat	8.05	**	2.05	ns	1.32	ns	[-]	1.07	0.31	13.6	0.31
lodging	2.93	*	2.67	ns	2.61	*	[-]	1.57	0.68	38.5	1.28
podset	1.33	ns	-	ns	1.03	ns	[-]	2.71	0.69	26.1	1.50
SPAD1	4.02	**	11.57	**	2.06	+	[-]	41.87	1.84	3.2	2.82
SPAD2	1.29	ns	2.21	ns	1.40	ns	[-]	46.23	1.56	4.5	4.45
leaf size	8.34	**	0.17	ns	1.18	ns	[cm²]	49.80	9.12	8.0	8.40
d-stom	1.81	+	0.00	ns	10.28	**	[1/mm²]	251.45	26.63	11.0	58.89
height	4.91	**	1.13	ns	1.16	ns	[cm]	84.11	11.14	7.0	12.56
yield	2.47	*	4.56	*	1.78	ns	[dt/ha]	34.05	5.26	15.0	10.83

Correlation matrix - Pearson's correlation coefficient (r)

	emerg	**devscore**	**ttf**	**ttm**	**t-reprod**	**podshat**	**lodging**	**podset**	**SPAD1**	**SPAD2**	**leaf size**	**d-stom**	**height**
devscore	0.544**												
ttf	-0.143	-0.314*											
ttm	0.277	0.072	0.366*										
t-reprod	0.378*	0.273	-0.252	0.809**									
podshat	-0.016	-0.024	-0.081	-0.330*	-0.292								
lodging	-0.005	-0.133	0.084	0.085	0.035	0.330*							
podset	-0.036	-0.062	-0.157	-0.414**	-0.331*	-0.227	-0.386**						
SPAD1	-0.061	0.08	-0.239	-0.188	-0.044	-0.008	0.232	-0.144					
SPAD2	0.142	0.075	-0.184	-0.053	0.061	0.263	-0.183	0.072	-0.112				
leaf size	0.175	-0.065	0.654**	0.284	-0.118	0.016	-0.089	0.078	-0.258	0.004			
d-stom	0.234	0.06	0.179	0.166	0.059	-0.269	-0.074	0.259	0.153	0.063	0.216		
height	0.350*	0.287	0.196	0.375*	0.266	0.343*	0.385**	-0.608**	-0.057	0.004	0.202	-0.085	
yield	0.465**	0.371*	-0.091	0.206	0.272	-0.173	0.035	0.174	-0.171	0.016	0.191	0.16	0.196

Table S7: Trial Y3, statistical analysis from plabstat in all scored and measured traits; Anova with F-values between unadjusted Treatments (Varieties), Replications and Blocks (adjusted); correlation matrix with all traits (Pearson): colored cells show significant correlation; following significance levels (Sign.) are valid: +: p<0.1; ∗: p<0.05; ∗∗: p<0.01; ns: not significant.

Y3	30 Genotypes; Lattice 10x3 ; 2 rep		Software: Plabstat		Date: 20.01.2025					
ANOVA							**Distribution of traits**				
Trait	**Treatments (unadj.)**		**Replications**		**Blocks (adj.)**						
	F-value	Sign.	F-value	Sign.	F-value	Sign.	**Unit**	**Mean**	**St.Dev.**	**C.V.%**	**LSD5**
emerg	1.25	ns	1.29	ns	0.70	ns	[-]	7.63	0.92	11.9	2.00
devscore	2.97	*	0.14	ns	2.14	+	[-]	3.37	0.73	18.5	1.37
ttf	12.71	**	0.55	ns	1.72	ns	[doy]	183.93	6.71	1.4	5.77
ttm	9.51	**	0.30	ns	1.50	ns	[doy]	267.92	6.27	0.9	5.54
t-reprod	3.45	*	0.04	ns	1.11	ns	[day]	83.98	4.77	3.7	6.90
podshat	0.00	ns	0.29	ns	0	ns	[-]	1.20	-	-	0.00
lodging	2.12	+	0.35	ns	0.80	ns	[-]	2.15	0.8	30.4	1.44
podset	0	ns	0.14	ns	0	ns	[-]	2.70	-	-	0.00
SPAD	2.15	+	2.18	ns	1.37	ns	[-]	43.15	1.95	3.8	3.64
leaf size	5.47	**	0	ns	0.97	ns	[cm²]	60.87	8.37	7.1	9.50
height	3.39	*	3.68	+	0.65	ns	[cm]	92.67	8.90	5.1	10.37
yield	2.54	+	1.04	ns	1.32	ns	[dt/ha]	30.25	5.23	15.5	10.31

Correlation matrix - Pearson's correlation coefficient (r)

	emerg	**devscore**	**ttf**	**ttm**	**t-reprod**	**podshat**	**lodging**	**podset**	**SPAD**	**leaf size**	**height**
devscore	0.634**										
ttf	-0.234	-0.471**									
ttm	0.213	-0.188	0.709**								
t-reprod	0.595**	0.404*	-0.440*	0.318							
podshat	0.023	-0.267	0.451*	0.315	-0.243						
lodging	0.077	-0.175	0.697**	0.673**	-0.066	0.618**					
podset	0.115	0.448*	-0.535*	-0.849**	-0.181	-0.279	-0.549**				
SPAD	0.317	0.26	0.099	0.11	0.005	0.028	0.174	0.062			
leaf size	-0.386*	-0.25	0.223	0.007	-0.305	-0.212	-0.101	-0.382	-0.384*		
height	0.145	-0.05	0.379*	0.637**	0.3	0.121	0.535**	-0.791**	0.115	0.2	
yield	0.076	0.434*	-0.494**	-0.474**	0.071	-0.144	-0.14	0.547**	-0.088	-0.073	-0.203

Table S8: Trial Y1, statistical analysis from plabstat in all scored and measured traits; Anova with F-values between unadjusted Treatments (Varieties), Replications and Blocks (adjusted); correlation matrix with all traits (Pearson): colored cells show significant correlation; following significance levels (Sign.) are valid: +: p<0.1; ∗: p<0.05; ∗∗: p<0.01; ns: not significant.

Food 70 Genotypes; Lattice 10x7 ; 2 rep **Software:** Plabstat **Date:** 20.01.2025

ANOVA

Trait	Treatments (unadj.)		Replications		Blocks (adj.)		Distribution of traits				
	F-value	Sign.	F-value	Sign.	F-value	Sign.	Unit	MEAN	St.Dev.	C.V.%	LSD5
emerg	1.82	*	0.02	ns	0.75	ns	[-]	7.71	0.66	8.2	1.27
devscore	1.51	+	0.01	ns	1.87	*	[-]	3.44	0.59	20.0	1.38
ttf	21.59	**	11.45	**	1.44	ns	[doy]	176.48	6.03	1.0	3.60
ttm	20.68	**	0.44	ns	1.21	ns	[doy]	256.80	6.73	0.8	4.06
t-reprod	5.18	**	8.98	**	1.91	*	[day]	80.32	3.77	3.0	4.81
podshat	9.44	**	0.06	ns	0.90	ns	[-]	1.44	0.82	24.4	0.70
lodging	7.07	**	5.45	*	1.75	+	[-]	2.33	1.02	24.0	1.12
podset	4.27	**	1.33	ns	1.64	+	[-]	2.88	0.71	17.3	1.00
SPAD	3.51	**	0.43	ns	1.43	ns	[-]	42.75	1.58	2.8	2.44
leaf size	11.83	**	2.40	ns	1.80	+	[cm²]	57.80	11.35	8.1	9.36
height	10.02	**	3.16	+	1.84	*	[cm]	81.36	10.99	6.2	10.08
yield	2.41	**	1.21	ns	1.28	ns	[dt/ha]	29.03	4.79	15.0	8.74

Correlation matrix - Pearson's correlation coefficient (r)

	emerg	devscore	ttf	ttm	t-reprod	podshat	loding	podset	SPAD	leaf size	height
devscore	0.690**										
ttf	-0.138	-0.154									
ttm	-0.082	-0.052	0.830**								
t-reprod	0.067	0.139	-0.117	0.456**							
podshat	-0.002	-0.102	-0.191	-0.306*	-0.23						
lodging	-0.18	-0.176	0.460**	0.307**	-0.185	-0.005					
podset	0.166	0.237*	-0.358**	-0.275*	0.089	0.03	-0.663**				
SPAD	0.123	-0.001	-0.197	-0.118	0.102	0.219	-0.203	0.133			
leaf size	-0.104	-0.028	0.492**	0.538**	0.176	-0.286*	0.103	-0.197	-0.008		
height	-0.124	-0.085	0.645**	0.669**	0.166	-0.148	0.675**	-0.471**	-0.255*	0.332**	
yield	0.06	0.273*	-0.307**	-0.278*	-0.011	-0.320**	-0.218	0.293*	0.031	0.063	-0.108

Table S9a: Trial Y1, Vegetation + Chlorophyll indices at five timepoints (A, D, G, J, K): Anova with F-values between all varieties; correlation matrix with Pearson's correlation coefficients (r): colored cells show significant correlation; following significance levels (Sign.) are valid: +: p<0.1; *: p<0.05; **: p<0.01; ns: not significant.

Y1	60 Genotypes; Lattice 10x6; 2 rep							Software: Plabstat			Date: 25.11./2.12.2024				
ANOVA			**Correlation matrix - Pearson's correlation coefficient (r)**												
F-value	**Sign.**	**Index-TP**	**emerg**	**ttf**	**SPAD**	**leaf size**	**ttm**	**podshat**	**lodging**	**pod set**	**height**	**yield**	*Index-* **A**	*Index-* **D**	*Index-* **G**	*Index-* **J**
2.99	**	NDVI-A	0.320*	-0.013	0.06	0.303*	0.203	-0.217	-0.306*	0.355**	-0.033	0.347**			NDVI	
2.26	**	NDVI-D	0.510**	0.083	-0.245	0.271*	0.203	-0.067	-0.008	0.06	0.25	0.270*	0.678**			
1.91	*	NDVI-G	0.312*	0.068	-0.145	0.111	0.275*	-0.11	-0.268*	0.194	0.051	0.276*	0.690**	0.686**		
2.65	**	NDVI-J	0.360**	0.186	-0.178	0.179	0.397**	-0.222	-0.054	0.256*	0.214	0.468**	0.633**	0.697**	0.709**	
3.43	**	NDVI-K	-0.086	0.304*	-0.072	0.117	0.503**	-0.24	0.062	0.174	0.221	0.336**	0.278*	0.307*	0.423**	0.543**
2.41	**	NRI-A	0.177	0.204	-0.273*	0.339**	0.067	0.03	-0.176	0.204	0.069	0.139			NRI	
3.28	**	NRI-D	0.248	0.280*	-0.404**	0.291*	0.174	0.074	0.058	-0.122	0.280*	0.083	0.704**			
5.01	**	NRI-G	0.119	0.228	-0.367**	0.027	0.085	0.234	-0.125	-0.128	-0.019	-0.212	0.539**	0.702**		
4.34	**	NRI-J	0.23	0.004	-0.316*	-0.158	-0.245	0.445**	-0.033	-0.223	-0.17	-0.416**	0.300*	0.363**	0.711**	
2.05	**	NRI-K	0.032	0.112	-0.233	-0.075	0.04	0.204	0.135	-0.18	-0.005	-0.146	0.152	0.297*	0.491**	0.504**
3.22	**	CI-A	0.233	-0.188	0.275*	0.07	0.156	-0.262*	-0.21	0.275*	-0.035	0.264*			CI	
2.51	**	CI-D	0.335**	-0.19	0.047	-0.002	0.081	-0.182	-0.079	0.203	0.081	0.255*	0.801**			
3.21	**	CI-G	0.186	-0.07	0.11	0.145	0.232	-0.324*	-0.158	0.324*	0.118	0.485**	0.827**	0.741**		
8.16	**	CI-J	0.107	0.195	0.026	0.233	0.464**	-0.406**	-0.005	0.300*	0.288*	0.585**	0.711**	0.642**	0.850**	
5.50	**	CI-K	-0.083	0.270*	0.044	0.211	0.628**	-0.407**	-0.038	0.292*	0.232	0.480**	0.541**	0.401**	0.634**	0.809**
3.00	**	REIP-A	0.209	-0.148	0.262*	0.037	0.147	-0.268*	-0.09	0.195	0.091	0.301*			REIP	
2.78	**	REIP-D	0.280*	-0.198	0.107	-0.042	0.051	-0.213	-0.035	0.198	0.124	0.293*	0.851**			
4.86	**	REIP-G	0.16	-0.046	0.128	0.147	0.218	-0.338**	-0.034	0.300*	0.226	0.535**	0.825**	0.796**		
7.71	**	REIP-J	0.078	0.219	0.018	0.224	0.472**	-0.421**	0.05	0.282*	0.344**	0.611**	0.722**	0.673**	0.851**	
7.95	**	REIP-K	-0.082	0.340**	0.022	0.257*	0.643**	-0.478**	0.018	0.290*	0.306*	0.567**	0.536**	0.406**	0.637**	0.868**
2.73	**	PSSRa-A	0.302*	0.007	0.043	0.324*	0.233	-0.25	-0.335**	0.371**	-0.039	0.343**			PSSRa	
2.48	**	PSSRa-D	0.469**	0.08	-0.241	0.253	0.2	-0.098	-0.016	0.056	0.24	0.273*	0.648**			
1.86	*	PSSRa-G	0.308*	0.051	-0.148	0.126	0.247	-0.137	-0.259*	0.208	0.04	0.302*	0.692**	0.681**		
2.09	**	PSSRa-J	0.370**	0.169	-0.163	0.168	0.360**	-0.227	-0.064	0.239	0.18	0.451**	0.627**	0.697**	0.687**	
3.09	**	PSSRa-K	-0.055	0.176	-0.054	0.074	0.508**	-0.236	-0.06	0.182	0.057	0.262*	0.293*	0.356**	0.478**	0.432**
3.54	**	PSSRb-A	0.274*	-0.033	0.117	0.307*	0.241	-0.291*	-0.304*	0.367**	-0.055	0.364**			PSSRb	
2.74	**	PSSRb-D	0.451**	0.031	-0.135	0.257*	0.191	-0.149	-0.062	0.137	0.166	0.304*	0.715**			
2.05	**	PSSRb-G	0.261*	0.041	-0.059	0.157	0.263*	-0.188	-0.257*	0.222	0.04	0.335**	0.723**	0.711**		
3.73	**	PSSRb-J	0.253	0.169	-0.06	0.224	0.419**	-0.340**	-0.059	0.266*	0.201	0.517**	0.712**	0.723**	0.743**	
3.73	**	PSSRb-K	-0.071	0.185	-0.009	0.106	0.546**	-0.282*	-0.081	0.22	0.079	0.302*	0.392**	0.389**	0.547**	0.578**

Table S9b: Trial Y1, MA1_R and Water indices (WI) at five timepoints (A, D, G, J, K): Anova with F-values between all varieties; correlation matrix with Pearson's correlation coefficients (r): colored cells show significant correlation; following significance levels (Sign.) are valid: +: p<0.1; *: p<0.05; **: p<0.01; ns: not significant.

Y1	60 Genotypes; Lattice 10x6; 2 rep							**Software:** Plabstat			**Date:**	25.11./2.12.2024			
ANOVA			**Correlation matrix - Pearson's correlation coefficient (r)**												
F-value	**Sign.**	**Index-TP**	**emerg**	**ttf**	**SPAD**	**leaf size**	**ttm**	**podshat**	**lodging**	**pod set**	**height**	**yield**	*Index-* **A**	*Index-* **D**	*Index-* **G**	*Index-* **J**
3.68	**	**MA1R-A**	0.012	0.14	-0.257*	-0.032	-0.112	0.199	-0.013	-0.061	0.085	-0.135			**MA1-R**	
5.49	**	**MA1R-D**	0.07	0.188	-0.352**	0.008	0.026	0.175	0.127	-0.275*	0.249	-0.122	0.747**			
3.74	**	**MA1R-G**	0.128	0.089	-0.355**	-0.146	-0.135	0.348**	0.032	-0.178	0.003	-0.297*	0.720**	0.658**		
8.03	**	**MA1R-J**	0.134	-0.16	-0.194	-0.270*	-0.401**	0.464**	-0.029	-0.222	-0.232	-0.496**	0.486**	0.421**	0.770**	
2.71	**	**MA1R-K**	0.101	-0.187	-0.131	-0.237	-0.465**	0.475**	0.082	-0.245	-0.171	-0.449**	0.416**	0.281*	0.645**	0.759**
1.87	*	**WI-A**	0.136	0.058	0.096	-0.075	0.014	-0.055	0.204	-0.095	0.382**	0.109			**WI**	
1.25	ns	**WI-D**	0.427**	0.05	-0.199	-0.023	0.072	0.021	0.228	-0.028	0.419**	0.243	0.624**			
2.43	**	**WI-G**	0.295*	-0.074	0.009	-0.085	-0.058	-0.09	0.196	0.101	0.313*	0.409**	0.587**	0.673**		
4.19	**	**WI-J**	0.343**	-0.025	-0.186	-0.139	-0.051	0.065	0.214	-0.078	0.261*	0.191	0.369**	0.622**	0.697**	
4.01	**	**WI-K**	0.139	0.212	-0.124	0.118	0.263*	-0.234	0.222	0.019	0.393**	0.446**	0.412**	0.383**	0.513**	0.489**
1.09	ns	**WI1-A**	0.02	-0.029	-0.209	0.084	0.121	-0.045	-0.285*	0.096	-0.400**	-0.064			**WI-1**	
1.73	*	**WI1-D**	-0.079	-0.249	0.2	-0.072	-0.165	0.16	-0.443**	0.103	-0.624**	-0.462**	0.403**			
2.28	**	**WI1-G**	-0.02	-0.317*	-0.021	-0.181	-0.174	0.144	-0.272*	-0.133	-0.594**	-0.535**	0.601**	0.501**		
2.80	**	**WI1-J**	-0.195	-0.077	0.089	0.006	0.077	-0.041	-0.312*	0.004	-0.380**	-0.292*	0.404**	0.495**	0.616**	
7.26	**	**WI1-K**	-0.136	-0.330**	0.107	-0.216	-0.332**	0.279*	-0.331**	-0.063	-0.609**	-0.674**	0.318*	0.570**	0.715**	0.561**
2.00	*	**WI2-A**	-0.235	-0.05	-0.03	0.063	-0.026	0.045	-0.073	0.127	-0.23	-0.013			**WI-2**	
1.09	ns	**WI2-D**	-0.492**	0.028	0.17	0.057	-0.066	-0.088	-0.085	0.021	-0.21	-0.073	0.500**			
2.11	**	**WI2-G**	-0.429**	0.161	0	0.102	0.161	0.007	-0.191	-0.034	-0.211	-0.284*	0.454**	0.593**		
3.07	**	**WI2-J**	-0.368**	0.107	0.165	0.178	0.086	-0.086	-0.136	0.062	-0.14	-0.105	0.311*	0.595**	0.723**	
2.29	**	**WI2-K**	-0.146	-0.081	0.126	-0.025	-0.156	0.177	-0.089	0.032	-0.19	-0.244	0.388**	0.264*	0.340**	0.383**
1.49	+	**WI3-A**	-0.254	-0.033	0.122	0.007	-0.115	0.083	0.134	0.064	0.055	0.033			**WI-3**	
1.68	*	**WI3-D**	-0.433**	0.21	0.037	0.106	0.057	-0.196	0.246	-0.05	0.247	0.291*	0.368**			
1.51	+	**WI3-G**	-0.509**	0.398**	-0.015	0.229	0.310*	-0.073	-0.006	0.048	0.145	0.014	0.196	0.449**		
2.51	**	**WI3-J**	-0.391**	0.162	0.213	0.258*	0.082	-0.083	-0.06	0.178	-0.015	0.034	0.199	0.398**	0.577**	
1.78	*	**WI3-K**	-0.048	0.186	0.057	0.151	0.122	-0.037	0.172	0.118	0.290*	0.315*	0.393**	0.314*	0.125	0.311**

Table S9c: Trial Y1, Normalized water indices (NWI) at five timepoints (A, D, G, J, K): Anova with F-values between all varieties; correlation matrix with Pearson's correlation coefficients (r): colored cells show significant correlation; following significance levels (Sign.) are valid: +: p<0.1; ∗: p<0.05; ∗∗: p<0.01; ns: not significant.

Y1	60 Genotypes; Lattice 10x6; 2 rep							Software: Plabstat				Date: 25.11./2.12.2024			
ANOVA			Correlation matrix - Pearson's correlation coefficient (r)												
F-value	Sign.	Index-TP	emerg	ttf	SPAD	leaf size	ttm	podshat	lodging	pod set	height	yield	*Index-* **A**	*Index-* **D**	*Index-* **G**	*Index-* **J**
1.89	*	NWI1-A	-0.137	-0.059	-0.095	0.075	-0.014	0.053	-0.206	0.097	-0.384**	-0.109			NWI-1	
1.25	ns	NWI1-D	-0.429**	-0.051	0.2	0.023	-0.073	-0.021	-0.228	0.029	-0.419**	-0.242	0.625**			
2.43	**	NWI1-G	-0.294*	0.071	-0.011	0.083	0.057	0.091	-0.197	-0.1	-0.316*	-0.409**	0.588**	0.672**		
4.18	**	NWI1-J	-0.343**	0.025	0.186	0.141	0.05	-0.065	-0.213	0.079	-0.262*	-0.19	0.370**	0.622**	0.696**	
4.00	**	NWI1-K	-0.137	-0.214	0.124	-0.118	-0.265*	0.235	-0.223	-0.019	-0.394**	-0.448**	0.413**	0.384**	0.515**	0.488**
1.55	+	NWI2-A	-0.081	-0.031	-0.139	0.035	0.028	0.021	-0.21	0.017	-0.398**	-0.126			NWI-2	
1.99	*	NWI2-D	-0.316*	-0.135	0.248	-0.033	-0.09	0.036	-0.362**	0.075	-0.581**	-0.352**	0.632**			
2.16	**	NWI2-G	-0.17	-0.054	0.008	0.028	-0.017	0.106	-0.258*	-0.065	-0.439**	-0.449**	0.697**	0.710**		
4.40	**	NWI2-J	-0.293*	-0.088	0.188	0.041	0.009	-0.04	-0.311*	0.097	-0.408**	-0.284*	0.376**	0.640**	0.678**	
6.81	**	NWI2-K	-0.126	-0.319*	0.158	-0.199	-0.328*	0.227	-0.351**	0.014	-0.581**	-0.559**	0.442**	0.552**	0.634**	0.617**
2.03	**	NWI3-A	-0.159	-0.072	-0.084	0.066	-0.028	0.067	-0.213	0.147	-0.374**	-0.109			NWI-3	
1.11	ns	NWI3-D	-0.435**	0.015	0.165	0.063	0.019	-0.015	-0.202	0.075	-0.352**	-0.19	0.649**			
2.65	**	NWI3-G	-0.346**	0.107	-0.014	0.082	0.083	0.076	-0.184	-0.097	-0.272*	-0.393**	0.573**	0.689**		
4.56	**	NWI3-J	-0.357**	0.055	0.174	0.156	0.06	-0.069	-0.166	0.066	-0.221	-0.17	0.400**	0.646**	0.713**	
3.56	**	NWI3-K	-0.132	-0.179	0.108	-0.092	-0.239	0.233	-0.202	-0.012	-0.346**	-0.404**	0.403**	0.332**	0.465**	0.453**
1.68	*	NWI4-A	-0.09	-0.052	-0.135	0.044	0.007	0.056	-0.256*	0.062	-0.441**	-0.173			NWI-4	
1.69	**	NWI4-D	-0.328*	-0.122	0.223	-0.012	-0.098	0.054	-0.355**	0.062	-0.570**	-0.372**	0.661**			
2.53	**	NWI4-G	-0.201	-0.037	-0.009	0.01	-0.015	0.13	-0.258*	-0.097	-0.427**	-0.481**	0.706**	0.716**		
4.4	**	NWI4-J	-0.308*	-0.064	0.184	0.06	0.008	-0.029	-0.286*	0.081	-0.383**	-0.285*	0.412**	0.646**	0.696**	
6.11	**	NWI4-K	-0.129	-0.305*	0.144	-0.192	-0.320*	0.248	-0.329*	-0.008	-0.559**	-0.564**	0.472**	0.531**	0.633**	0.584**
1.65	*	NWI5-A	-0.175	-0.026	-0.055	0.087	-0.085	0.111	-0.1	0.078	-0.193	-0.032			NWI-5	
1.44	ns	NWI5-D	-0.384**	0.295*	0.041	0.266*	0.188	-0.045	0.103	0.056	0.04	0.126	0.467**			
2.56	**	NWI5-G	-0.367**	0.145	-0.079	0.156	0.119	0.01	-0.17	-0.02	-0.198	-0.289*	0.343**	0.417**		
4.26	**	NWI5-J	-0.324*	0.08	0.158	0.209	0.059	-0.052	-0.078	0.02	-0.147	-0.127	0.300*	0.387**	0.638**	
2.75	**	NWI5-K	-0.115	-0.073	0.073	-0.068	-0.158	0.174	-0.189	0.019	-0.277*	-0.263*	0.350**	0.104	0.339**	0.438**

Table S10a: Trial Y2, Vegetation + Chlorophyll indices at five timepoints (A, D, G, J, K): Anova with F-values between all varieties; correlation matrix with Pearson's correlation coefficients (r): colored cells show significant correlation; following significance levels (Sign.) are valid: +: p<0.1; *: p<0.05; **: p<0.01; ns: not significant.

Y2	45 Genotypes; Lattice 15x3; 2 rep			Software: Plabstat						Date: 26.11./2.12.2024				
ANOVA			Correlation matrix - Pearson's correlation coefficient (r)											
F-value	Sign.	Index-TP	emerg	ttf	SPAD	leaf size	ttm	podshat	lodging	pod set	height	yield	*Index-* A	*Index-* D	*Index-* G	*Index-* J
3.93	**	NDVI-A	0.309*	0.105	-0.086	0.175	0.099	-0.232	-0.133	0.132	-0.222	0.317*			NDVI	
4.48	**	NDVI-D	0.074	0.04	-0.033	0.204	0.061	-0.162	-0.158	0.302*	-0.380*	0.263	0.747**			
3.64	**	NDVI-G	-0.293	-0.054	-0.026	0.093	-0.255	-0.089	-0.304*	0.475**	-0.518**	0.107	0.377*	0.640**		
2.98	*	NDVI-J	0.063	-0.019	0.122	-0.055	-0.05	-0.363*	-0.271	0.06	-0.096	0.316*	0.427**	0.352*	0.398**	
2.70	*	NDVI-K	-0.437**	-0.07	0.113	-0.034	-0.175	-0.021	0.086	0.168	-0.310*	-0.064	-0.054	0.191	0.548**	0.142
2.15	**	NRI-A	-0.151	0.354*	-0.401**	0.397**	0.083	0.09	0.029	-0.147	0.111	-0.072			NRI	
4.05	*	NRI-D	-0.157	0.484**	-0.357*	0.514**	0.249	-0.034	-0.083	-0.076	0.078	0.069	0.755**			
2.55	*	NRI-G	-0.249	0.292	-0.255	0.393**	0.009	0.068	-0.063	-0.007	-0.045	-0.144	0.606**	0.754**		
6.90	**	NRI-J	-0.07	0.018	-0.118	0.069	-0.156	-0.078	-0.219	-0.042	-0.063	-0.115	0.321*	0.375*	0.631**	
5.55	**	NRI-K	-0.172	-0.318*	0.003	-0.017	-0.435**	0.168	-0.172	0.205	-0.272	-0.153	0.01	0.093	0.540**	0.269**
8.35	**	CI-A	0.358*	-0.168	0.199	-0.112	0.062	-0.264	-0.165	0.184	-0.289	0.342*			CI	
6.41	**	CI-D	0.242	-0.386**	0.277	-0.252	-0.086	-0.112	-0.044	0.263	-0.314*	0.237	0.808**			
4.03	**	CI-G	-0.048	-0.336*	0.12	-0.175	-0.279	-0.123	-0.276	0.489**	-0.459**	0.278	0.576**	0.647**		
4.43	**	CI-J	0.174	-0.104	0.205	-0.099	0.031	-0.267	-0.151	0.189	-0.075	0.443**	0.628**	0.497**	0.702**	
3.13	**	CI-K	-0.238	0.041	0.1	-0.081	0.162	-0.203	0.119	0.07	-0.143	0.129	0.251	0.206	0.469**	0.583**
7.04	**	REIP-A	0.491**	-0.253	0.185	-0.158	0.085	-0.217	-0.128	0.137	-0.17	0.403**			REIP	
6.91	**	REIP-D	0.383**	-0.445**	0.239	-0.316*	-0.081	-0.046	0.013	0.19	-0.179	0.252	0.829**			
2.98	*	REIP-G	0.189	-0.396**	0.138	-0.309*	-0.204	-0.195	-0.221	0.363*	-0.327*	0.357*	0.725**	0.714**		
3.69	**	REIP-J	0.309*	-0.12	0.232	-0.099	0.126	-0.215	-0.06	0.1	0.064	0.445**	0.679**	0.527**	0.699**	
3.77	**	REIP-K	-0.038	0.171	0.031	-0.053	0.366*	-0.256	0.129	-0.061	0.055	0.174	0.332*	0.172	0.371*	0.666**
4.85	**	PSSRa-A	0.278	0.119	-0.097	0.169	0.114	-0.243	-0.179	0.124	-0.229	0.299*			PSSRa	
3.72	**	PSSRa-D	0.085	0.025	-0.003	0.173	0.067	-0.16	-0.123	0.286	-0.347*	0.27	0.696**			
3.57	**	PSSRa-G	-0.265	-0.125	-0.006	0.036	-0.265	-0.094	-0.301*	0.460**	-0.496**	0.151	0.360*	0.606**		
3.22	**	PSSRa-J	0.065	-0.062	0.132	-0.041	-0.098	-0.359*	-0.334*	0.136	-0.132	0.352*	0.439**	0.366*	0.484**	
2.61	*	PSSRa-K	-0.440**	-0.127	0.12	-0.086	-0.15	-0.033	0.084	0.187	-0.314*	-0.046	-0.091	0.149	0.516**	0.118
7.02	**	PSSRb-A	0.291	0.099	-0.015	0.153	0.097	-0.269	-0.201	0.187	-0.279	0.314*			PSSRb	
5.38	**	PSSRb-D	0.07	-0.042	0.069	0.109	-0.004	-0.17	-0.135	0.356*	-0.415**	0.269	0.741**			
4.50	**	PSSRb-G	-0.256	-0.12	0.024	0.032	-0.255	-0.115	-0.320*	0.486**	-0.510**	0.17	0.440**	0.656**		
3.75	**	PSSRb-J	0.042	-0.002	0.098	-0.008	-0.048	-0.340*	-0.300*	0.15	-0.151	0.380**	0.559**	0.438**	0.560**	
3.03	**	PSSRb-K	-0.441**	-0.067	0.114	-0.076	-0.095	-0.094	0.095	0.173	-0.309*	-0.017	0.02	0.22	0.533**	0.234

Table S10b: Trial Y2, MA1_R and Water indices (WI) at five timepoints (A, D, G, J, K): Anova with F-values between all varieties; correlation matrix with Pearson's correlation coefficients (r): colored cells show significant correlation; following significance levels (Sign.) are valid: +: p<0.1; *: p<0.05; **: p<0.01; ns: not significant.

Y2	45 Genotypes; Lattice 15x3; 2 rep							**Software:** Plabstat				**Date:**	26.11./2.12.2024			
ANOVA			**Correlation matrix - Pearson's correlation coefficient (r)**													
F-value	**Sign.**	**Index-TP**	**emerg**	**ttf**	**SPAD**	**leaf size**	**ttm**	**podshat**	**lodging**	**pod set**	**height**	**yield**	*Index-* **A**	*Index-* **D**	*Index-* **G**	*Index-* **J**
5.08	**	**MA1R-A**	-0.226	0.097	-0.308*	0.069	0.013	0.219	0.175	-0.300*	0.300*	-0.23			**MA1-R**	
4.11	**	**MA1R-D**	-0.07	0.336*	-0.300*	0.277	0.214	0.091	0.094	-0.318*	0.325*	-0.121	0.771**			
5.23	**	**MA1R-G**	0.002	-0.023	-0.052	0.012	0.024	0.105	0.156	-0.268	0.192	-0.202	0.638**	0.667**		
6.26	**	**MA1R-J**	0.074	-0.202	0.07	-0.094	-0.137	0.042	-0.032	-0.056	0.075	-0.155	0.407**	0.355*	0.692**	
7.08	**	**MA1R-K**	0.15	-0.330*	0.015	-0.072	-0.307*	0.273	-0.12	0.016	0.038	-0.104	0.227	0.213	0.593**	0.716**
2.14	+	**WI-A**	0.418**	-0.346*	0.086	-0.357*	0.128	-0.009	0.116	-0.135	0.177	0.352*			**WI**	
2.92	*	**WI-D**	0.343*	-0.371*	-0.029	-0.330*	-0.161	0.295*	0.043	-0.07	0.063	-0.005	0.663**			
1.79	ns	**WI-G**	0.194	-0.424**	0.039	-0.406**	-0.152	-0.01	-0.097	0.125	-0.041	0.339*	0.715**	0.556**		
1.57	ns	**WI-J**	0.314*	-0.114	0.381**	-0.108	0.061	0.021	0.271	-0.086	0.351*	0.337*	0.466**	0.149	0.282	
0.98	ns	**WI-K**	0.04	0.004	0.149	-0.128	0.148	0.202	0.535**	-0.264	0.390**	0.224	0.152	-0.062	0.078	0.349*
1.63	ns	**WI1-A**	-0.08	0.216	-0.15	0.167	-0.057	-0.083	-0.136	0.144	-0.301*	-0.116			**WI-1**	
2.34	*	**WI1-D**	-0.348*	0.212	-0.182	0.152	-0.061	-0.388**	-0.356*	0.449**	-0.578**	-0.101	0.494**			
1.38	ns	**WI1-G**	-0.231	0.109	-0.05	0.07	-0.037	-0.189	-0.166	0.123	-0.364*	-0.435**	0.345*	0.416**		
1.30	ns	**WI1-J**	-0.397**	-0.015	-0.126	0.009	-0.201	-0.128	-0.181	0.254	-0.504**	-0.234	0.454**	0.589**	0.197	
2.46	*	**WI1-K**	-0.216	-0.14	-0.083	-0.045	-0.464**	-0.025	-0.433**	0.390**	-0.521**	-0.469**	0	0.23	0.267	0.258
2.91	*	**WI2-A**	-0.369*	0.143	-0.024	0.288	-0.288	0.2	-0.106	0.111	-0.034	-0.317*			**WI-2**	
3.26	**	**WI2-D**	-0.229	0.261	0.156	0.226	0.259	-0.246	0.096	-0.114	0.164	0.143	0.424**			
2.08	+	**WI2-G**	-0.104	0.372*	-0.045	0.408**	0.187	0.074	0.241	-0.241	0.238	-0.18	0.635**	0.563**		
1.46	ns	**WI2-J**	-0.265	0.148	-0.359*	0.116	0.047	0.046	-0.115	-0.13	-0.157	-0.403**	0.346*	0.022	0.312*	
0.87	ns	**WI2-K**	0.156	0.095	-0.196	0.314*	0.138	-0.081	-0.405**	0.022	0.036	0.007	0.094	-0.034	0.03	0.276
3.34	**	**WI3-A**	-0.274	-0.14	0.208	0.002	-0.216	0.213	0.088	-0.054	0.213	-0.168			**WI-3**	
2.56	*	**WI3-D**	-0.023	0.137	0.279	0.129	0.304*	-0.028	0.339*	-0.386**	0.517**	0.247	0.441**			
2.38	*	**WI3-G**	0.054	0.308*	-0.05	0.387**	0.185	0.166	0.349*	-0.334*	0.441**	0.082	0.466**	0.606**		
1.22	ns	**WI3-J**	-0.046	0.118	-0.238	0.091	0.147	0.132	0.088	-0.416**	0.201	-0.326*	0.197	0.094	0.346*	
1.69	ns	**WI3-K**	0.282	0.199	-0.125	0.404**	0.473**	0.082	0.045	-0.426**	0.562**	0.304*	0.103	0.488**	0.364*	0.354*

Table S10c: Trial Y2, Normalized water indices (NWI) at five timepoints (A, D, G, J, K): Anova with F-values between all varieties; correlation matrix with Pearson's correlation coefficients (r): colored cells show significant correlation; following significance levels (Sign.) are valid: +: p<0.1; *: p<0.05; **: p<0.01; ns: not significant.

Y2	45 Genotypes; Lattice 15x3; 2 rep						Software: Plabstat				Date: 26.11./2.12.2024				
ANOVA			**Correlation matrix - Pearson's correlation coefficient (r)**												
F-value	**Sign.**	**Index-TP**	**emerg**	**ttf**	**SPAD**	**leaf size**	**ttm**	**podshat**	**lodging**	**pod set**	**height**	**yield**	*Index-* **A**	*Index-* **D**	*Index-* **G**	*Index-* **J**
2.15	*	**NWI1-A**	-0.421**	0.347*	-0.086	0.357*	-0.127	0.009	-0.118	0.135	-0.177	-0.353*			**NWI-1**	
2.96	*	**NWI1-D**	-0.345*	0.371*	0.03	0.328*	0.162	-0.296*	-0.044	0.068	-0.063	0.004	0.663**			
1.79		**NWI1-G**	-0.195	0.425**	-0.039	0.406**	0.152	0.01	0.095	-0.126	0.041	-0.339*	0.716**	0.557**		
1.58		**NWI1-J**	-0.315*	0.115	-0.381**	0.108	-0.059	-0.021	-0.273	0.084	-0.350*	-0.338*	0.465**	0.149	0.282	
0.97		**NWI1-K**	-0.04	-0.004	-0.149	0.128	-0.148	-0.201	-0.534**	0.263	-0.389**	-0.225	0.152	-0.063	0.078	0.350*
2.22	*	**NWI2-A**	-0.273	0.322*	-0.138	0.266	-0.093	-0.088	-0.147	0.172	-0.286	-0.293			**NWI-2**	
4.04	**	**NWI2-D**	-0.369*	0.351*	-0.112	0.249	0.002	-0.350*	-0.195	0.285	-0.372*	-0.121	0.742**			
2.27	*	**NWI2-G**	-0.259	0.355*	-0.05	0.256	0.012	-0.143	-0.064	0.072	-0.275	-0.414**	0.745**	0.674**		
1.90	+	**NWI2-J**	-0.341*	0.073	-0.267	0.052	-0.153	-0.128	-0.297*	0.219	-0.513**	-0.363*	0.631**	0.467**	0.467**	
1.64		**NWI2-K**	-0.222	-0.013	-0.117	0.012	-0.321*	-0.149	-0.462**	0.331*	-0.495**	-0.451**	0.351*	0.231	0.358*	0.415**
2.18	*	**NWI3-A**	-0.407**	0.317*	-0.058	0.383**	-0.135	0.046	-0.13	0.113	-0.111	-0.355*			**NWI-3**	
2.96	*	**NWI3-D**	-0.296*	0.390**	0.056	0.386**	0.179	-0.256	-0.023	0.017	0.048	0.045	0.620**			
1.81	+	**NWI3-G**	-0.151	0.447**	-0.049	0.453**	0.194	0.035	0.104	-0.163	0.109	-0.295*	0.689**	0.537**		
1.57		**NWI3-J**	-0.274	0.12	-0.401**	0.115	-0.017	-0.008	-0.269	0.036	-0.28	-0.306*	0.351*	0.092	0.251	
0.93		**NWI3-K**	0.002	-0.003	-0.128	0.161	-0.121	-0.193	-0.545**	0.228	-0.352*	-0.2	0.113	-0.121	0.054	0.333*
2.28	*	**NWI4-A**	-0.318*	0.349*	-0.125	0.297*	-0.095	-0.077	-0.145	0.163	-0.29	-0.307*			**NWI-4**	
3.78	**	**NWI4-D**	-0.402**	0.381**	-0.08	0.285	0.048	-0.366*	-0.187	0.239	-0.333*	-0.095	0.709**			
1.9	+	**NWI4-G**	-0.258	0.385**	-0.065	0.323*	0.049	-0.098	-0.036	0.015	-0.191	-0.423**	0.710**	0.603**		
1.91	+	**NWI4-J**	-0.354*	0.091	-0.314*	0.079	-0.147	-0.1	-0.312*	0.203	-0.495**	-0.350*	0.595**	0.390**	0.371*	
1.45		**NWI4-K**	-0.186	-0.039	-0.133	0.019	-0.313*	-0.16	-0.494**	0.334*	-0.497**	-0.408**	0.27	0.123	0.262	0.387**
2.68	*	**NWI5-A**	-0.328*	0.192	0.032	0.327*	-0.079	0.025	-0.157	0.059	-0.018	-0.265			**NWI-5**	
2.66	*	**NWI5-D**	-0.118	0.368*	0.036	0.447**	0.167	-0.052	0.026	-0.141	0.343*	0.097	0.546**			
2.19	*	**NWI5-G**	-0.086	0.467**	-0.06	0.519**	0.189	0.122	0.149	-0.209	0.187	-0.232	0.565**	0.563**		
1.12		**NWI5-J**	-0.24	0.116	-0.368*	0.042	0.021	0.086	-0.153	-0.158	-0.02	-0.341*	0.228	0.032	0.301*	
0.85		**NWI5-K**	0.02	0.072	-0.085	0.271	-0.017	-0.142	-0.467**	0.095	-0.19	-0.122	0.257	-0.089	0.097	0.235

Table S11a: Trial Y3, Vegetation + Chlorophyll indices at five timepoints (A, D, G, J, K): Anova with F-values between all varieties; correlation matrix with Pearson's correlation coefficients (r): colored cells show significant correlation; following significance levels (Sign.) are valid: +: p<0.1; *: p<0.05; **: p<0.01; ns: not significant.

Y3	30 Genotypes; Lattice 10x3; 2 rep							**Software:** Plabstat				**Date:** 26.11./2.12.2024			
ANOVA			**Correlation matrix - Pearson's correlation coefficient (r)**												
F-value	**Sign.**	**Index-TP**	**emerg**	**ttf**	**SPAD**	**leaf size**	**ttm**	**podshat**	**lodging**	**pod set**	**height**	**yield**	*Index-* **A**	*Index-* **D**	*Index-* **G**	*Index-* **J**
3.06	*	NDVI-A	0.323	0.338	0.364*	-0.296	0.482**	0.228	0.399*	-0.05	0.286	0.087			NDVI	
3.45	*	NDVI-D	0.186	0.461*	0.273	-0.196	0.370*	0.415*	0.478**	0.272	0.149	-0.076	0.705**			
1.57	*	NDVI-G	0.019	0.297	0.266	-0.065	0.139	0.215	0.229	0.122	0.047	0.009	0.421*	0.646**		
2.25	+	NDVI-J	0.014	0.082	0.183	-0.03	0.003	0.098	-0.04	0.137	-0.046	0.074	0.467**	0.496**	0.721**	
3.02	*	NDVI-K	-0.218	-0.047	-0.149	0.252	-0.191	0.122	-0.2	0.159	-0.304	0.109	-0.022	0.21	0.418*	0.484**
4.67	**	NRI-A	-0.201	0.136	-0.487**	0.343	0.144	0.018	0.189	-0.108	0.136	-0.056			NRI	
9.53	**	NRI-D	-0.208	0.367*	-0.349	0.306	0.242	0.359	0.321	-0.153	0.093	-0.208	0.790**			
2.99	*	NRI-G	-0.226	0.33	-0.364*	0.363*	0.132	0.312	0.239	-0.161	0.023	-0.177	0.616**	0.836**		
3.29	*	NRI-J	-0.31	0.05	-0.439*	0.490**	-0.247	0.081	-0.083	0.141	-0.277	-0.017	0.532**	0.647**	0.683**	
4.96	**	NRI-K	-0.149	-0.267	-0.17	0.195	-0.550**	-0.036	-0.233	0.489*	-0.547**	0.227	0.304	0.355	0.372*	0.662**
4.19	**	CI-A	0.465**	0.27	0.541**	-0.486**	0.396*	0.231	0.322	0.106	0.19	0.091			CI	
8.74	**	CI-D	0.422*	0.199	0.540**	-0.537**	0.233	0.193	0.286	0.4	0.045	0.061	0.891**			
2.36	+	CI-G	0.242	0.191	0.515**	-0.464**	0.133	0.15	0.162	0.383	-0.024	0.128	0.720**	0.690**		
6.10	**	CI-J	0.268	0.082	0.433*	-0.389*	0.148	0.158	0.092	0.153	0.071	0.134	0.665**	0.548**	0.824**	
4.78	**	CI-K	0.037	0.256	0.058	-0.077	0.291	0.412*	0.098	-0.149	0.032	-0.081	0.380*	0.263	0.519**	0.676**
4.01	**	REIP-A	0.583**	0.167	0.587**	-0.525**	0.352	0.209	0.275	0.136	0.181	0.121			REIP	
51.23	**	REIP-D	0.551**	0.026	0.600**	-0.546**	0.173	0.144	0.179	0.286	0.021	0.096	0.911**			
1.87	**	REIP-G	0.346	0.172	0.513**	-0.519**	0.227	0.222	0.176	0.252	0.06	0.119	0.812**	0.705**		
7.93	**	REIP-J	0.384*	0.158	0.532**	-0.469**	0.332	0.289	0.249	-0.023	0.218	0.074	0.788**	0.617**	0.829**	
8.08	**	REIP-K	0.249	0.419*	0.206	-0.249	0.613**	0.457*	0.373*	-0.338	0.35	-0.179	0.608**	0.430*	0.663**	0.808**
3.85	*	PSSRa-A	0.347	0.327	0.375*	-0.361	0.488**	0.245	0.418*	-0.029	0.271	0.09			PSSRa	
4.49	**	PSSRa-D	0.2	0.469**	0.285	-0.243	0.400*	0.445*	0.480**	0.246	0.171	-0.097	0.749**			
1.63	ns	PSSRa-G	0.004	0.3	0.269	-0.115	0.117	0.234	0.184	0.165	0.004	-0.02	0.417*	0.634**		
2.56	+	PSSRa-J	0.037	0.089	0.197	-0.055	0.014	0.104	-0.04	0.159	-0.054	0.056	0.453*	0.530**	0.745**	
2.85	*	PSSRa-K	-0.19	-0.027	-0.132	0.167	-0.19	0.198	-0.219	0.134	-0.348	0.08	0.028	0.227	0.452*	0.550**
4.61	**	PSSRb-A	0.354	0.32	0.457*	-0.409*	0.479**	0.226	0.402*	-0.026	0.262	0.082			PSSRb	
4.49	**	PSSRb-D	0.234	0.459*	0.425*	-0.288	0.398*	0.31	0.471**	0.297	0.194	-0.061	0.793**			
1.47	ns	PSSRb-G	0.012	0.273	0.364*	-0.119	0.08	0.151	0.151	0.207	0.007	-0.002	0.394*	0.602**		
2.91	*	PSSRb-J	0.039	0.082	0.265	-0.078	0.022	0.04	-0.056	0.144	-0.006	0.078	0.447*	0.498**	0.760**	
2.84	*	PSSRb-K	-0.22	0.014	-0.143	0.168	-0.117	0.206	-0.208	0.017	-0.291	0.016	-0.011	0.087	0.437*	0.521**

Table S11b: Trial Y3, MA1_R and Water indices (WI) at five timepoints (A, D, G, J, K): Anova with F-values between all varieties; correlation matrix with Pearson's correlation coefficients (r): colored cells show significant correlation; following significance levels (Sign.) are valid: +: p<0.1; *: p<0.05; **: p<0.01; ns: not significant.

Y3	30 Genotypes; Lattice 10x3; 2 rep			**Software:** Plabstat							**Date:** 26.11./2.12.2024			
ANOVA			**Correlation matrix - Pearson's correlation coefficient (r)**											
F-value	**Sign.**	**Index-TP**	**emerg**	**ttf**	**SPAD**	**leaf size**	**ttm**	**podshat**	**lodging**	**pod set**	**height**	**yield**	*Index-* **A**	*Index-* **D**	*Index-* **G**	*Index-* **J**
4.66	**	**MA1R-A**	-0.276	-0.063	-0.633**	0.424*	-0.141	-0.017	-0.071	-0.047	-0.05	-0.035			**MA1-R**	
5.96	**	**MA1R-D**	-0.192	0.034	-0.553**	0.212	0.009	0.353	0.029	-0.156	-0.079	-0.155	0.842**			
2.89	*	**MA1R-G**	-0.175	0.088	-0.621**	0.086	-0.051	0.3	0.091	0.074	-0.251	-0.083	0.556**	0.669**		
2.11	+	**MA1R-J**	-0.082	-0.124	-0.422*	0.132	-0.256	0.181	0	0.193	-0.374*	-0.037	0.564**	0.584**	0.733**	
5.86	**	**MA1R-K**	0.148	-0.373*	0.01	-0.104	-0.557**	-0.099	-0.169	0.659**	-0.459*	0.406*	0.178	0.026	0.257	0.547**
2.81	*	**WI-A**	0.640**	-0.006	0.338	-0.523**	0.146	0.191	0.29	0.306	0.139	0.183			**WI**	
3.67	*	**WI-D**	0.650**	-0.084	0.345	-0.543**	0.116	0.206	0.136	0.233	0.076	0.042	0.866**			
0.69	ns	**WI-G**	0.434*	0.057	0.324	-0.540**	0.235	0.222	0.273	0.197	0.268	0.014	0.783**	0.819**		
0.96	ns	**WI-J**	0.515**	0.084	0.296	-0.380*	0.388*	0.358	0.286	-0.162	0.450*	-0.047	0.697**	0.671**	0.727**	
2.29	**+**	**WI-K**	0.404*	0.172	0.103	-0.283	0.464**	0.466*	0.449*	-0.213	0.519**	0.131	0.583**	0.530**	0.722**	0.824*
2.94	*	**WI1-A**	-0.495**	0.198	-0.378*	0.564**	-0.051	-0.04	-0.15	-0.163	-0.218	-0.276			**WI-1**	
5.96	**	**WI1-D**	-0.689**	0.192	-0.425*	0.452*	-0.023	-0.152	-0.131	-0.148	-0.144	-0.197	0.726**			
2.73	*	**WI1-G**	-0.325	-0.132	-0.343	0.356	-0.215	-0.272	-0.344	-0.028	-0.369*	0.007	0.707**	0.564**		
1.15	ns	**WI1-J**	-0.278	0.014	-0.238	-0.012	-0.163	-0.225	-0.166	0.29	-0.430*	-0.092	0.446*	0.36	0.473**	
3.98	*	**WI1-K**	-0.172	-0.003	0.007	0.04	-0.229	-0.305	-0.315	0.371	-0.585**	-0.269	0.390*	0.359	0.559**	0.564**
2.54	+	**WI2-A**	-0.590**	-0.136	-0.32	0.450*	-0.217	-0.221	-0.338	-0.351	-0.104	-0.02			**WI-2**	
2.27	+	**WI2-D**	-0.627**	0.074	-0.296	0.486**	-0.1	-0.237	-0.103	-0.273	0.015	0.012	0.812**			
0.58	ns	**WI2-G**	-0.428*	-0.031	-0.405*	0.556**	-0.177	-0.104	-0.236	-0.311	-0.161	0.01	0.744**	0.759**		
1.06	ns	**WI2-J**	-0.493**	-0.045	-0.215	0.453*	-0.341	-0.430*	-0.303	0.078	-0.379*	0.029	0.614**	0.642**	0.654**	
1.46	**ns**	**WI2-K**	-0.482**	-0.006	-0.072	0.377*	-0.33	-0.345	-0.333	-0.098	-0.318	-0.276	0.544**	0.515**	0.618**	0.768**
2.51	+	**WI3-A**	-0.424*	-0.277	-0.198	0.174	-0.213	-0.259	-0.323	-0.258	0.037	0.163			**WI-3**	
1.25	ns	**WI3-D**	-0.27	0.021	-0.16	0.304	0.037	-0.211	0.042	-0.38	0.326	0.133	0.574**			
0.4	ns	**WI3-G**	-0.171	0.108	-0.368*	0.370*	0.113	0.138	-0.069	-0.449*	0.105	-0.011	0.347	0.308		
0.83	ns	**WI3-J**	-0.448*	0.275	-0.117	0.271	0.081	-0.346	-0.11	-0.168	-0.09	-0.253	0.348	0.266	0.306	
1.53	ns	**WI3-K**	-0.269	0.146	0.199	0.349	0.034	-0.251	-0.064	-0.371	0.207	-0.307	0.319	0.152	0.132	0.427*

Table S11c: Trial Y3, Normalized water indices (NWI) at five timepoints (A, D, G, J, K): Anova with F-values between all varieties; correlation matrix with Pearson's correlation coefficients (r): colored cells show significant correlation; following significance levels (Sign.) are valid: +: p<0.1; *: p<0.05; **: p<0.01; ns: not significant.

Y3	30 Genotypes; Lattice 10x3; 2 rep		**Software:** Plabstat									**Date:** 26.11./2.12.2024			
ANOVA			**Correlation matrix - Pearson's correlation coefficient (r)**												
F-value	**Sign.**	**Index-TP**	**emerg**	**ttf**	**SPAD**	**leaf size**	**ttm**	**podshat**	**lodging**	**pod set**	**height**	**yield**	***Index-* A**	***Index-* D**	***Index-* G**	***Index-* J**
2.76	*	**NWI1-A**	-0.641**	0.006	-0.337	0.522**	-0.145	-0.19	-0.288	-0.306	-0.139	-0.184			**NWI-1**	
3.69	*	**NWI1-D**	-0.651**	0.085	-0.345	0.542**	-0.116	-0.206	-0.135	-0.232	-0.075	-0.042	0.865**			
0.69	ns	**NWI1-G**	-0.434*	-0.056	-0.325	0.540**	-0.234	-0.222	-0.271	-0.197	-0.267	-0.014	0.784**	0.819**		
0.96	ns	**NWI1-J**	-0.516**	-0.083	-0.295	0.380*	-0.387*	-0.359	-0.285	0.162	-0.449*	0.046	0.696**	0.670**	0.727**	
2.29	+	**NWI1-K**	-0.403*	-0.173	-0.101	0.279	-0.465**	-0.465*	-0.448*	0.215	-0.521**	-0.13	0.581**	0.527**	0.720**	0.824*
4.03	**	**NWI2-A**	-0.630**	0.04	-0.309	0.499**	-0.165	-0.143	-0.312	-0.224	-0.225	-0.212			**NWI-2**	
7.24	**	**NWI2-D**	-0.624**	0.051	-0.345	0.534**	-0.129	-0.165	-0.236	-0.26	-0.175	-0.094	0.914**			
1.40	ns	**NWI2-G**	-0.435*	-0.149	-0.261	0.456*	-0.316	-0.263	-0.380*	-0.094	-0.381*	0.014	0.828**	0.859**		
1.19	ns	**NWI2-J**	-0.507**	-0.14	-0.259	0.253	-0.415*	-0.32	-0.391*	0.186	-0.549**	0.018	0.736**	0.687**	0.771**	
3.27	*	**NWI2-K**	-0.334	-0.174	-0.05	0.201	-0.425*	-0.434*	-0.491**	0.292	-0.599**	-0.115	0.635**	0.602**	0.790**	0.833**
2.56	+	**NWI3-A**	-0.660**	0.004	-0.362*	0.535**	-0.161	-0.221	-0.284	-0.292	-0.12	-0.156			**NWI-3**	
3.66	*	**NWI3-D**	-0.632**	0.098	-0.362*	0.553**	-0.099	-0.215	-0.105	-0.232	-0.027	-0.039	0.852**			
0.61	ns	**NWI3-G**	-0.442*	-0.002	-0.33	0.553**	-0.199	-0.202	-0.212	-0.202	-0.228	-0.032	0.777**	0.803**		
1.00	ns	**NWI3-J**	-0.504**	-0.077	-0.29	0.454*	-0.351	-0.368	-0.257	0.058	-0.367*	0.059	0.720**	0.694**	0.756**	
2.30	+	**NWI3-K**	-0.418*	-0.128	-0.106	0.31	-0.428*	-0.449*	-0.403*	0.147	-0.471**	-0.147	0.584**	0.516**	0.706**	0.825**
3.53	*	**NWI4-A**	-0.660**	0.102	-0.342	0.537**	-0.124	-0.136	-0.257	-0.239	-0.183	-0.252			**NWI-4**	
5.88	**	**NWI4-D**	-0.659**	0.131	-0.367*	0.565**	-0.078	-0.162	-0.166	-0.261	-0.125	-0.122	0.895**			
1.05	ns	**NWI4-G**	-0.451*	-0.091	-0.279	0.501**	-0.278	-0.262	-0.318	-0.116	-0.339	-0.034	0.793**	0.823**		
1.08	ns	**NWI4-J**	-0.530**	-0.055	-0.291	0.27	-0.372*	-0.324	-0.314	0.222	-0.526**	-0.017	0.709**	0.655**	0.698**	
3.25	*	**NWI4-K**	-0.338	-0.157	-0.055	0.209	-0.439*	-0.451*	-0.466**	0.337	-0.605**	-0.13	0.577**	0.537**	0.744**	0.798**
1.80	ns	**NWI5-A**	-0.654**	-0.087	-0.391*	0.498**	-0.279	-0.221	-0.3	-0.209	-0.103	-0.012			**NWI-5**	
2.91	*	**NWI5-D**	-0.533**	0.049	-0.359	0.558**	-0.112	-0.222	-0.141	-0.258	-0.013	-0.004	0.761**			
0.63	ns	**NWI5-G**	-0.458*	-0.082	-0.382*	0.542**	-0.25	-0.218	-0.198	-0.178	-0.193	0.045	0.777**	0.742**		
0.98	ns	**NWI5-J**	-0.482**	0.007	-0.28	0.506**	-0.234	-0.345	-0.231	-0.163	-0.26	-0.022	0.698**	0.655**	0.799**	
2.24	+	**NWI5-K**	-0.425*	-0.013	-0.134	0.412*	-0.291	-0.338	-0.347	-0.173	-0.355	-0.229	0.567**	0.531**	0.702**	0.835**

Table S12a: Trial Food, Vegetation + Chlorophyll indices at five timepoints (A, D, G, J, K): Anova with F-values between all varieties; correlation matrix with Pearson's correlation coefficients (r): colored cells show significant correlation; following significance levels (Sign.) are valid: +: p<0.1; *: p<0.05; **: p<0.01; ns: not significant.

Food	70 Genotypes; Lattice 10x7; 2 rep		**Software:** Plabstat								**Date:** 26.11./2.12.2024			
ANOVA			**Correlation matrix - Pearson's correlation coefficient (r)**												
F-value	**Sign.**	**Index-TP**	**emerg**	**ttf**	**SPAD**	**leaf size**	**ttm**	**podshat**	**lodging**	**pod set**	**height**	**yield**	*Index-* **B**	*Index-* **E**	*Index-* **G**	*Index-* **J**
6.75	**	NDVI-B	0.273*	0.308**	0.071	0.346**	0.418**	-0.313**	-0.174	0.108	0.059	0.079			NDVI	
3.25	**	NDVI-E	0.259*	0.176	0.18	0.301*	0.355**	-0.159	-0.214	0.151	-0.073	0.052	0.817**			
2.50	**	NDVI-G	0.177	0.048	0.219	0.171	0.212	-0.156	-0.272*	0.165	-0.201	0.043	0.515**	0.668**		
5.18	**	NDVI-J	0.044	-0.011	-0.077	0.203	0.137	-0.175	-0.240*	0.249*	-0.117	0.278*	0.464**	0.537**	0.518**	
4.33	**	NDVI-L	-0.109	0.222	-0.126	0.298*	0.347**	-0.260*	0.041	0.045	0.302*	0.137	0.336**	0.271*	0.208	0.705**
9.97	**	NRI-B	0.067	0.396**	-0.314**	0.183	0.485**	-0.232	0.108	-0.213	0.254*	-0.174			NRI	
8.46	**	NRI-E	-0.018	0.380**	-0.248*	0.306**	0.569**	-0.246*	0.117	-0.208	0.269*	-0.17	0.837**			
4.34	**	NRI-G	-0.067	0.226	-0.047	0.193	0.329**	0.017	0.128	-0.321**	0.103	-0.194	0.536**	0.736**		
6.56	**	NRI-J	0.013	-0.194	0.061	-0.071	-0.197	0.393**	-0.083	-0.168	-0.275*	-0.055	0.16	0.294*	0.568**	
3.68	**	NRI-L	-0.143	-0.152	-0.008	0.055	-0.126	0.206	-0.103	-0.053	-0.127	0.143	-0.004	0.077	0.199	0.354**
6.08	**	CI-B	0.301*	0.147	0.319**	0.300*	0.204	-0.156	-0.233	0.255*	-0.041	0.198			CI	
3.90	**	CI-E	0.286*	-0.102	0.407**	0.031	-0.072	0.036	-0.292*	0.375**	-0.227	0.219	0.815**			
2.48	**	CI-G	0.271*	-0.041	0.260*	0.12	0.096	-0.217	-0.352**	0.430**	-0.181	0.226	0.622**	0.625**		
8.08	**	CI-J	0.073	0.142	-0.08	0.231	0.294*	-0.361**	-0.099	0.264*	0.13	0.254*	0.522**	0.478**	0.665**	
11.77	**	CI-L	0.044	0.493**	-0.091	0.478**	0.693**	-0.433**	0.042	0.063	0.466**	0.01	0.499**	0.244*	0.505**	0.797**
4.41	**	REIP-B	0.377**	0.058	0.320**	0.257*	0.106	-0.145	-0.173	0.280*	0.003	0.296*			REIP	
4.57	**	REIP-E	0.327**	-0.112	0.323**	0.041	-0.087	0.008	-0.188	0.341**	-0.095	0.288*	0.865**			
3.12	**	REIP-G	0.269*	0.001	0.158	0.147	0.149	-0.242*	-0.204	0.395**	0.055	0.286*	0.733**	0.703**		
9.57	**	REIP-J	0.009	0.250*	-0.113	0.298*	0.398**	-0.363**	0.086	0.112	0.335**	0.185	0.494**	0.476**	0.704**	
9.03	**	REIP-L	-0.02	0.437**	-0.107	0.439**	0.615**	-0.399**	0.128	0.02	0.506**	0.05	0.419**	0.290*	0.632**	0.902**
6.56	**	PSSRa-B	0.280*	0.332**	0.059	0.344**	0.442**	-0.300*	-0.168	0.094	0.071	0.05			PSSRa	
3.15	**	PSSRa-E	0.255*	0.179	0.175	0.279*	0.358**	-0.151	-0.212	0.15	-0.071	0.028	0.817**			
2.48	*	PSSRa-G	0.17	0.053	0.208	0.179	0.211	-0.152	-0.263*	0.148	-0.193	0.064	0.487**	0.683**		
4.37	**	PSSRa-J	0.098	-0.035	-0.044	0.179	0.113	-0.14	-0.283*	0.265*	-0.188	0.275*	0.485**	0.618**	0.588**	
8.77	**	PSSRa-L	0.028	0.405**	-0.049	0.481**	0.605**	-0.363**	-0.114	0.107	0.285*	0.051	0.678**	0.602**	0.456**	0.653**
6.34	**	PSSRb-B	0.280*	0.268*	0.147	0.368**	0.374**	-0.295*	-0.235	0.178	-0.001	0.114			PSSRb	
3.5	**	PSSRb-E	0.287*	0.096	0.279*	0.267*	0.239*	-0.138	-0.295*	0.253*	-0.161	0.103	0.841**			
2.37	**	PSSRb-G	0.18	0.035	0.243*	0.195	0.188	-0.19	-0.317**	0.227	-0.225	0.095	0.530**	0.694**		
4.99	**	PSSRb-J	0.11	0.012	-0.057	0.216	0.169	-0.284*	-0.298*	0.322**	-0.135	0.281*	0.559**	0.620**	0.588**	
10.69	**	PSSRb-L	0.042	0.458**	-0.068	0.500**	0.656**	-0.427**	-0.08	0.098	0.331**	0.021	0.683**	0.555**	0.464**	0.713**

Table S12b: Trial Food, MA1_R and Water indices (WI) at five timepoints (A, D, G, J, K): Anova with F-values between all varieties; correlation matrix with Pearson's correlation coefficients (r): colored cells show significant correlation; following significance levels (Sign.) are valid: +: p<0.1; *: p<0.05; **: p<0.01; ns: not significant.

Food	70 Genotypes; Lattice 10x7; 2 rep		**Software:** Plabstat								**Date:** 26.11./2.12.2024			
ANOVA			**Correlation matrix - Pearson's correlation coefficient (r)**												
F-value	**Sign.**	**Index-TP**	**emerg**	**ttf**	**SPAD**	**leaf size**	**ttm**	**podshat**	**lodging**	**pod set**	**height**	**yield**	*Index-* **B**	*Index-* **E**	*Index-* **G**	*Index-* **J**
11.64	**	**MA1R-B**	-0.028	0.235	-0.361**	-0.172	0.237*	0.017	0.295*	-0.332**	0.268*	-0.247*			**MA1-R**	
15.71	**	**MA1R-E**	-0.167	0.262*	-0.344**	-0.029	0.360**	-0.034	0.298*	-0.343**	0.311**	-0.22	0.836**			
3.85	**	**MA1R-G**	-0.076	0.088	-0.164	-0.12	0.088	0.224	0.339**	-0.404**	0.166	-0.187	0.699**	0.756**		
7.74	**	**MA1R-J**	-0.001	-0.176	0.114	-0.233	-0.280*	0.482**	0.074	-0.238*	-0.215	-0.145	0.286*	0.330**	0.591**	
6.98	**	**MA1R-L**	-0.048	-0.443**	0.138	-0.378**	-0.571**	0.560**	-0.061	-0.059	-0.404**	0.052	0.04	0.031	0.314**	0.714**
3.17	**	**WI-B**	0.291*	-0.013	0.017	-0.154	-0.024	0.009	0.23	-0.053	0.256*	0.137			**WI**	
3.85	**	**WI-E**	0.225	-0.005	-0.071	-0.188	0.032	0.111	0.202	-0.088	0.277*	0.014	0.751**			
1.66	*	**WI-G**	0.287*	-0.2	-0.1	-0.356**	-0.122	0.076	0.075	0.195	0.182	0.213	0.573**	0.590**		
3.26	**	**WI-J**	0.077	-0.02	-0.045	-0.16	0.02	0.206	0.409**	-0.257*	0.417**	0.045	0.570**	0.586**	0.515**	
4.38	**	**WI-L**	0.115	0.175	-0.1	0.058	0.296*	-0.079	0.255*	-0.05	0.521**	0.031	0.496**	0.498**	0.515**	0.677**
2.03	**	**WI1-B**	-0.023	-0.007	-0.023	0.125	0.023	-0.027	-0.271*	0.05	-0.292*	-0.244*			**WI-1**	
2.54	**	**WI1-E**	-0.12	-0.03	0.004	0.116	-0.05	-0.003	-0.312**	0.04	-0.329**	-0.16	0.631**			
2.57	**	**WI1-G**	-0.025	0.027	0.134	0.254*	0.028	-0.007	-0.298*	-0.074	-0.354**	-0.303*	0.609**	0.583**		
2.94	**	**WI1-J**	0.025	-0.166	0.066	0.002	-0.191	-0.127	-0.508**	0.270*	-0.596**	-0.058	0.515**	0.584**	0.478**	
3.99	**	**WI1-L**	-0.019	-0.380**	0.167	-0.146	-0.451**	0.149	-0.348**	0.037	-0.670**	-0.072	0.402**	0.415**	0.527**	0.662**
2.16	**	**WI2-B**	-0.354**	-0.065	0.037	0.069	-0.052	0.039	-0.158	0.043	-0.201	-0.045			**WI-2**	
2.69	**	**WI2-E**	-0.269*	-0.01	0.086	0.127	-0.084	-0.119	-0.109	0.102	-0.227	0.068	0.682**			
1.38	ns	**WI2-G**	-0.422**	0.252*	-0.017	0.317**	0.179	-0.112	0.114	-0.268*	0.016	-0.083	0.480**	0.484**		
2.80	**	**WI2-J**	-0.11	0.093	-0.013	0.197	0.058	-0.255*	-0.347**	0.22	-0.343**	-0.015	0.476**	0.531**	0.481**	
3.16	**	**WI2-L**	-0.165	-0.037	0.058	0.024	-0.175	0.051	-0.161	0.031	-0.371**	-0.005	0.441**	0.491**	0.490**	0.685**
1.35	ns	**WI3-B**	-0.377**	-0.064	0.067	-0.004	-0.071	0.06	0	0.013	-0.033	0.117			**WI-3**	
1.82	*	**WI3-E**	-0.246*	0.028	0.103	0.101	-0.05	-0.148	0.075	0.077	-0.051	0.176	0.555**			
1.68	ns	**WI3-G**	-0.393**	0.276*	-0.086	0.182	0.191	-0.131	0.351**	-0.288*	0.304*	0.119	0.395**	0.332**		
2.37	**	**WI3-J**	-0.152	0.238*	-0.067	0.287*	0.217	-0.309**	-0.196	0.104	-0.117	0.027	0.275*	0.246*	0.390**	
2.16	**	**WI3-L**	-0.202	0.241*	-0.048	0.149	0.105	-0.044	0.046	0.003	0.002	0.046	0.251*	0.357**	0.420**	0.612**

Table S12c: Trial Food, Normalized water indices (NWI) at five timepoints (A, D, G, J, K): Anova with F-values between all varieties; correlation matrix with Pearson's correlation coefficients (r): colored cells show significant correlation; following significance levels (Sign.) are valid: +: p<0.1; *: p<0.05; **: p<0.01; ns: not significant.

Food	70 Genotypes; Lattice 10x7; 2 rep			**Software:**	Plabstat					**Date:**	26.11./2.12.2024			
ANOVA			**Correlation matrix - Pearson's correlation coefficient (r)**											
F-value	**Sign.**	**Index-TP**	**emerg**	**ttf**	**SPAD**	**leaf size**	**ttm**	**podshat**	**lodging**	**pod set**	**height**	**yield**	*Index-* **B**	*Index-* **E**	*Index-* **G**	*Index-* **J**
3.18	**	NWI1-B	-0.291*	0.014	-0.017	0.154	0.025	-0.008	-0.23	0.052	-0.255*	-0.138			NWI-1	
3.86	**	NWI1-E	-0.225	0.004	0.07	0.189	-0.033	-0.112	-0.202	0.087	-0.277*	-0.013	0.750**			
1.66	*	NWI1-G	-0.287*	0.199	0.099	0.355**	0.122	-0.077	-0.076	-0.194	-0.182	-0.213	0.574**	0.591**		
3.26	**	NWI1-J	-0.078	0.018	0.045	0.159	-0.021	-0.207	-0.409**	0.256*	-0.418**	-0.045	0.571**	0.586**	0.516**	
4.45	**	NWI1-L	-0.114	-0.177	0.1	-0.058	-0.296*	0.079	-0.256*	0.05	-0.520**	-0.032	0.496**	0.498**	0.516**	0.676**
4.91	**	NWI2-B	-0.149	-0.026	-0.032	0.124	-0.005	-0.041	-0.296*	0.1	-0.331**	-0.116			NWI-2	
5.52	**	NWI2-E	-0.103	-0.085	0.085	0.137	-0.092	-0.087	-0.303*	0.133	-0.392**	-0.003	0.850**			
2.3	*	NWI2-G	-0.049	-0.019	0.189	0.228	-0.049	-0.064	-0.291*	-0.025	-0.436**	-0.135	0.680**	0.698**		
3.83	**	NWI2-J	0.015	-0.138	0.086	0.078	-0.166	-0.205	-0.486**	0.296*	-0.576**	0.02	0.660**	0.694**	0.607**	
5.07	**	NWI2-L	-0.018	-0.298*	0.152	-0.14	-0.393**	0.09	-0.336**	0.104	-0.649**	-0.031	0.516**	0.538**	0.572**	0.703**
3.07	**	NWI3-B	-0.309**	0.046	-0.032	0.188	0.054	-0.037	-0.216	0.059	-0.229	-0.126			NWI-3	
3.95	**	NWI3-E	-0.246*	0.046	0.073	0.221	0.017	-0.13	-0.173	0.093	-0.23	-0.006	0.734**			
1.52	+	NWI3-G	-0.373**	0.249*	0.048	0.377**	0.175	-0.055	0.008	-0.22	-0.09	-0.241*	0.543**	0.564**		
3.16	**	NWI3-J	-0.092	0.059	0.041	0.182	0.012	-0.201	-0.378**	0.233	-0.372**	-0.063	0.551**	0.538**	0.486**	
4.15	**	NWI3-K	-0.142	-0.122	0.098	-0.014	-0.244*	0.074	-0.235	0.044	-0.479**	-0.031	0.494**	0.484**	0.523**	0.686**
4.52	**	NWI4-B	-0.196	0.043	-0.058	0.173	0.063	-0.043	-0.272*	0.062	-0.277*	-0.178			NWI-4	
4.94	**	NWI4-E	-0.154	-0.009	0.06	0.189	-0.023	-0.107	-0.273*	0.095	-0.336**	-0.055	0.814**			
2.16	**	NWI4-G	-0.112	0.086	0.155	0.289*	0.042	-0.065	-0.235*	-0.095	-0.349**	-0.213	0.652**	0.658**		
3.60	**	NWI4-J	-0.023	-0.083	0.074	0.094	-0.12	-0.186	-0.474**	0.282*	-0.534**	-0.027	0.620**	0.653**	0.550**	
5.07	**	NWI4-L	-0.053	-0.282*	0.14	-0.133	-0.388**	0.099	-0.326**	0.086	-0.631**	-0.04	0.484**	0.507**	0.531**	0.698**
2.23	**	NWI5-B	-0.228	0.062	-0.038	0.209	0.042	-0.092	-0.159	0.061	-0.158	-0.022			NWI-5	
2.72	**	NWI5-E	-0.274*	0.028	0.082	0.269*	0.021	-0.139	-0.125	0.073	-0.194	0.096	0.757**			
1.3	ns	NWI5-G	-0.408**	0.215	0.013	0.303*	0.136	-0.038	0.033	-0.159	-0.073	-0.113	0.412**	0.528**		
2.31	**	NWI5-J	-0.157	0.078	0.009	0.229	0.033	-0.213	-0.310**	0.164	-0.314**	-0.05	0.504**	0.509**	0.519**	
3.14	**	NWI5-L	-0.208	-0.024	0.037	0.044	-0.144	0.043	-0.158	0.001	-0.377**	-0.055	0.395**	0.442**	0.602**	0.717**

Table S13: Spearman's rank correlation coefficients (r) for siCWSI and several plant traits, departed in daytime (12:00 and 15:00) and stress levels according to VPD (low: VPD =< 1.5 kPa, mid: 1.5<VPD=<2.0 kPa, high: VPD > 2.0 kPa, average: all timepoints); probability level p to determine significant correlation; with following significance levels (Sign.): $+$: p$<$0.1; $*$: p$<$0.05; $**$: p$<$0.01; ns: not significant.

Stress level		**low**			**mid**			**high**			**average**		
Trait	Time	r(Spearman)	p	Sign.	r(Spearman)	p	Sign.	r(Spearman)	p	Sign.	r(Spearman)	p	Sign.
emerg	12:00	-0.191	0.163	ns	0.048	0.791	ns	0.134	0.552	ns	-0.055	0.572	ns
devsc	12:00	-0.040	0.775	ns	0.127	0.482	ns	-0.397	0.068	+	-0.041	0.672	ns
ttf	12:00	-0.280	0.038	*	-0.031	0.863	ns	-0.013	0.955	ns	-0.153	0.111	ns
ttm	12:00	-0.273	0.044	*	-0.057	0.753	ns	0.039	0.865	ns	-0.147	0.125	ns
t_reprod	12:00	-0.168	0.219	ns	-0.064	0.724	ns	-0.099	0.662	ns	-0.117	0.222	ns
SPAD1	12:00	-0.221	0.106	ns	-0.249	0.163	ns	-0.612	0.003	**	-0.301	0.001	**
SPAD2	12:00	-0.121	0.378	ns	-0.377	0.030	*	-0.288	0.194	ns	-0.230	0.016	*
leaf size	12:00	-0.336	0.012	*	-0.221	0.216	ns	-0.091	0.688	ns	-0.260	0.006	**
height	12:00	-0.182	0.184	ns	0.077	0.672	ns	0.009	0.968	ns	-0.060	0.532	ns
yield	12:00	-0.191	0.162	ns	0.048	0.790	ns	-0.134	0.553	ns	-0.097	0.316	ns
d_stom	12:00	-0.258	0.057	+	-0.123	0.496	ns	-0.378	0.083	+	-0.233	0.014	*
emerg	15:00	0.304	0.024	*	0.365	0.015	*	0.292	0.017	*	0.286	0.000	**
devsc	15:00	-0.024	0.865	ns	0.008	0.959	ns	0.040	0.750	ns	-0.005	0.952	ns
ttf	15:00	0.288	0.033	*	0.333	0.027	*	0.383	0.002	**	0.304	0.000	**
ttm	15:00	0.281	0.038	*	0.359	0.017	*	0.372	0.002	**	0.305	0.000	**
t_reprod	15:00	0.100	0.469	ns	0.212	0.167	ns	0.106	0.396	ns	0.127	0.104	ns
SPAD1	15:00	-0.225	0.099	+	-0.172	0.264	ns	-0.198	0.110	ns	-0.178	0.022	*
SPAD2	15:00	-0.278	0.040	*	-0.232	0.130	ns	-0.243	0.049	*	-0.221	0.004	**
leaf size	15:00	0.011	0.937	ns	0.100	0.518	ns	0.093	0.458	ns	0.050	0.521	ns
height	15:00	0.362	0.053	+	0.337	0.025	*	0.341	0.005	**	0.312	0.000	**
yield	15:00	0.262	0.053	+	0.366	0.015	*	0.233	0.060	+	0.264	0.001	**
d_stom	15:00	-0.010	0.944	ns	0.182	0.236	ns	-0.031	0.806	ns	0.051	0.512	ns